NASA CONTRACTOR REPORT

NASA CR-7
c.1

NASA CR-788

APPLICATION OF ALLOY 718 IN M-1 ENGINE COMPONENTS

by F. T. Inouye, V. Hunt, G. R. Janser, and V. Frick

Prepared by
AEROJET-GENERAL CORPORATION
Sacramento, Calif.
for Lewis Research Center

NATIONAL AERONAUTICS AND SPACE ADMINISTRATION • WASHINGTON, D. C. • JUNE 1967

NASA CR-788

APPLICATION OF ALLOY 718 IN M-1 ENGINE COMPONENTS

By F. T. Inouye, V. Hunt, G. R. Janser,
and V. Frick

Prepared under Contract No. NAS 3-2555 by
AEROJET-GENERAL CORPORATION
Sacramento, Calif.

for Lewis Research Center

NATIONAL AERONAUTICS AND SPACE ADMINISTRATION

For sale by the Clearinghouse for Federal Scientific and Technical Information
Springfield, Virginia 22151 – CFSTI price $3.00

FOREWORD

The research described herein, which was conducted by the Aerojet-General Corporation, Liquid Rocket Operations, was performed under NASA Contract NAS3-2555 with Mr. J. M. Kazaroff, Chemical Rocket Division, NASA Lewis Research Center, as Technical Manager.

ABSTRACT

Large quantities of Alloy 718 were used in fabricating components for the M-1 Engine, which is a 1.5-million-pound-thrust, liquid hydrogen/liquid oxygen, engine. The development work performed to evaluate the alloy during the design and initial production phases is reported herein. The establishment of heat treatment criteria and properties of Alloy 718 for applications from -423°F to 1350°F are described in Part I of this report. Critical welding of heavy sections was performed by electron-beam welding (EBW) and tungsten inert gas arc welding (TIG) and are described for specific components in Parts II and III, respectively.

TABLE OF CONTENTS

TABLE OF CONTENTS (CONT.)

TABLE OF CONTENTS (CONT.)

SUMMARY

This report summarizes the experience in using Alloy 718 in the M-1 Engine. It does not delineate all of the detailed aspects of metallurgical research undertaken in this connection.

The design phase and material selection for components of the M-1, a 1.5-million-lb thrust, liquid oxygen/liquid hydrogen engine, began in 1962. Before that time (1960), the International Nickel Company introduced Inconel 718, a nickel-base precipitation hardened alloy. The alloy possessed exceptionally good elevated temperature properties at temperatures ranging from 1000°F to 1350°F and later proved to have excellent properties at cryogenic temperatures.

Alloy 718, which is strengthened with columbium in addition to aluminum and titanium, displays a low rate of precipitation of the metastable, columbium rich, gamma prime phase. This results in improved weldability over the well-known nickel-base super-alloys.

This alloy was selected for numerous applications in the M-1 engine because of its good strength and toughness at temperatures ranging from -423°F to 1350°F as well as its good weldability. Alloy 718 is used in such major M-1 components as the liquid hydrogen and liquid oxygen turbopumps, engine lines, and thrust chamber jacket.

The alloy was evaluated during the design and initial production phases of the M-1 program. This evaluation of Alloy 718 properties is discussed in Part I of this report. Critical welding of heavy sections was required and the results of this weld development for electron-beam (EB) welding and gas tungsten arc welding (TIG) are reported in Parts II and III, respectively.

INTRODUCTION

The Aerojet-General Corporation began design work for the M-1, a 1.5-million-lb thrust, liquid oxygen/liquid hydrogen engine in 1962. A materials evaluation and materials selection study for applications from cryogenic to elevated temperatures was undertaken shortly after the introduction of Inconel® 718 by the International Nickel Company. The available property data indicated exceptionally good strength and ductility in the range of 1000°F to 1350°F. Numerous high strength alloys were available for application to approximately 1000°F (e.g., precipitation-hardenable stainless steels, A-286, etc.) and the nickel-base precipitation-hardened super alloys (e.g., Udimets, Hastelloy R-235, etc.) were candidates for applications at temperatures in excess of 1400°F. Alloy 718 filled the temperature-range gap at which the M-1 hydrogen and oxygen pump turbines would operate. The results of initial tests at cryogenic temperatures showed that the alloy also possessed excellent low temperature toughness.

Alloy 718, which is a precipitation-hardening nickel-base alloy, has a nominal composition of 55% nickel, 19% chromium, 5% columbium, 3% molybdenum, 1% titanium, 0.5% aluminum, 0.8% maximum carbon, and the balance iron. It is

® Inconel is the registered trademark of the International Nickel Company.

strengthened by a columbium-rich, gamma-prime precipitate believed to be Ni_3 (Cb, Ti, Al); this phase is face-centered-cubic and is coherent with the matrix. The lattice parameter of gamma prime is approximately 0.8% greater than that of the matrix, thereby producing strengthening by lattice strain. Although gamma prime precipitates heavily from solid solution during aging at temperatures between 1300 to 1400°F, the precipitation hardening reaction is sluggish, because of the slow diffusion rates of the hardening elements. The slow aging response is beneficial in that it produces low-annealed hardness during the cooling from the annealing temperature; this enhances formability and weldability. In addition to gamma prime, primary massive carbides, both blocky and granular types, are present in Alloy 718. They have been identified as MC or Cb, Ti (C) and are relatively insensitive to temperature. Grain boundary carbide film may also exist, depending upon temperature and time during heat treatment. The grain boundary carbide film (probably columbium-rich M_6C) does not generally occur in Alloy 718 that is annealed at 1700°F to 1750°F. With higher annealing temperatures, there is an increased possibility for the existence of intergranular carbide film after aging. Very high temperature aging for extended periods causes overaging by transforming the metastable face-centered-cubic precipitate to a stable orthorhombic Ni_3Cb compound that is non-coherent with the matrix.

The heat treatment of Alloy 718 is relatively simple, consisting of an anneal (1750 to 1950°F) and a double aging cycle. The secondary lower temperature age is used to obtain maximum precipitate of the face-centered-cubic gamma prime without suffering overaging effects.

The heat treatment studies resulted in two Aerojet-General standard heat treatments. The 1800°F solution anneal plus aging is used for stress rupture limited applications (i.e., applications at temperature exposure in excess of 1170°F), and the 1950°F solution anneal and aging provides optimum tensile limited and cryogenic properties. These heat treatments are described in Part I of this report.

Specific study programs were undertaken to evaluate Alloy 718 for heat treatment, material properties, and weldability. Minimum design properties were established from these tests and from the results of other investigators. These are shown in Appendix A.

As a result of the excellent properties and weldability, numerous components of the M-1 engine were made of Alloy 718. The liquid hydrogen turbopump ranged in operational temperature from -423°F in the axial flow pump to 1200°F in the hot gas turbine. Weldments of heavy sections of Alloy 718 were made by both the gas tungsten-arc weld (TIG) and electron-beam (EB) welding processes. The turbine components of the liquid oxygen turbopump were made from this alloy, as were most of the engine lines and the thrust chamber jacket. Cutaway views of these areas are presented in Appendix B.

The specific studies performed for Alloy 718 prior to and concurrent with the production of prototype M-1 hardware are described in Part I of this report.

The evolution of the unique electron beam weld design of the turbines and joint properties are described in Part II. The TIG process was used in all other welded fabrication. Of particular interest was the TIG welded fuel pump rotor; this welding of Alloy 718 in heavy sections is described in Part III.

PART I. HEAT TREATMENT AND PROPERTIES OF ALLOY 718 FOR APPLICATIONS AT TEMPERATURES FROM -423° TO 1350° F

I. TEST PROCEDURES AND RESULTS

The general testing procedure was to prepare representative test samples from the sheet, bars, forgings and other forms and shapes, heat-treat them to specified conditions, final machine the test samples, and test the finished specimens in accordance with standard test methods.

Tension tests were conducted in accordance with Federal Standard 151a, normally at 0.005-in./in./min strain rate. Tests were made at -320°F by immersion in liquid nitrogen, and at -423°F by immersion in liquid hydrogen; a 60,000-lb-capacity Baldwin testing machine was used.

Fatigue tests were conducted with a Tatnall-Krouse Rotating Beam Fatigue Tester at a frequency of 2500 rpm, and with a Type VSP-150 Budd Fatigue Tester at a frequency of 2100 cycles per minute. Specimens were stressed by bending under complete-stress reversal to failure or 10^8 run-out, whichever occurred first.

Metallographic specimens were prepared by standard techniques, and an etchant containing 50 HCl, 30 H_2O, 20 HF, and 10 HNO_3 was used in most cases for revealing the structure of Alloy 718.

Specific testing procedures are outlined in the discussion of the individual study phases presented in the following sections. Unless otherwise stated, all test material conformed to the standard composition and heat-treat conditions described in Table I-I.

A. VARIATION OF HEAT-TREATED MECHANICAL PROPERTIES WITH ANNEALING TEMPERATURES

Many potential uses of Alloy 718 require that it is heated above 1750°F. This is particularly true in the case of brazing, where the melting points of the common braze alloys may exceed the normally used annealing temperatures for Alloy 718. Also, the parts may require in-process stress relieving or re-annealing. Therefore, a study was made of the variation of heat-treated mechanical properties as a function of annealing temperatures.

One 4.5-in. diameter bar in the mill-annealed condition was machined into smooth and notched longitudinal tensile specimens (notch-acuity factor $K_t = 8$), and then annealed for one hour at the following temperatures: 1750°F, 1850°F, 1950°F, and 2050°F. The specimens were subsequently given the following aging treatment: 1325°F for eight hours, furnace cooled to 1150°F, held at 1150°F for 14 hours, and air cooled to room temperature. The specimens were tensile tested at ambient temperature.

Test results are listed in Table I-II and are graphically shown in Figures No. I-1 and No. I-2. Increasing the annealing temperature from 1750°F to 2050°F resulted in decreased strength and increased ductility. Annealing at 1750°F produced very little change in the microstructure when viewed with the

TABLE I-I

STANDARD COMPOSITION AND HEAT TREATMENTS FOR ALLOY 718

A. STANDARD COMPOSITION

Element	Percent Minimum	Percent Maximum
Ni	50.0	55.0
Cr	17.0	21.0
Cb	4.75	5.5
Mo	2.8	3.3
Ti	0.65	1.40
Co		1.0
Mn		0.45
Si		0.45
Cu		0.30
C		0.08
S		0.015
P		0.015
Al		0.80
B		0.006
Fe		Balance

B. STANDARD HEAT TREATMENTS

Designation	Use	Treatment
Condition A	All stress-rupture limited applications	Annealed 1 hr at 1800°F, air cooled. Aged 8 hr at 1325°F furnace-cooled to 1150°F, and held at 1150°F until a total aging time of 18 hr has elapsed.
Condition B	All cryogenic and other tensile-limited applications	Annealed 1 hr at 1950°F, air cooled. Aged 8-10 hr at 1350°F, furnace-cooled to 1200°F, and held at 1200°F until a total aging time of 20 hr has elapsed.
Condition C	All cryogenic and other tensile-limited applications	Annealed 1 hr at 1950°F, air cooled. Aged 8-10 hr at 1400°F, furnace-cooled to 1200°F, and held at 1200°F until a total aging time of 20 hr has elapsed.

TABLE I-II

VARIATION OF HEAT-TREATED MECHANICAL PROPERTIES WITH ANNEALING TEMPERATURES*

Annealing Temperature °F	Testing Temperature °F	F_{tu} ksi	F_{ty} ksi	Elongation % in 4D	Reduction of Area %	Hardness R_c	Notch Tensile ksi	Notch** Ultimate Ratio
1750	73	185.2	154.3	25	43.7	42	253.2	1.37
	-320	239.3	168.1	33	34.5	--	282.2	1.18
1850	73	176.6	135.4	30	36.0	39	234.4	1.33
	-320	227.0	145.1	31	47.1	--	275.9	1.22
1950	73	171.6	130.2	34	52.5	37.5	230.2	1.34
	-320	233.1	147.5	41	45.6	--	266.9	1.15
2050	73	163.3	120.2	52	50.0	34	201.3	1.24
	-320	210.8	125.2	40	49.5	--	243.5	1.16

* All values reported are averages of two tests

** $K_t = 8$

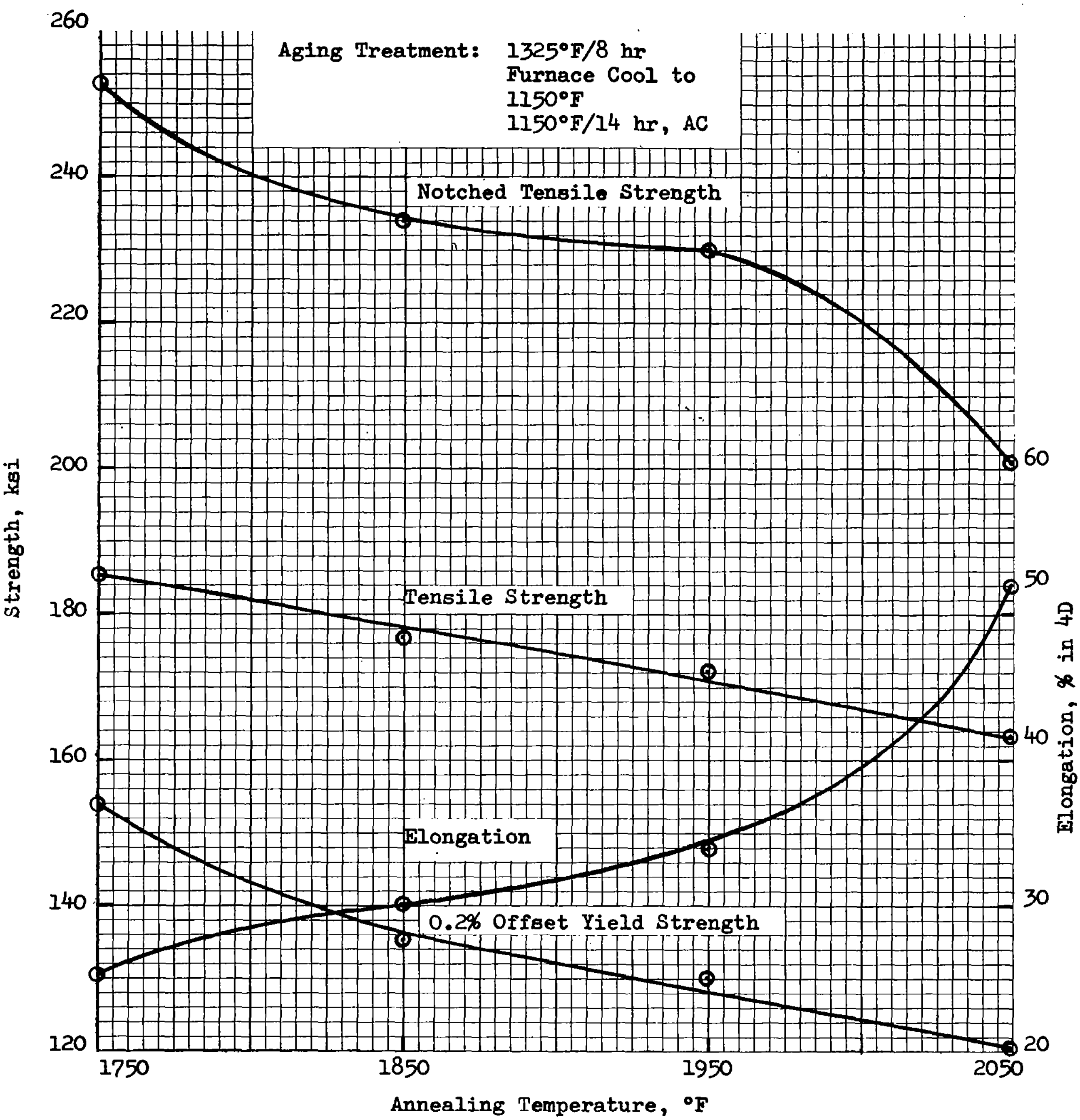

Figure I-I

Variation of As-Heat-Treated Room Temperature
Mechanical Properties with Annealing Temperature

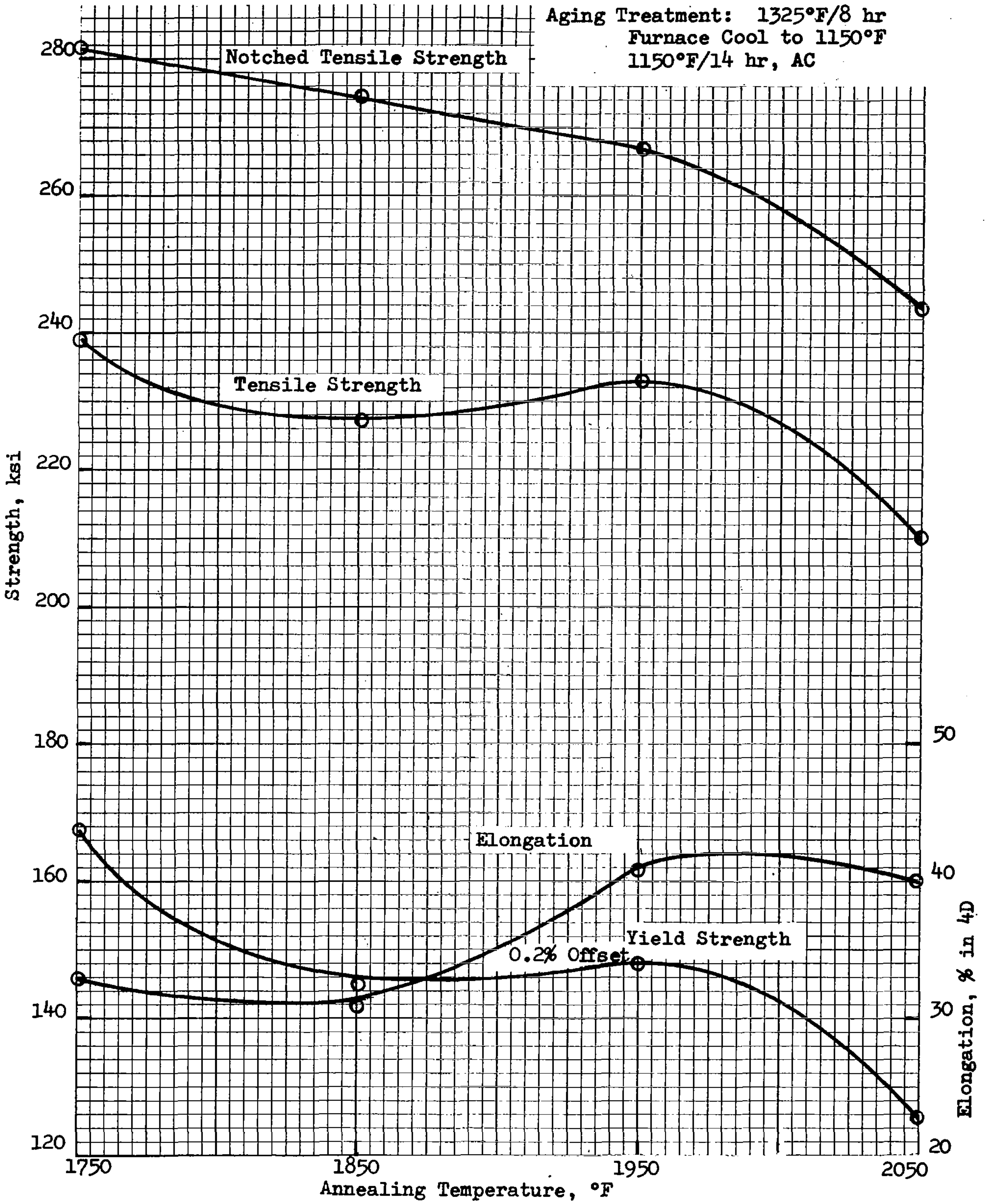

Figure I-2

Variation of As-Heat-Treated Minus 320°F Mechanical Properties with Annealing Temperature light microscope, while annealing at 1950°F and 2050°F produced considerable grain growth. The strength reduction appears to be partly caused by stress relaxation and stress relief when annealed at 1750°F and 1850°F and caused by recrystallization when annealed at 1950°F and 2050°F, with the grain growth being associated with a warm-worked structure.

The optimum combination of cryogenic strength and ductility with the 1950°F solution-anneal temperature (see Figure No. I-2) is of particular interest. This solution anneal has been selected for the cryogenic applications of Alloy 718 as well as for higher-temperature, tensile-limited applications. An 1800°F solution anneal temperature is used for stress rupture limited applications (see Table I-I).

Masking of properties of mill-annealed (1750°F to 1800°F) and aged material because of warm work is a serious consideration. Material with poor mill practice can sometimes meet specification requirements for an 1800°F solution anneal and age but prove substandard after process annealing and welding during fabrication. Procurement specifications should contain a capability requirement wherein stated minimum properties must be met with a higher (1950°F) solution anneal.

B. COOLING RATE EFFECTS ON ANNEALED HARDNESS AND ON ANNEALED AND AGED TENSILE PROPERTIES

The effect of cooling rates upon annealed hardness and upon annealed and aged properties was studied to provide in-process heat-treatment criteria for massive parts such as the thrust chamber fuel torus and jacket.

Test specimens were annealed at 1950°F for one hour, and furnace-cooled from 1950°F to 1350°F at the following rates: 2400°F/hr, 1200°F/hr, 600°F/hr, 200°F/hr, 100°F/hr; and then air cooled to room temperature. Additional specimens were annealed at 1950°F for one hour and furnace-cooled to 1350°F at rates of 2400°F/hr, 600°F/hr, and 200°F/hr, followed by aging (1350°F for 8 hours, furnace cooled to 1200°F, and holding at 1200°F, until a total aging time of 20 hours has elapsed), and finally air cooling to room temperature.

The effect of these cooling rates upon annealed hardness is shown in Figure No. I-3. As the cooling rate decreased, the hardness increased; this results from aging with a longer time exposure in the aging range. If the cooling rate were slower than 2400°F/hr, the hardness will be above Rockwell C 28 and the material will become more difficult to form. The higher hardness resulting from a cooling rate less than 2400°F/hr would not be detrimental if no subsequent forming is planned.

The effect of cooling rates upon annealed and aged properties is shown in Figure No. 1-4 and Table I-III. As the cooling rate decreased, the yield strength gradually decreased until a cooling rate of 600°F/hr was reached. The yield strength then decreased rapidly but exceeded the design minimum requirement of 150 ksi.

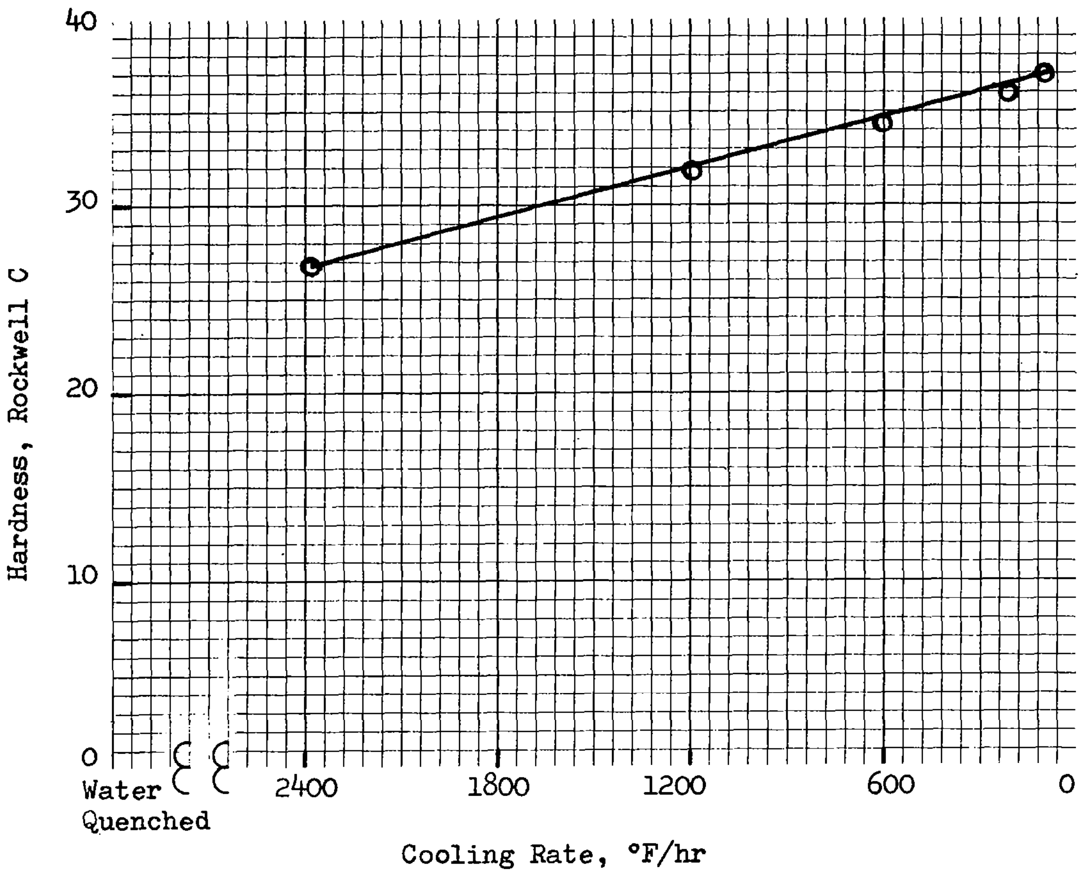

Figure I-3

Solution Annealed Hardness Vs. Cooling Rate from 1950°F to 1350°F

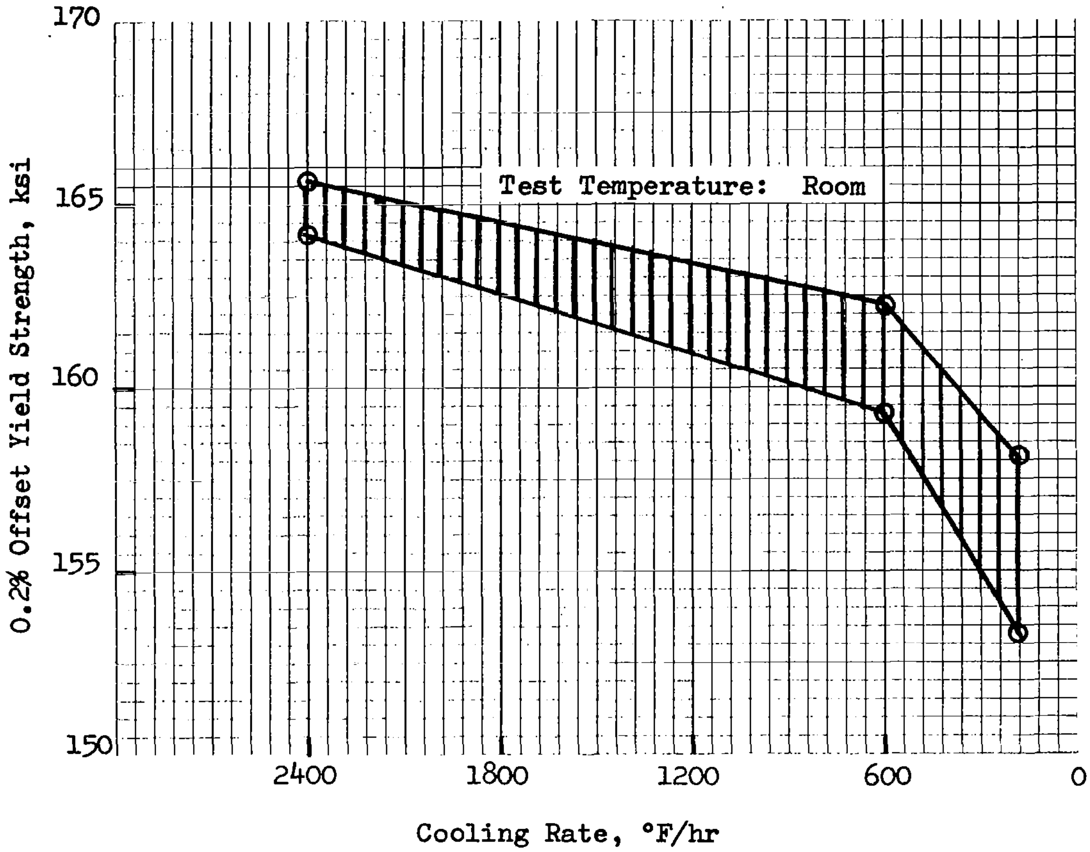

Figure I-4

The 0.2% Offset Yield Strength after Aging at 1350°/1200°F Vs. Cooling Rate from the Solution Annealing Temperature of 1950°F to 1350°F

TABLE I-III

EFFECT OF COOLING RATE, FROM THE ANNEAL, UPON THE PROPERTIES OF ALLOY 718 PLATE, CONDITION B*

Cooling Rate, °F/hr	F_{tu} ksi	F_{ty} ksi	Elongation %	Reduction in Area %	Hardness R_c
2400	203.9	164.4	21.5	29.5	44
2400	208.6	165.8	20.0	30.3	43
600	199.2	162.3	21.0	33.9	46
600	198.0	159.4	20.0	36.4	44
200	202.0	158.3	22.0	36.6	43
200	201.9	153.4	21.5	34.0	41

* See Table I-I

C. FORGING

1. Fatigue Properties of Fuel Rotor Material

Fatigue strength and fatigue strength/tensile ratios for parent metal and weldments were studied to provide design data for the M-1 fuel rotor weldment configuration.

Fatigue specimens were tested in two heat-treatment conditions: Condition A and Condition C (see Table I-I). The Condition A specimens were tested in a Tatnall-Krouse Rotating Beam Fatigue Tester at a frequency of 2500 rpm. The Condition C specimens were tested in a Type VSP-150 Budd Fatigue Tester at a frequency of 2100 cycles per minute. Two testers were used because of the difference in specimen sizes. Larger specimens were tested in the Tatnall-Krouse tester while smaller specimens were tested in the Budd unit. Specimens were stressed by bending under complete-stress reversal to failure or 10^8 cycles run-out, whichever occurred first.

Ambient temperature fatigue results are listed in Tables I-IV through I-VII and shown in Figures No. I-5 and No. I-6. The tensile properties of the material used in the fatigue investigation is shown in Table I-VIII. At 10^8 cycles, the parent metal and weld metal fatigue strengths ranged from 55 to 58 ksi with the fatigue strength/tensile strength and fatigue strength/yield strength ratios ranging from 0.30 to 0.31 and 0.35 to 0.38, respectively. At lower cycles (10^5 and 10^6) the fatigue strengths of the Condition A specimens were slightly higher than those of the Condition C specimens. In all cases, welded specimens exhibited lower fatigue strengths than parent metal specimens.

The higher fatigue strength of Condition A specimens is ascribed to the finer grain structure. The grain size of Condition A specimens was generally ASTM 5 and finer while the grain size of Condition C was ASTM 3 and coarser. The difference in testers does not appear to have significantly affected fatigue results. Although Condition B specimens were not evaluated, it is believed that their fatigue strengths would be similar to the results obtained for Condition C specimens based upon the similarity of the heat treatment cycles and essentially equivalent strength levels conferred to Alloy 718 by the heat treatments.

2. Evaluation of Forging for Injector Applications

The mechanical properties of an Alloy 718 forging were studied for suitability to injector applications at room temperature and -320°F.

An 11-in.-diameter by 1-1/2-in. thick forging was obtained and machined into smooth and notched tensile specimens. Specimens were obtained from the following locations: a. at the centerline, b. along the radius, c. perpendicular to the radius at the midpoint, and d. perpendicular to the radius at the end. Specimens were not obtained in the thickness directions. Notched tensile specimens were machined to give a notch acuity factor

TABLE I-IV

FATIGUE TEST RESULTS OF ROTOR MATERIAL IN CONDITION A

Specimen	Stress ksi	Cycles to Failure	Remarks
Parent Metal			
P7	120	23,300	--
P8	80	251,000	--
P10	60	7,724,900	--
P11	50	100,000,000	No failure
P12	55	100,000,000	No failure
P13	70	19,519,300	--
Welds			
W7	120	19,900	Failed in weld
W8	80	241,000	Failed in weld
W9	60	43,267,200	Failed in weld
W10	55	104,378,300	No failure
W11	57.5	117,250,300	No failure
W12	58.5	116,573,200	No failure
W13	60	709,400	Failed in weld

TABLE I-V

FATIGUE TEST RESULTS OF ROTOR MATERIAL IN CONDITION C

Specimen	Stress ksi	Cycles to Failure	Remarks
Parent Metal			
P1	120	29,200	--
P2	80	147,600	--
P3	50	101,595,400	No failure
P5	60	4,124,000	--
P6	60	100,000,000	No failure
Welds			
W1	120	20,300	Failed in weld
W2	80	243,000	Failed in weld
W3	60	394,200	Failed in weld
W4	40	102,105,800	No failure
W5	60	3,862,000	Failed in weld
W6	60	5,919,400	Failed in weld

TABLE I-VI

FATIGUE STRENGTH AND ULTIMATE STRENGTH RATIOS FOR ROTOR MATERIAL TESTED AT ROOM TEMPERATURE

Condition	Specimen	Tensile Strength F_{tu} ksi	Fatigue Strength (ksi) and Fatigue Strength/ Ultimate Strength Ratio (in parentheses) for Indicated Life (cycles)			
			10^5	10^6	10^7	10^8
A	Parent Metal	184.8	95 (0.51)	72 (0.39)	59 (0.32)	55 (0.30)
C	Parent Metal	184.2	89 (0.48)	68 (0.37)	59 (0.32)	55 (0.30)
A	Weld	184.2	92 (0.50)	60 (0.32)	59 (0.32)	58 (0.31)
C	Weld	184.6	87 (0.47)	60 (0.32)	*	*

* Insufficient test data

TABLE I-VII

FATIGUE STRENGTH AND 0.2% OFFSET YIELD STRENGTH RATIOS FOR ROTOR MATERIAL AT ROOM TEMPERATURE

Condition	Specimen	F_{ty}, ksi	Fatigue Strength (ksi) and Fatigue Strength/Yield Strength Ratio (in parentheses) for Indicated Life (cycles)			
			10^5	10^6	10^7	10^8
A	Parent Metal	155.2	95 (0.61)	72 (0.46)	59 (0.38)	55 (0.35)
C	Parent Metal	157.4	89 (0.56)	68 (0.43)	59 (0.38)	55 (0.35)
A	Weld	154.0	92 (0.60)	60 (0.39)	59 (0.38)	58 (0.38)
C	Weld	157.1	87 (0.55)	60 (0.38)	*	*

* Insufficient test data

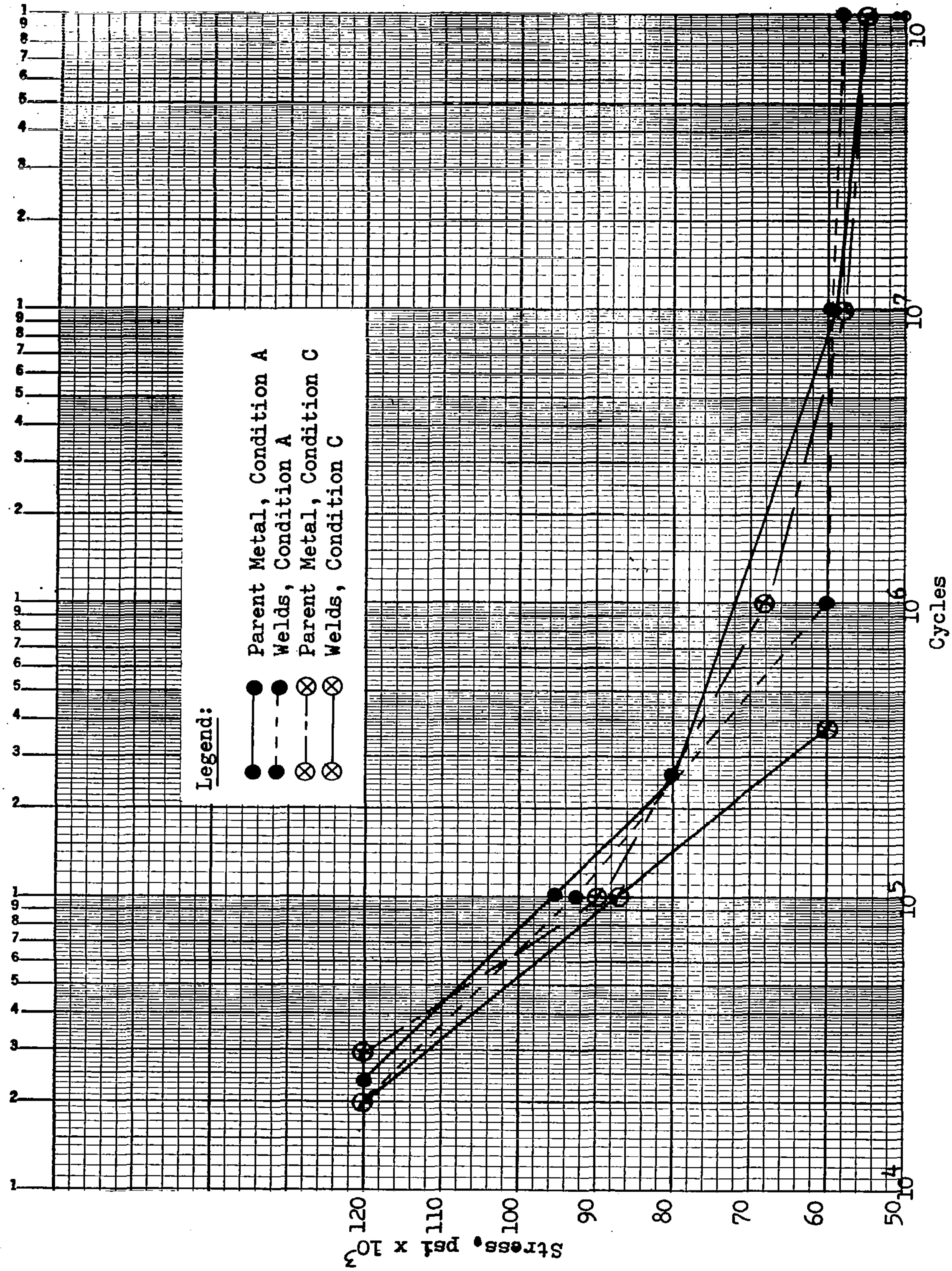

Figure I-5

Stress-Log Cycle Fatigue Curves for Rotor Material

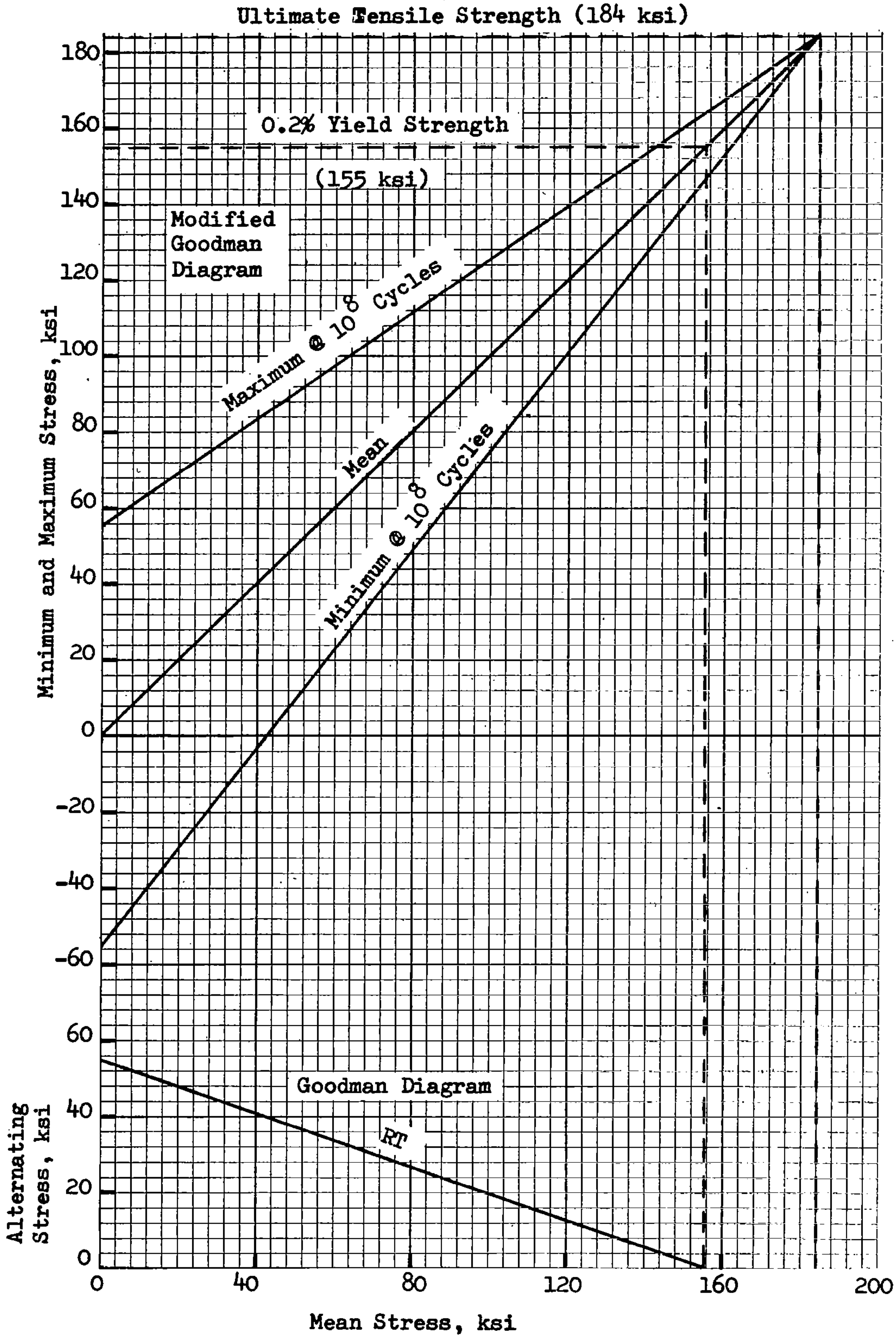

Figure I-6

Goodman and Modified Goodman Diagram for M-1 Fuel Rotor at Room Temperature

TABLE I-VIII

TENSILE PROPERTIES OF ROTOR MATERIAL USED IN THE FATIGUE INVESTIGATION

Condition	Specimen Type	F_{tu} ksi	F_{ty} ksi	Elongation %	Notch Strength* ksi	Notch/Ultimate Ratio
A	Unwelded	184.8	155.2	28.8	239.0	1.29
A	Welded	184.2	154.0	11.5	231.3	1.26
C	Unwelded	184.2	157.4	24.3	237.2	1.29
C	Welded	184.6	157.1	19.3	237.5	1.29

* Notched-bar stress concentration factor K = 6.3

of K_t = 6.3. All specimens were heat treated to Condition A.

The tensile properties are listed in Table I-IX. The centerline ductilities are lower than those from other directions. The forging possessed good strength and ductility as well as notch toughness at ambient temperature and -320°F.

3. Fuel Turbine Pump Rotor Forging Properties

The mechanical properties of M-1 fuel turbine pump rotor material were established to provide design data.

Standard 1/4-in.-round and notched tensile specimens (with a notch acuity factor of K_t = 6.3) were machined from the parent metal and the weldment sections of the fuel turbine pump rotor. The specimens were heat-treated to Condition C to obtain optimum match toughness in Alloy 718.

Specimens were tested at temperatures of ambient, -423°F, and 1200°F.

The experimental results of mechanical property tests are listed in Table I-X. The strength characteristics of the parent metal and weldments reflected consistent age hardening response. Satisfactory metal toughness was observed at room temperature and was retained at -423°F and 1200°F although elongation and reduction of area were slightly reduced. Weld joint efficiency of 100% was obtained in the TIG welded specimens, which were welded with Alloy 718 wire.

4. Mechanical Properties of Large Cone Forging and Octagon Forging

Heat-treatment response tests were performed with one cone forging because of the difficulty experienced by a forging vendor in meeting mechanical property minimums of 180 ksi ultimate strength, 150 ksi 0.2% effect yield strength, and 12% elongation in a large fuel pump rotor forging.

The effect of various aging treatments upon properties of one 7-in. octagon forging was also studied by the alloy developer (Huntington Alloy Products Division of the International Nickel Company) in connection with the heat treatment analysis of Alloy 718 and results are reported herein.

The testing procedures and results are listed below:

a. Cone Forging

The part measured approximately 7-in. diameter on one end, 14-in. diameter on the opposite end, and was 18.5-in. long. One-inch-thick increments were machined from each end. Specimen blanks taken from tangential locations were separated into two groups, annealed per Condition A (at 1800°F) and per Condition C (at 1950°F), respectively, then machined into

TABLE I-IX

MECHANICAL PROPERTIES OF INJECTOR FORGING IN CONDITION A

A. TESTED AT ROOM-TEMPERATURE

Specimen No.	Specimen Type	Specimen Location	F_{tu} ksi	F_{ty} (.2%) ksi	Elongation % in 1 in.	Reduction of Area %	Hardness R_c	Notch/ Ultimate Ratio
1	R-3 Smooth	Tangential	195.9	155.0	22	30.2	44	
2	R-3 Smooth	Tangential	192.1	163.7	20	31.0		
Average			194.0	159.4	21	30.6		
5	Notched	Tangential	238.5	NA	NA	NA		
6	Notched	Tangential	241.8	NA	NA	NA	43	
Average			240.2					1.24
9	R-3 Smooth	Center	187.1	159.5	16	20.7	43	
10	R-3 Smooth	Center	185.7	159.0	15	17.5		
Average			186.4	159.3	15.5	19.1		
11	Notched	Center	242.4	NA	NA	NA		
12	Notched	Center	230.9	NA	NA	NA		
Average			136.7					1.27
13	R-3 Smooth	Mid-Radius	188.5	161.0	22	31.8	44	
14	R-3 Smooth	Mid-Radius	189.3	161.7	20	24.3		
Average			188.9	161.4	21	28.1		
15	Notched	Mid-Radius	237.9	NA	NA	NA		
16	Notched	Mid-Radius	242.4	NA	NA	NA		
Average			240.2					1.27
17	R-3 Smooth	Radial	189.7	162.1	24	34.9		
18	R-3 Smooth	Radial	188.6	163.7	22	36.1	44	

TABLE I-IX (CONT.)

MECHANICAL PROPERTIES OF INJECTOR FORGING IN CONDITION A

A. TESTED AT ROOM-TEMPERATURE (CONT.)

Specimen No.	Specimen Type	Specimen Location	F_{tu} ksi	F_{ty} (.2%) ksi	Elongation % in 1 in.	Reduction of Area %	Hardness R_c	Notch/ Ultimate Ratio
Average			189.2	162.9	23	35.5		
21	Notched	Radial	242.0	NA	NA	NA		
22	Notched	Radial	242.6	NA	NA	NA		
Average			242.3					1.32
B. TESTED AT 320°F								
3	R-3 Smooth	Tangential	246.1	179.9	22	23.1		
4	R-3 Smooth	Tangential	247.2	164.9	25	28.1	43	
Average			246.7	172.4	23.5	25.6		
7	Notched	Tangential	282.5	NA	NA	NA		
8	Notched	Tangential	281.4	NA	NA	NA	43	
Average			282.0					1.14
19	R-3 Smooth	Radial	240.6	178.9	28	34.4		
20	R-3 Smooth	Radial	242.7	183.0	26	28.4	NA	
Average			241.6	180.9	27	31.4		
23	Notched	Radial	275.4	NA	NA	NA		
24	Notched	Radial	279.3	NA	NA	NA	NA	
Average			277.4					1.15

TABLE I-X

MECHANICAL PROPERTIES OF A FUEL PUMP ROTOR, CONDITION C

A. TESTED AT ROOM TEMPERATURE

Specimen	Type	K_{tu} (ksi)	F_{ty} (0.2%) ksi	Elongation (% in 1 inch)	Reduction of Area %	Notch/Ultimate Ratio (%)
8-P-11	Parent Metal	205.1	162.6	24.5	36.0	
8-P-12	Parent Metal	194.4	165.1	25.0	40.0	
8-P-13	Parent Metal	193.0	**	27.0	39.0	
Average		197.5	163.6	25.5	38.5	
8-P-1	Parent Metal*	290.6				
8-P-2	Parent Metal*	266.9				
8-P-3	Parent Metal*	261.0				
Average		272.8				1.38
8-W-11	Weldment	190.1	**	20.0	40.4	
8-W-12	Weldment	189.0	162.0	19.0	37.6	
8-W-13	Weldment	190.1	169.2	19.0	36.2	
Average		189.7	165.6	19.3	38.0	
8-W-1	Weldment*	266.2				
8-W-2	Weldment*	262.4				
8-W-3	Weldment*	260.8				
Average		263.1				1.38

* Notched round specimens, stress concentration factor of 6.3

** Extensometer slippage

TABLE I-X (CONT.)

B. TESTED AT 1200°F

Specimen	Type	F_{tu} (ksi)	F_{ty} (0.2%) ksi	Elongation (% in 1 inch)	Reduction of Area %	Notch/Ultimate Ratio (%)
9-P-7	Parent Metal	143.0	122.1	21.0	44.1	
9-P-8	Parent Metal	144.7	125.6	20.0	43.5	
9-P-11	Parent Metal	144.0	126.3	21.5	35.3	
9-P-12	Parent Metal	144.1	127.3	21.5	39.0	
9-P-13	Parent Metal	143.0	127.0	21.5	41.4	
Average		143.8	125.7	21.5	40.7	
9-P-5	Parent Metal*	206.8				
9-P-6	Parent Metal*	211.9				
9-P-9	Parent Metal*	206.2				
9-P-10	Parent Metal*	204.5				
Average		207.4				1.44
9-W-7	Weldment	145.5	127.5	15.5	41.5	
9-W-8	Weldment	150.4	130.2	14.0	37.3	
9-W-11	Weldment	145.5	126.8	7.5	20.2	
9-W-12	Weldment	147.7	124.7	10.5	21.8	
Average		147.3	127.3	11.9	30.2	
9-W-5	Weldment*	209.2				
9-W-6	Weldment*	214.1				
9-W-9	Weldment*	196.9				
9-W-10	Weldment*	196.5				
Average		204.2				1.39

*Notched round specimens, stress concentration factor of 6.3

TABLE I-X (CONT.)

C. TESTED AT -423°F

Specimen	Type	F_{tu} (ksi)	F_{ty} (0.2%) ksi	Elongation (% in 1 inch)	Reduction of Area %	Notch/Ultimate Ratio (%)
8-P-6	Parent Metal	253.3	208.8	23.0	32.7	
8-P-7	Parent Metal	244.0	198.2	23.0	32.8	
8-P-8	Parent Metal	249.1	210.0	23.0	32.7	
Average		248.8	204.3	23.0	32.7	
8-P-4	Parent Metal*	325.3				
8-P-9	Parent Metal*	323.6				
8-P-10	Parent Metal*	322.4				
Average		323.8				1.30
8-W-5	Weldments	238.3	205.5	20.0	31.4	
8-W-6	Weldments	242.6	202.9	19.0	30.0	
8-W-8	Weldments	232.9	194.7	20.0	30.7	
Average		267.9	201.0	19.7	30.7	
8-W-4	Weldments*	312.7				
8-W-9	Weldments*	308.1				
8-W-10	Weldments*	305.5				
Average		308.8				1.15

*Notched round specimens, stress concentration factor of 6.3

standard 1/4-in.-diameter tensile specimens, and aged. Specimens were tested at ambient temperature for tensile properties.

The test results obtained for the cone forging are listed in Table I-XI. The results illustrated the following points.

(1) Samples in Condition A generally possessed low strength and ductility.

(2) Samples in Condition C had superior properties.

(3) The primary reason for the low properties of the cone forging has been insufficient hot work with the resultant coarse grain structure (Figure No. I-7). More hot working would break up the coarse structure and yield a smaller grain in the forging, with improved mechanical properties.

(4) High solution-annealing temperature is effective in dissolving grain boundary precipitates which affect ductility and in solutioning the Ni_3Cb.

b. Octagon Forging

Tensile specimens were sectioned longitudinally at mid-radius, annealed at 1950°F for one hour, air-cooled, and aged using various primary aging cycles (1325°F/8 hr, 1350°F/10 hr, 1375°F/10 hr, 1400°F/1 hr, 1400°F/10 hr), furnace-cooled at 100°F/hr to 1200°F, and holding at 1200°F/8 hr, air-cooled.

Specimens were tested at room temperature for strength and ductility.

Data for the 7-in. octagon forging are listed in Table I-XII. The effects of primary aging at 1350°F, 1375°F, and 1400°F upon yield strength are shown in Figure No. I-8. These data show no difficulty in meeting the strength requirements with any of the heat treatments used for this heat of material.

D. SHEET

1. Stress-Rupture Properties of 1/8-in. Sheet

Stress-rupture tests of sheet material were conducted to compare the effect of the Conditions A and B (Table I-I) heat treatments upon rupture strength and ductility.

A 12-in. square by 0.128-in. thick test sample was machined into 24 test coupons and split into two equal lots of 12 pieces with one lot heat-treated to Condition A and the second lot to Condition B. The heat-treated coupons were machined into notched and unnotched tensile specimens and tested

TABLE I-XI

MECHANICAL PROPERTIES OF LARGE CONE FORGING

A. CONDITION A (1800°F/1 HOUR + 1325°F/8 HOURS + 1150°F/TOTAL AGE 18 HOURS)

Specimen	F_{tu} ksi	F_{ty} (0.2%) ksi	Elongation % in 4D	Reduction of Area %
1	180.3	151.5	17.0	31.0
4	178.1	144.6	21.0	28.4
7	139.2	137.9	4.0	10.1
9	178.7	146.9	13.0	18.7
12	178.1	147.7	10.0	14.5
13	175.9	Extensometer slipped	18.7	23.4
16	150.0	145.3	1.6	10.9
19	122.4	121.9	1.6	7.7
21	139.8	Fractured prior to 0.2% Yield	1.6	11.9
24	172.5	149.5	7.8	15.7
25	175.0	146.4	9.4	17.0
28	161.9	148.3	3.1	8.5
29	167.8	147.4	3.1	13.3
Average	161.3	144.1	11.2	16.2

B. CONDITION C (1950°F/1-1/2 HOUR + 1400°F/10 HOURS + 1200°F/TOTAL AGE 20 HOURS)

Specimen	F_{tu} ksi	F_{ty} (0.2%) ksi	Elongation % in 4D	Reduction of Area %
2	185.8	159.8	23.0	35.5
5	189.3	163.0	21.0	29.8
8	181.5	156.3	14.0	21.5
10	185.8	159.7	19.0	27.0
14	190.8	163.1	18.8	31.6
17	140.1	Broke prior to 0.2% yield	4.7	16.9
22	189.1	159.2	17.2	31.6
26	182.8	146.8	15.6	24.5
Average	180.6	158.3	16.7	27.3
Requirements:	180	150	12	--

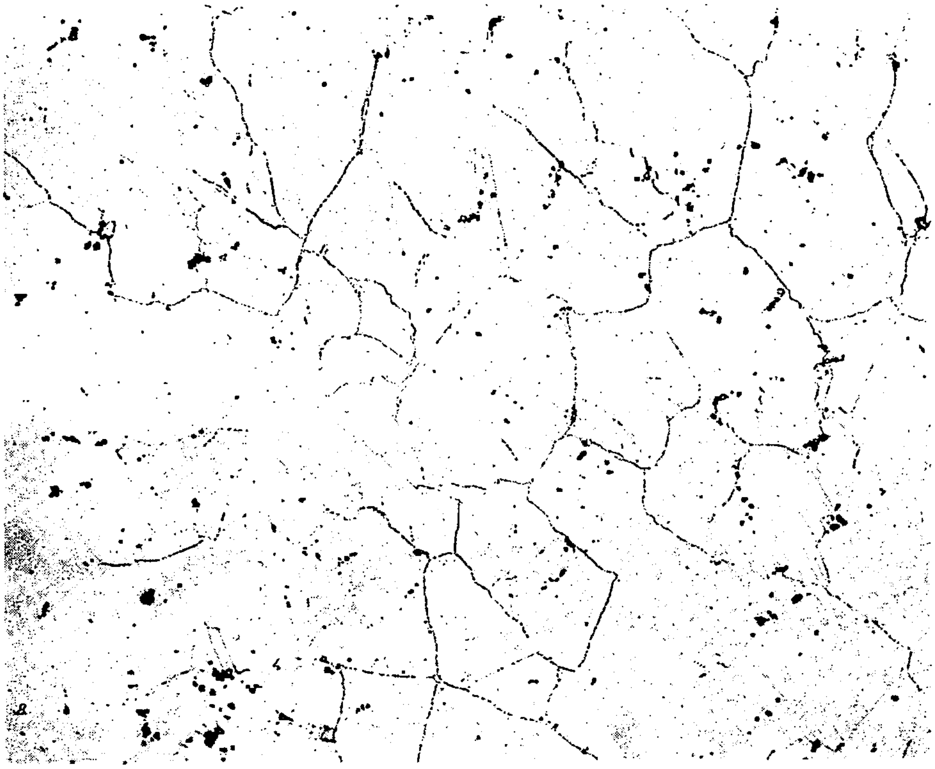

Etchant used: $FeCl_3$ + HCL + H_2O Magnification is 100X.

The grain structure is extremely coarse, being ASTM 1-3 predominantly with several grains larger than ASTM 1. Mechanical properties of this specimen were 122.4 ksi ultimate strength, 121.9 ksi 0.2% offset yield strength, 1.6% elongation and 7.7% reduction of area.

Figure I-7

Microstructure of Large Cone Forging (Condition A)

TABLE I-XII

THE EFFECT OF VARIOUS PRIMARY AGING CYCLES UPON PROPERTIES OF AN OCTAGON HAND FORGING*

1950°F/1 hr A.C. + Primary Aging Cycle Listed Below + Furnace - Cool 100°F/hr to 1200°F/8 hr, A.C.	F_{ty} 0.2% ksi	F_{tu} ksi	Elongation (%)	R.A. (%)	Hardness R_c
1400°F/10 hrs	159.5	184.0	13.0	11.0	42
1400°F/1 hr	156.0	178.5	18.0	24.0	41
1375°F/10 hrs	163.5	186.0	12.0	12.0	42
1350°F/10 hrs	159.5	183.5	12.0	18.0	42
1325°F/8 hrs	161.5	183.5	18.0	23.7	42

CHEMISTRY (%)

C	Mn	Fe	S	Si	Cu	Ni	Cr	Al	Ti	Mo	Cb + Ta
0.04	0.16	18.77	0.007	0.30	0.04	52.88	18.57	0.28	0.86	3.04	5.03

* Data from private communication with Huntington Alloy Products Division, International Nickel Company

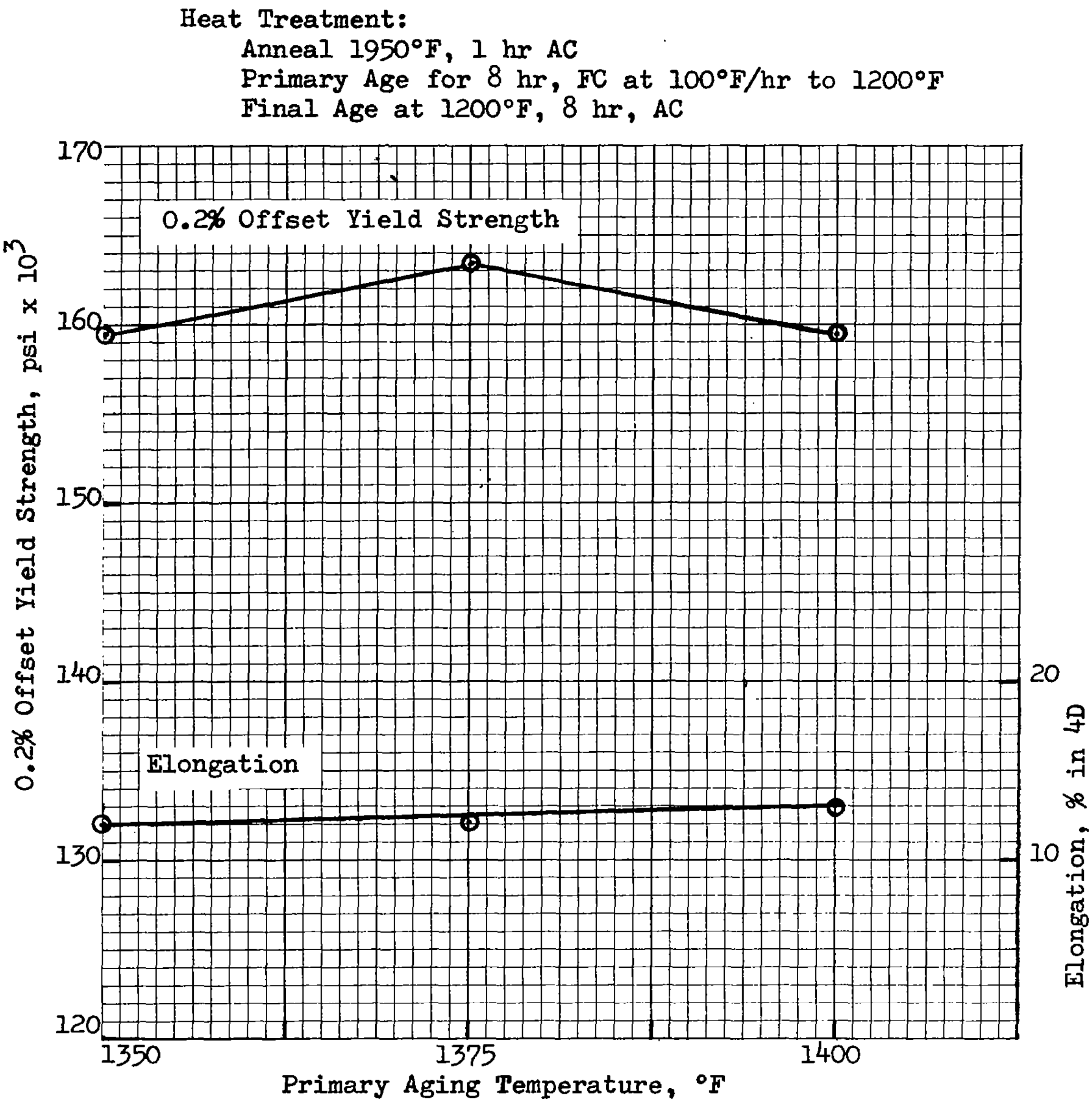

Figure I-8

Variation of Heat-Treated Properties of Octagon Forging with Primary Aging Cycles per ASTM-E 139 for stress-rupture life and elongation at 1350°F with stresses of 75, 80, and 85 ksi.

The stress-rupture results are listed in Table I-XIII and shown in Figure No. I-9. Condition A specimens had superior stress-rupture life and ductility.

The study indicates that Alloy 718 requires a low temperature anneal at 1800°F (and possibly lower) in combination with the 1325°F/1150°F aging cycle to obtain optimum stress-rupture properties. This is considered applicable to welds as well as to parent metal specimens.

Microstructures were studied and it was indicated that grain boundary carbide film in the samples in Condition B most probably contributed to low stress-rupture ductility. The carbide film formed in Inconel 718 samples that were annealed at very high temperature (2200°F) are illustrated in an existing publication.(1)

2. Effect of Heat Treatment Upon the Mechanical Properties of Single-Vacuum-Induction Melted Sheet

Sheet specimens were studied to compare the effects of the Condition A and B treatments (Table I-I) upon the mechanical properties and microstructure of single-vacuum-induction melted Alloy 718.

Type F-1 sheet tensile specimens per Federal Standard 151 were machined longitudinally from the sheets of Alloy 718. Thicknesses of the three sheets were: 0.125-in. (Heat 1) and 0.132-in. (Heats 2 and 3). After machining, specimens were heat-treated per Conditions A and B. The tests were conducted at -320°F to 1350°F in accordance with Federal Standard 151. Microstructures of the single-vacuum-induction melted heats were examined and compared with a later heat produced by the same vendor using the consumable-vacuum-melting (CEVM) practice for upgraded material.

The tensile results are listed in Table I-XIV and shown in Figures No. I-10, No. I-11, and No. I-12. In the -320°F to 1350°F temperature range, the Condition A heat treatment resulted in higher strength, while the Condition B resulted in higher ductility.

The single-vacuum-induction-melted material in Condition A contained globular primary Laves phase segregation and a finer acicular phase believed to be orthorhombic Ni_3Cb (see Figure No. I-13). The material in Condition B also contained Laves phase segregation; however, the finer orthorhombic Ni_3Cb secondary phase was not evident, apparently being solutioned by the 1950°F annealing (see Figure No. I-14). Sheet melted by the same vendor by multiple-vacuum melting using the consumable-vacuum-melting (CEVM) practice in the remelt cycle is illustrated in Figure No. I-15. The CEVM product is relatively

(1) Recent Investigations of the Metallurgy of Inconel Alloy 718, International Nickel Company (undated)

TABLE I-XIII

STRESS RUPTURE OF 0.128-IN. SHEET AT 1350°F

Specimen No.	Specimen Type	Test Stress (ksi)	Time to Failure (hr)	Elongation % in 2 in.	Remarks
Group A Condition A					
1	Smooth, Flat	85	5.5	5.5	Broke in gage mark
2	Smooth, Flat	85	5.5	13.5	Twisted during test
3	Smooth, Flat	80	20.0	18.0	
4	Smooth, Flat	80	21.0	16.0	
5	Smooth, Flat	75	36.4	14.5	
6	Smooth, Flat	75	24.9	16.0	
Group B Condition A					
7	Edge-notched, Flat	85	1.4	Less than 1.0	
8	Edge-notched, Flat	85	2.7	Less than 1.0	
9	Edge-notched, Flat	80	2.3	1.0	
10	Edge-notched, Flat	80	3.6	1.0	
11	Edge-notched, Flat	75	8.1	1.0	
12	Edge-notched, Flat	75	18.1	2.0	
Group C Condition B					
13	Smooth, Flat	85	2.8	1.0	Broke in gage mark
14	Smooth, Flat	85	8.3 (Total)	0.5	Broke in hole, rerun
15	Smooth, Flat	80	7.3 (Total)	1.0	Broke in hole, rerun
16	Smooth, Flat	80	5.6	1.5	
17	Smooth, Flat	75	20.0	2.0	
18	Smooth, Flat	75	14.9	1.0	
Group D Condition B					
19	Edge-notched, Flat	85	0.1	1.0	
20	Edge-notched, Flat	85	0.2	0.5	
21	Edge-notched, Flat	80	0.3	1.0	
22	Edge-notched, Flat	80	0.5	0.5	
23	Edge-notched, Flat	75	1.0	0.5	
24	Edge-notched, Flat	75	0.8	1.0	

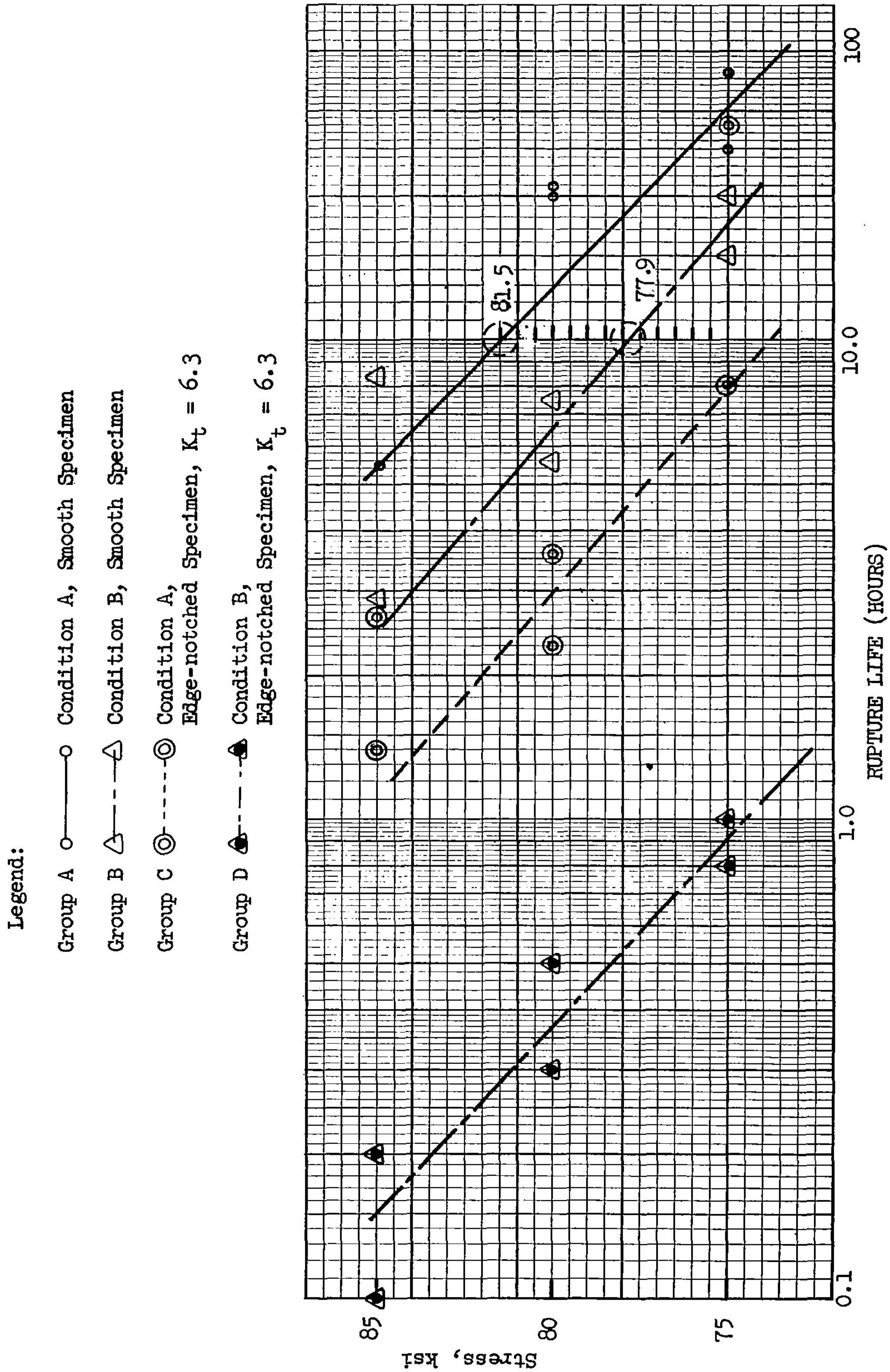

Figure I-9

Stress Vs. Rupture Life of 0.128-in. Sheet, at 1350°F

TABLE I-XIV

MECHANICAL PROPERTIES OF SINGLE VACUUM-INDUCTION MELTED SHEET

A. CONDITION A

Heat No.	Specimen No.	Sheet Thickness (inch)	Test Temp (°F)	F_{tu} (ksi)	F_{ty} 0.2%-Offset (ksi)	Elongation (% in 2 in.)	Hardness at Room Temp R_c
1	24	0.123	-320	252.5	186.0	--	45
2	24	0.134	-320	251.9	188.1	16.0	45
3	24	0.135	-320	249.3	184.0	17.0	45
Average				251.2	186.0	16.5	45
1	23	0.124	RT	195.8	160.2	19.0	45
2	23	0.135	RT	196.5	161.9	18.5	45
3	23	0.133	RT	200.9	165.3	20.5	45
Average				197.7	162.5	19.3	45
1	21	0.124	1200	161.6	136.0	18.5	45
2	21	0.132	1200	153.3	129.2	16.5	45
3	21	0.135	1200	162.1	135.6	16.5	45
Average				159.0	133.6	17.2	45
1	19	0.124	1300	134.3	114.4	11.5	45
2	19	0.132	1300	139.9	121.2	12.0	45
3	19	0.135	1300	142.8	122.1	10.5	45
Average				139.0	119.2	11.3	45
1	20	0.124	1350	134.2	112.1	11.5	45
2	20	0.131	1350	126.3	112.1	9.0	45
3	20	0.135	1350	129.8	110.4	10.5	45
Average				130.1	111.5	10.3	45

TABLE I-XIV (CONT.)

MECHANICAL PROPERTIES OF SINGLE VACUUM-INDUCTION MELTED SHEET

B. CONDITION B

Heat No.	Specimen No.	Sheet Thickness (inch)	Test Temp (°F)	F_{tu} (ksi)	F_{ty} 0.2%-Offset (ksi)	Elongation (% in 2 in.)	Hardness at Room Temp R_C
1	13	0.124	-320	236.9	174.7	30.5	41
1	14	0.124	-320	236.8	176.6	29.5	42
1	15	0.124	-320	236.9	--	29.0	43
Average				236.9	175.7	29.7	42
2	13	0.132	-320	235.9	--	28.5	42
2	14	0.130	-320	237.6	174.5	20.0	43
2	15	0.131	-320	239.3	177.0	27.5	42
Average				237.6	176.3	25.3	42
3	13	0.132	-320	235.9	172.5	22.5	42
3	14	0.135	-320	238.7	176.3	25.0	42
3	15	0.135	-320	239.3	177.7	22.5	43
Average				237.9	175.5	23.3	42
1	10	0.124	RT	179.7	147.1	20.5	41
1	11	0.124	RT	180.0	147.4	21.0	42
1	12	0.124	RT	180.2	147.4	22.0	43
Average				179.9	147.3	21.2	42
2	10	0.131	RT	180.5	149.1	24.5	41
2	11	0.132	RT	179.4	148.3	21.5	43
2	12	0.132	RT	180.1	150.1	22.0	41
Average				180.0	149.2	22.7	42
3	10	0.134	RT	183.9	151.7	23.5	41
3	11	0.135	RT	183.0	149.7	19.5	42
3	12	0.135	RT	184.1	151.7	21.5	42
Average				183.7	151.0	21.5	42
1	1	0.125	1200	140.1	117.8	17.0	42
1	2	0.124	1200	142.4	120.0	19.0	42
1	3	0.123	1200	142.2	120.8	18.5	41
Average				141.6	119.5	18.2	42

TABLE I-XIV (CONT.)

MECHANICAL PROPERTIES OF SINGLE VACUUM-INDUCTION MELTED SHEET

B. CONDITION B

Heat No.	Specimen No.	Sheet Thickness (inch)	Test Temp (°F)	F_{tu} (ksi)	F_{ty} 0.2%-Offset (ksi)	Elongation (% in 2 in.)	Hardness at Room Temp R_c
2	1	0.130	1200	141.4	120.8	17.5	41
2	2	0.132	1200	142.9	118.3	18.5	41
2	3	0.130	1200	141.3	119.7	17.5	41
Average				141.9	119.6	17.8	41
3	1	0.135	1200	143.7	121.7	15.5	42
3	2	0.133	1200	146.0	118.7	17.5	42
3	3	0.132	1200	145.6	123.3	18.0	41
Average				145.1	121.2	17.0	42
1	4	0.124	1300	133.0	113.0	11.5	41
1	5	0.125	1300	131.6	105.0	15.0	42
1	6	0.124	1300	131.4	108.4	11.0	42
Average				132.0	108.8	12.5	42
2	4	0.132	1300	133.6	105.7	16.5	41
2	5	0.132	1300	137.8	--	17.5	42
2	6	0.131	1300	136.3	115.5	16.0	43
Average				135.9	110.6	16.7	42
3	4	0.134	1300	137.8	112.8	14.0	42
3	5	0.134	1300	138.4	112.4	13.0	41
3	6	0.135	1300	134.9	111.5	8.5	41
Average				137.0	112.2	11.8	41
1	7	0.123	1350	128.8	107.7	10.5	42
1	8	0.124	1350	127.3	101.6	11.0	41
1	9	0.124	1350	126.0	92.4	9.5	41
Average				127.4	100.6	10.3	41
2	7	0.132	1350	126.6	103.5	13.0	41
2	8	0.132	1350	126.7	--	14.0	42
2	9	0.132	1350	126.9	103.0	11.5	41
Average				126.7	103.3	12.8	41
3	7	0.134	1350	129.5	106.4	8.0	41
3	8	0.135	1350	132.3	110.1	9.0	42
3	9	0.134	1350	130.0	106.9	11.0	42
Average				130.6	107.8	9.3	42

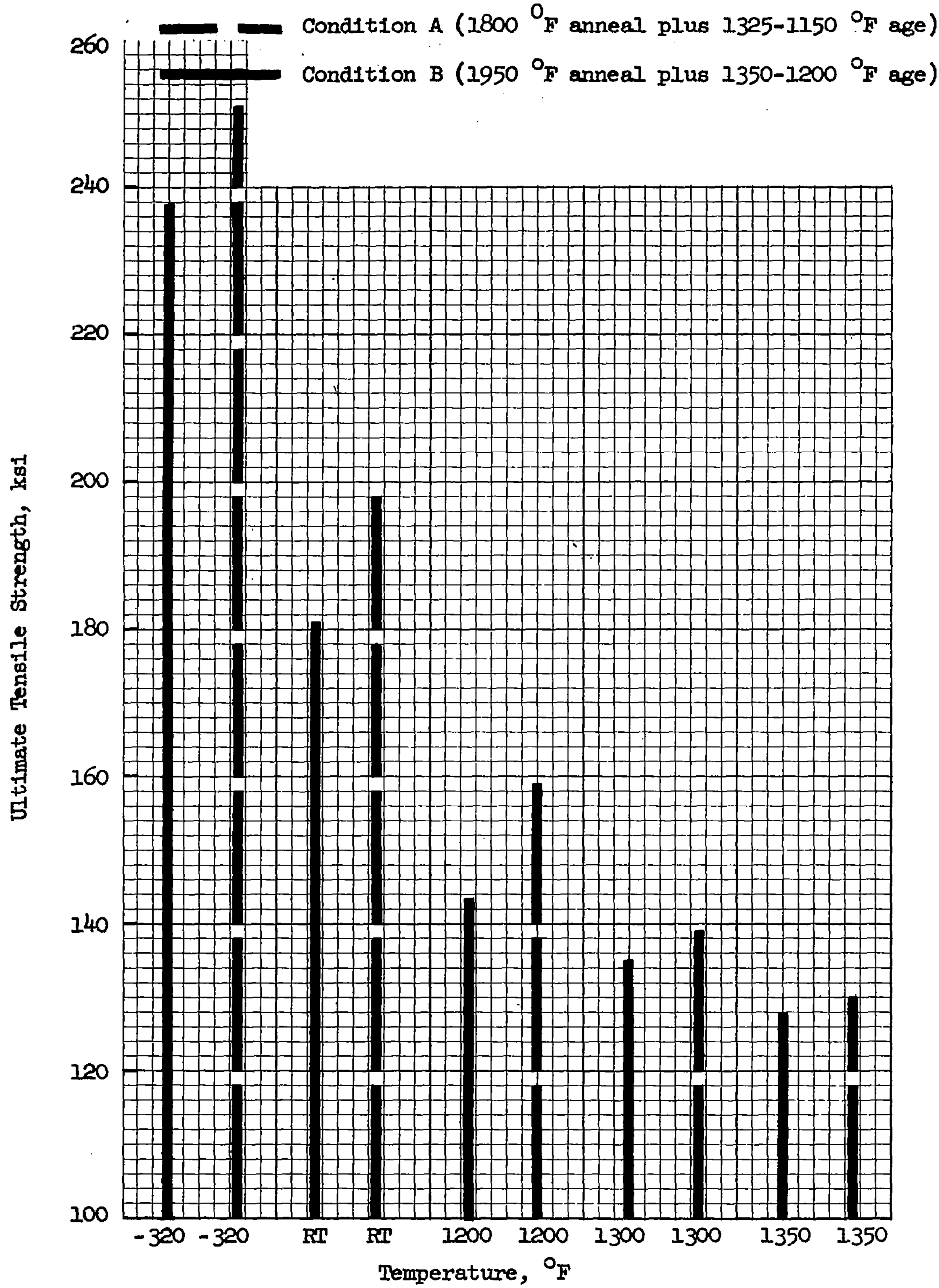

Figure I-10

Ultimate Tensile Strength of Sheet in Heat-Treat Conditions A and B in the -320°F to 1350°F Temperature Range

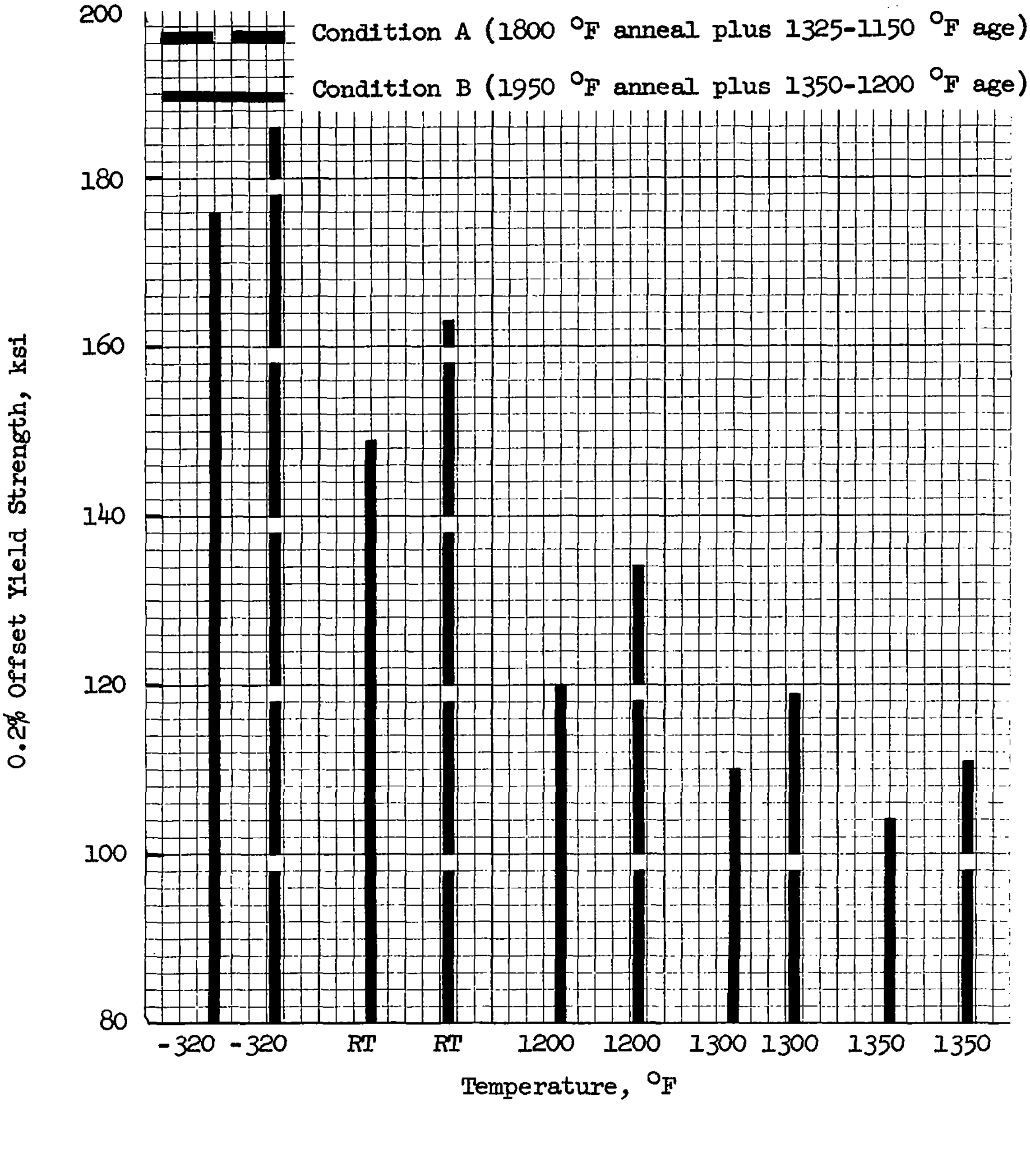

Figure I-11

The 0.2% Off-Set Yield Strength of Sheet in Heat-Treatment Conditions A and B in -320°F to 1350°F Temperature Range

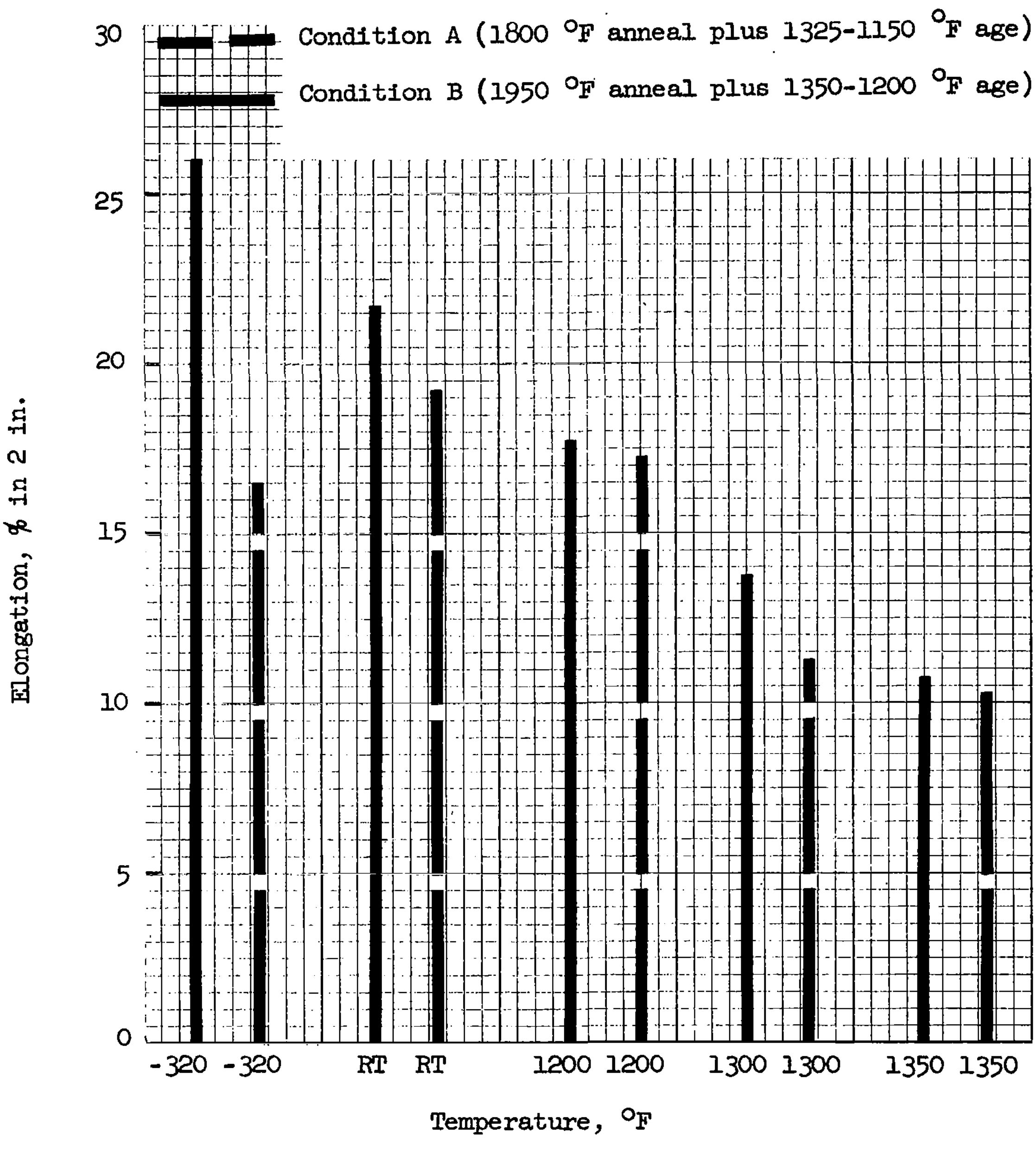

Figure I-12

Elongation of Sheet in Heat-Treat Conditions A and B in the -320°F to 1350°F Temperature Range

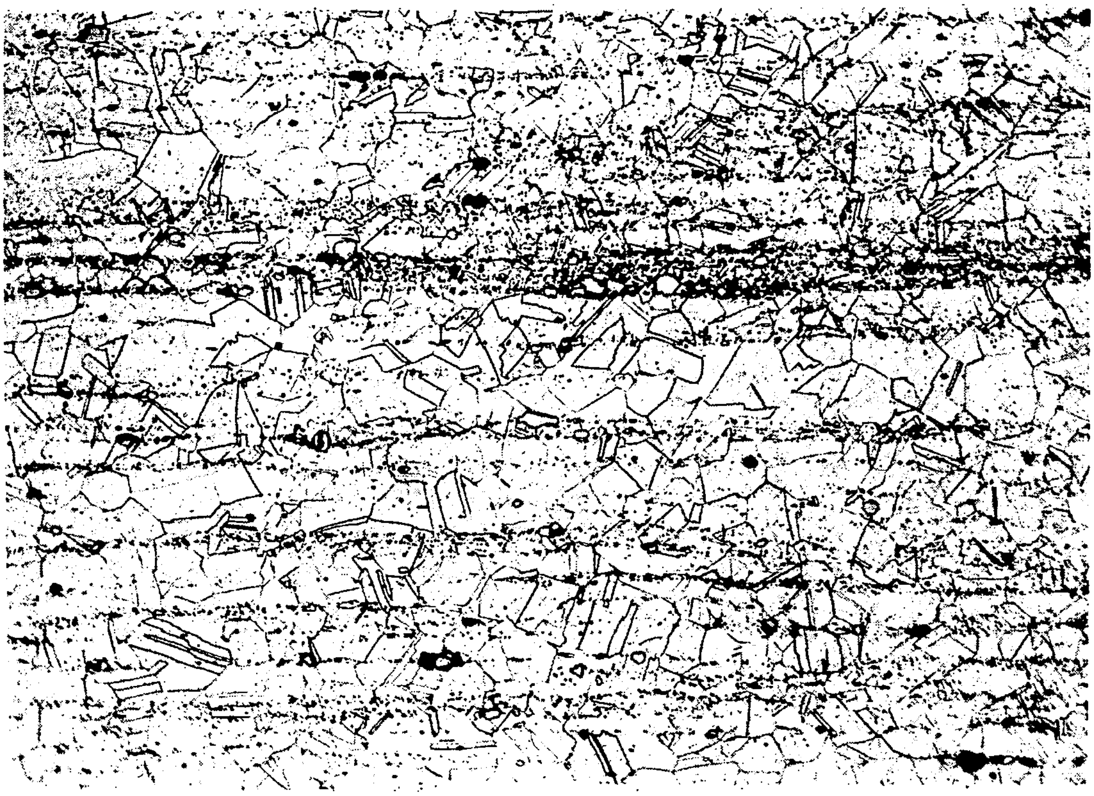

Magnification: 100X

Etchant: 50 HCL + 30 H_2O + 20 HF + 10 HNO_3

Figure I-13

Microstructure of Single Vacuum Induction Melted Sheet (Condition A)

Magnification: 100X

Etchant: 50 HCL + 30 H_2O + 20 HF + 10 HNO_3

Figure I-14

Microstructure of Single Vacuum Induction Melted Sheet (Condition B)

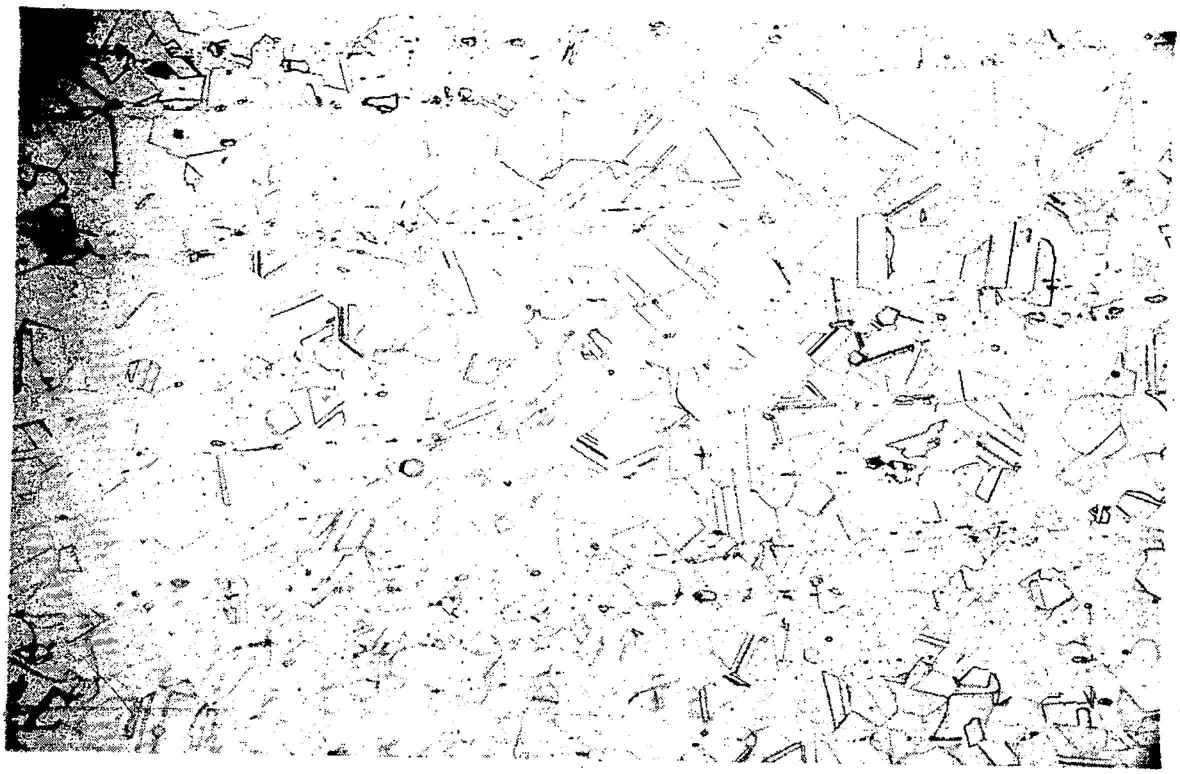

Magnification: 250X

Etchant: 50 HCL + 30 H_2O + 20 HF + 10 HNO_3

Figure I-15

Microstructure of Double Vacuum Induction Melted Sheet (Mill Annealed) free from Laves phase segregation. Alloy 718 that is free from segregation generally possesses better aging response characteristics. Therefore, double vacuum melting using the CEVM process in the remelt cycle is recommended for Alloy 718.

3. Ambient and Cryogenic Mechanical Properties of Alloy 718 Sheet

Mechanical properties of Alloy 718 sheet in the annealed and heat-treated condition were studied at ambient temperatures, -320°F, and -423°F to obtain design data.

Tensile specimens were machined from a 0.125-in.-thick sheet from both longitudinal and transverse directions. Both standard and notched sheet specimens were prepared. Notched specimens were prepared to give a notch acuity factory K_t = 6.0. Several specimens were tested in the 1800°F/1 hr annealed condition. Other specimens were treated to Condition A. Specimens were tested at room temperature, -320°F, and -423°F.

The tensile results are listed in Table I-XV. The Alloy 718 sheet material retained excellent ductility at -320°F and -423°F in both the longitudinal and transverse directions.

4. Age-Hardening Response and Elevated Temperature Tensile Properties of Thin Gage Sheet

The age-hardening response of 8-mil-thick Alloy 718 sheet used in hot gas line bellows applications was studied.

Tensile specimens were prepared from 8-mil sheet and heat-treated as follows:

Group I was annealed at 1800°F for 10 min., aged 1325°F for 16 hr per the original heat treatment developed for Alloy 718 by the alloy developer.

Group II was annealed at 1800°F for 10 min. then aged per standard Condition A. Specimens were tensile tested at room, 1200°F, 1300°F, and 1400°F in accordance with Federal Standard 151.

The results, listed in Table I-XVI, illustrated the following points:

a. Aging as in Condition A conferred higher strength in the thin gage Alloy 718.

b. Aging as in Condition A also resulted in slightly higher elongation at elevated temperatures.

TABLE I-XV

MECHANICAL PROPERTIES OF 0.125-IN. SHEET AT AMBIENT AND CRYOGENIC TEMPERATURES

A. ANNEALED (1800°F/1 HR) SHEET TESTED AT 75°F

Specimen Number	Specimen Orientation	F_{tu} ksi	F_{ty} (0.02%) ksi	F_{ty} (0.2%) ksi	Elongation (% in 2 in.)	Hardness R_c
L-13	Long.	136.1	76.2	89.7	37.0	25
L-14	Long.	131.1	54.1	73.8	42.0	22
L-15	Long.	136.1	76.4	89.0	38.0	26
Average		134.4	68.9	84.2	39.0	24
T-13	Trans.	133.3	68.7	84.7	40.0	24
T-14	Trans.	132.9	66.9	87.1	39.0	25
T-15	Trans.	131.7	67.5	84.7	38.0	25
Average		132.6	67.7	85.5	39.0	25

B. ANNEALED (1800°F/1 HR) SHEET TESTED AT -320°F

Specimen Number	Specimen Orientation	F_{tu} ksi	F_{ty} (0.02%) ksi	F_{ty} (0.2%) ksi	Elongation (% in 2 in.)	Hardness R_c
L-16	Long.	185.6	99.2	114.8	45.5	25
L-17	Long.	189.7	96.1	115.8	48.0	26
L-18	Long.	186.9	81.1	115.2	43.0	26
Average		187.4	92.1	115.3	45.5	26
T-16	Trans.	183.7	96.7	111.8	47.5	25.5
T-17	Trans.	177.4	100.0	112.9	52.0	25
T-18	Trans.	179.7	--	--	44.0	25
Average		180.2	98.4	112.4	47.8	25

TABLE I-XV (CONT.)

C. HEAT TREATED SHEET (CONDITION A) TESTED AT 75°F

Specimen Number	Specimen Orientation	F_{tu} ksi	(0.02%) ksi	(0.2%) ksi	Elongation (% in 2 in.)	Hardness R_c
L-1	Long.	190.0	109.7	150.0	22.0	43.5
L-2	Long.	191.9	132.2	155.6	21.0	43.0
L-3	Long.	188.7	127.6	150.2	22.0	43.0
Average		190.2	123.2	151.9	21.7	43.0
T-1	Trans.	189.1	117.4	150.4	22.0	43.0
T-2	Trans.	188.6	121.9	150.2	21.0	43.5
T-3	Trans.	187.4	132.8	151.0	22.0	43.0
Average		188.4	124.0	150.5	21.7	43.0

Specimen Number	Specimen Orientation	Notch Strength ksi	Notch/Ultimate Ratio (K_t=6)	Notch/Yield Ratio
NL-1	Long.	201.0		
NL-2	Long.	208.2		
NL-3	Long.	207.9		
Average		205.7	1.08	1.35
NT-1	Trans.	202.9		
NT-2	Trans.	195.9		
NT-3	Trans.	196.2		
Average		198.3	1.05	1.32

TABLE I-XV (CONT.)

D. HEAT TREATED SHEET (CONDITION A) TESTED AT -320°F

Specimen Number	Specimen Orientation	F_{tu} ksi	F_{ty} (0.02%) ksi	F_{ty} (0.2%) ksi	Elongation (% in 2 in.)	Hardness R_c
L-4	Long.	245.7	151.8	174.8	27.0	43.0
L-5	Long.	245.6	150.6	175.6	30.0	42.5
L-6	Long.	249.2	158.0	184.0	28.0	44.0
Average		246.8	153.5	178.1	28.3	43.0
T-4	Trans.	242.8	152.7	176.2	28.0	43.0
T-5	Trans.	247.6	158.1	181.4	26.0	43.5
T-6	Trans.	243.9	154.3	170.0	26.0	43.0
Average		244.8	155.0	175.9	26.7	43.0

Specimen Number	Specimen Orientation	Notch Strength ksi	Notch/Ultimate Ratio (K_t=6)	Notch/Yield Ratio
NL-4	Long.	239.5		
NL-5	Long.	--		
NL-6	Long.	237.7		
Average		238.6	0.97	1.34
NT-4	Trans.	230.4		
NT-5	Trans.	236.6		
NT-6	Trans.	236.6		
Average		234.5	0.96	1.33

TABLE I-XV (CONT.)

E. HEAT TREATED SHEET (CONDITION A) TESTED AT -423°F

Designation	Orientation	F_{tu} ksi	F_{ty} (0.02%) ksi	F_{ty} (0.2%) ksi	Elongation (% in 2 in.)
CL 1	Long.	253.0	168.0	185.7	18.5
CL 2	Long.	247.0	No Curve	No Curve	18.5
CL 3	Long.	249.0	164.0	187.6	21.5
Average		249.7	166.0	186.7	19.5
CT 1	Trans.	250.0	180.0	200.0	16.5
CT 2	Trans.	248.1	170.0	184.5	19.5
CT 3	Trans.	252.0	171.0	187.5	17.5
Average		250.0	173.7	190.7	17.8

Specimen Number	Specimen Orientation	Notch Strength ksi	Notch/Ultimate Ratio	Notch/Yield Ratio
NL 7	Long.	235.0		
NL 8	Long.	247.0		
NL 9	Long.	239.0		
Average		243.7	0.97	1.3
NT 7	Trans.	229.0		
NT 8	Trans.	235.0		
Average		232.0	0.93	1.2

TABLE I-XVI

THE EFFECT OF AGING TREATMENT UPON THE MECHANICAL PROPERTIES OF THIN GAGE SHEET

(Thickness: 8 mils)

A. GROUP I: 1800°F/10 min. re-anneal plus 1325°F/16 hr age

Test Temp (°F)	F_{tu} ksi	(0.2%) ksi	Elongation % in 2 in.
R.T.	176.7	144.6	20.4
R.T.	178.6	146.0	22.6
1200	145.1	123.0	12.5
1200	148.6	123.8	11.0
1300	142.9	121.9	6.0
1300	150.0	125.2	7.5
1400	114.8	102.6	3.0
1400	103.8	93.1	3.0

B. GROUP II*: 1800°F/10 min. re-anneal plus age as in Condition A

R.T.	186.0	159.3	17.7
R.T.	186.5	149.3	18.0
1200	149.5	130.0	14.5
1200	148.6	130.2	16.6
1400	104.0	97.6	4.0

*One specimen was tested at 1300°F; results are unreliable and not included in the report. A second specimen tested at 1400°F failed through the grip hole.

c. Elongation decreased with increasing temperature in the temperature range tested.

Data in these and other tests with Alloy 718 sheet have shown an apparent lowering of elongation with a decrease in thickness.

5. The Effect of Heat Treatment Variables Upon Parent Metal and Weldment Properties of Sheet Material

The effects of aging sequence, weld filler wire, annealing temperature, and test temperature upon the tensile properties of 1/8-in. sheet was investigated for the M-1 turbine manifold application.

Welded panels were prepared for four conditions: age, then weld; weld, then age; weld, anneal, and age; age, weld, and age. These were processed as follows:

a. Group A Specimens

Mill anneal. Age as in Condition A. TIG weld one lot with Alloy 718 and a second lot with Rene' 41 filler wire. Flush grind the weld beads.

b. Group B Specimens

Mill anneal. TIG weld one lot with Alloy 718 and a second lot with Rene' 41 filler wire. Flush grind the weld beads. Age as in Condition A.

c. Group C Specimens

Mill anneal. TIG weld one lot with Alloy 718 and a second lot with Rene' 41 weld wire. Flush grind the weld beads. Heat treat to Condition A.

d. Group D Specimens

Mill anneal. Age as in Condition A alloy. TIG weld one lot with Alloy 718 and a second lot with Rene' 41 weld wire. Flush grind the weld beads. Age as in Condition A.

Standard sheet tensile specimens (unwelded) were annealed at various temperatures and aged as to Condition A, then tested at 1300°F after a 15-min hold at temperature. A second group of sheet tensile specimens, initially in the mill-annealed condition, were aged as to Condition A and tested at temperatures from -320°F to 1400°F.

The test results, listed in Table I-XVII, illustrated the following points:

TABLE I-XVII

MECHANICAL PROPERTIES OF TUNGSTEN-INERT-GAS WELDS
AND PARENT METAL SHEET

A. ROOM TEMPERATURE PROPERTIES OF WELDS

Group	Process Schedule (1)	Weld Wire	F_{tu}	F_{ty} .2%	Elongation % in 2 in.	Weld-Joint Efficiency (2)
Parent Metal	Heat Treat to Condition A	NA	190.0	150.0	22.0	NA
			191.9	155.6	21.0	
			188.7	150.2	22.0	
		Average	190.2	151.9	21.7	
A	Age as in Condition A TIG Weld	Alloy 718	106.2	59.2	8.5	
			111.8	63.8	8.0	
			114.5	64.5	9.0	
		Average	110.8	62.5	8.5	58
		Rene' 41	126.9	79.4	7.0	
			116.4	76.5	6.5	
			124.9	79.5	6.5	
		Average	122.7	78.5	6.7	64
B	TIG Weld Age as in Condition A	Alloy 718	184.7	154.9	4.0	
			177.4	160.6	2.5	
			188.8	160.2	5.0	
			190.8	164.8	7.5	
			189.0	148.5	9.0	
		Average	186.1	157.8	5.6	98
		Rene' 41	180.6	149.9	3.0	
			184.0	151.5	3.5	
			185.8	153.1	3.0	
			186.7	155.6	3.0	
			184.1	155.6	4.0	
			187.5	155.0	4.0	
		Average	184.8	153.5	3.4	97

TABLE I-XVII (CONT.)

A. ROOM TEMPERATURE PROPERTIES OF WELDS (CONT.)

Group	Process Schedule (1)	Weld Wire	F_{tu}	F_{ty} .2%	Elongation % in 2 in.	Weld-Joint Efficiency (2)
C	TIG Weld	Alloy 718	183.9	150.5	9.0	
	Heat Treat to		182.8	151.2	14.0	
	Condition A		184.2	149.7	12.0	
			181.0	148.6	12.0	
			181.6	148.4	11.5	
		Average	182.7	149.7	11.7	96
		Rene' 41	178.8	142.9	7.5	
			173.3	140.1	4.5	
			176.9	139.8	6.5	
			177.3	141.7	6.0	
			187.4	140.8	6.5	
			174.3	143.1	4.5	
		Average	176.5	141.4	5.9	93
D	Age as in	Alloy 718	187.3	152.8	10.0	
	Condition A		186.9	151.6	12.0	
	TIG Weld		182.7	148.7	8.5	
	Age as in		182.9	142.8	13.0	
	Condition A		172.4	141.0	4.0	
		Average	182.4	147.4	9.5	96
		Rene' 41	161.4	135.0	2.0	
			159.1	136.0	2.0	
			166.0	145.8	2.0	
			155.7	146.0	1.0	
			166.3	144.7	2.0	
			160.1	140.9	4.0	
		Average	161.4	141.4	2.2	85

TABLE I-XVII (CONT.)

B. THE 1300°F MECHANICAL PROPERTIES OF HEAT TREATED SHEET WITH VARIOUS ANNEALING TEMPERATURES, AGED AS IN CONDITION A (3)

Prior Anneal °F	F_{tu}	F_{ty} .2%	Elongation % in 2 in.	Hardness Before Test Rc
Mill Anneal	167.5	148.3	7.0	46
	158.4	144.9	OGM	
	166.8	148.6	5.0	
Average	164.2	147.3	6.0	
1800	148.0	124.1	12.0	43
	148.3	125.0	13.0	42
	147.0	124.0	12.0	44
Average	147.8	124.4	12.3	
1900	144.4	119.5	14.0	
	143.2	121.1	15.0	42
	142.1	118.8	15.0	
Average	143.2	119.8	14.7	
2000	136.7	113.0	20.0	40
	137.3	114.2	20.0	
	132.9	110.2	18.0	38
Average	135.6	112.5	19.3	
2100	125.6	106.4	16.0	36
	124.3	102.4	20.0	
	123.8	106.0	14.0	
Average	124.6	104.9	16.7	

TABLE I-XVII (CONT.)

C. MECHANICAL PROPERTIES OF HEAT-TREATED SHEET FROM -320°F TO 1400°F (MILL ANNEALED, AGED AS IN CONDITION A) (3)

Test Temp °F	F_{tu} ksi	F_{ty} (.2%)	Elongation % in 2 in.	Hardness Before Test Rc
-320	254.0	No Curve	25.0	47.0
	264.0	210.0	22.0	47.0
	262.2	208.9	20.0	46.0
Average	260.1	209.5	22.3	
+75	204.3	183.1	15.0	46.0
	203.8	182.2	15.0	46.0
	203.1	182.0	15.0	46.0
Average	203.7	182.4	15.0	
800	181.0	166.1	16.0	
	180.6	164.3	15.0	
	174.4	161.4	13.0	
Average	178.7	163.9	14.7	
1000	171.2	No Curve	12.0	
	173.2	159.0	14.0	
	171.5	159.0	13.0	
Average	172.0	159.0	13.0	
1200	170.1	158.8	9.0	
	169.3	153.2	13.0	
	169.2	151.4	9.0	
Average	169.5	154.5	10.3	
1300	167.5	148.3	7.0	
	158.4	144.9	OGM	46.0
	166.8	148.6	5.0	
Average	164.2	147.3	6.0	
1350	155.0	141.2	2.0	46.0
	156.9	145.5	5.0	
	154.3	147.1	4.0	

TABLE I-XVII (CONT.)

C. MECHANICAL PROPERTIES OF HEAT-TREATED SHEET FROM -320°F TO 1400°F (MILL ANNEALED, AGED AS IN CONDITION A) (3) (CONT.)

Test Temp °F	F_{tu} ksi	F_{ty} (.2%)	Elongation % in 2 in.	Hardness Before Test Rc
Average	155.4	144.6	3.7	
1400	141.3	126.4	2.0	
	143.3	130.4	2.0	
	144.2	131.4	OGM	
Average	142.9	129.4	2.0	

NOTES: (1) All sheet was initially in the mill annealed condition. All welds were ground flush.
(2) Joint efficiency is defined as the ratio of ultimate tensile strength of the weldment to the tensile strength of the parent metal.
(3) Tested by Method 211, Fed. Std. 151; 15-min soak at test temperature.
(4) Failed outside gage marks.

The best combination of ambient temperature strength and ductility using either Alloy 718 or Rene' 41 weld wire was obtained by solution annealing and aging after the welding cycle. Aging alone produced equivalent strength but the ductility was lower.

Alloy 718 weld wire yielded slightly higher strength and ductility than Rene' 41 with the same heat treatment. Note that the weld ductility is measured over a 2-in. gage length, which results in a low value when major deformation occurs in the weld.

Parent metal Alloy 718 in the heat-treated condition is not overaged by re-aging after heat treating and welding.

Heat-treated Alloy 718 retains a significant proportion of room temperature strength in short time tests at 1350°F.

The short-time 1300°F tensile strength of heat-treated Alloy 718 decreases with increase of solution annealing temperature.

An interesting observation is that the ambient and -320°F tensile properties for Alloy 718 aged directly from the mill anneal are higher than those for Alloy 718 which has been re-annealed and aged. This is because the mill anneal was lower than the 1800°F re-anneal and residual warm work contributed to the strength of material aged directly from the mill anneal. The exact mill anneal temperature is not known.

A second observation is the anomaly of the increase of 1300°F ductility with increase of annealing temperature prior to aging (Table I-XVII). The increase of ductility is not in agreement with vendor data which indicated a decrease of ductility in the 1200°F to 1400°F range with annealing temperatures above 1800°F. Testing of additional heats is required to clarify this point because the operational temperature range of Alloy 718 is within the low ductility range.

6. Mechanical Properties of Cold-Rolled and Mill-Annealed Sheet

The effect of various aging treatments upon the properties of cold-rolled and mill-annealed sheet was studied in cooperation with the alloy developer.

Standard flat F-1 tensile specimens per Federal Standard 151 were machined from the cold-rolled and mill-annealed sheet. These specimens were annealed at 1950°F/1 hr, primary aged using various cycles (1325°F/1 hr, 1350°F/8 hr, 1375°F/8 hr, and 1400°F/8 to 10 hr), furnace-cooled to the final aging temperature at either 1150°F or 1200°F, and aged during cooling or at the aging temperature for 8 hrs, and air-cooled.

Data for the cold-rolled and mill-annealed sheet are listed in Table I-XVIII and shown in Figure No. I-16.

TABLE I XVIII

ROOM TEMPERATURE MECHANICAL PROPERTIES OF SHEET ANNEALED AT 1950 F/1 HR USING VARIOUS PRIMARY AGING CYCLES*

	Hardener Content (%)				Aged 1325°F 18 Hr FC at 20°/Hr to 1150A				Aged 1350°F/8 Hr FC at 100°/Hr to 1200°F/8 Hr				Aged 1375°F/8 Hr FC at 100°/Hr to 1200°F/8 Hr				Aged 1400°F/10 Hr FC at 100°/Hr to 1200°F/8 Hr			
Gage (in.)	Al	Tl	Cs+ TA	B	.2% Y.S. KSI	Tensile Str. KSI	% Elong	Hard- ness	.2% Y.S. KSI	Tensile Str. KSI	% Elong	Hard- ness	.2% Y.S. KSI	Tensile Str. KSI	% Elong	Hard- ness	.2% Y.S. KSI	Tensile Str. KSI	% Elong	Hard- ness
								15N				15N				15N				15N
.016	.36	.99	5.57	.002	167.5	193.0	14.0	83	175.0	203.0	17.0	84	167.0	200.0	15.0	83	151.0	185.0	15.0	83
.021	.49	.94	5.25	.0036	151.0	178.0	18.0	82	158.0	190.0	20.0	83	153.0	188.5	18.0	83	147.0	184.0	16.0	81
								30N				30N				30N				30N
.025	.39	.98	5.08	.0027	158.5	186.0	18.0	62	162.0	198.0	17.0	63	159.0	191.0	19.0	64	147.0	184.5	15.0	63
.031	.41	.94	4.88	.0026	160.0	185.5	21.0	63	160.0	191.0	20.0	64	150.0	185.0	21.0	64	146.0	182.0	19.0	62
.031	.49	.92	5.03	.0034	162.0	188.0	20.0	63	160.0	189.0	20.0	64	157.0	190.0	19.0	65	154.0	186.5	17.0	62
								RC				RC				RC				RC
.062	.43	.82	4.95	.0032	157.0	182.0	21.0	41	159.0	186.0	22.5	44	157.0	189.5	21.0	43	150.0	185.5	20.0	40
.062	.53	.85	4.93	.0025	170.0	199.0	17.0	44	165.5	198.0	19.0	44	159.5	199.0	19.0	44	153.0	191.0	20.0	41
.062	.43	.86	5.09	.0024	161.0	184.5	22.0	41	159.0	187.0	22.0	43	154.0	181.5	20.0	43	153.0	188.5	20.0	41
.093	.41	.90	5.16	.0027	170.5	199.0	18.0	44	166.0	196.0	20.0	45	159.0	193.5	20.0	43	150.0	187.0	18.0	42
.093	.39	.87	5.04	.0027	160.0	185.5	21.0	43	163.0	190.0	23.0	44	160.0	192.0	22.0	44	156.0	190.5	19.0	41
.100	.34	.82	4.81	.0030	152.0	180.0	25.0	42	152.5	183.5	24.5	43	150.0	187.0	24.0	42	148.0	187.0	20.0	41
.100	.50	.78	4.94	.0028	157.5	185.5	20.0	42	153.0	185.0	23.0	42	145.0	182.0	21.0	41	138.5	177.5	21.0	39
.109	.39	.98	5.08	.0027	164.5	189.0	20.0	43	166.0	192.0	21.0	44	162.5	193.0	21.0	43	157.5	191.5	21.0	42
.109	.34	.83	4.83	.0029	158.0	184.0	20.0	42	157.5	186.5	23.0	43	147.5	182.0	23.5	42	143.0	180.0	21.0	41
.172	.69	1.01	5.43	.0038	151.0	180.0	22.0	42	160.0	185.0	21.0	44	165.0	191.0	20.0	45	165.0	196.0	18.0	44

*Data from private communication with Huntington Alloy Products Division, International Nickel Company.

	Al	Ti	Cb + Ta
Low Hardener	0.50	0.78	4.94
High Hardener	0.69	1.01	5.43

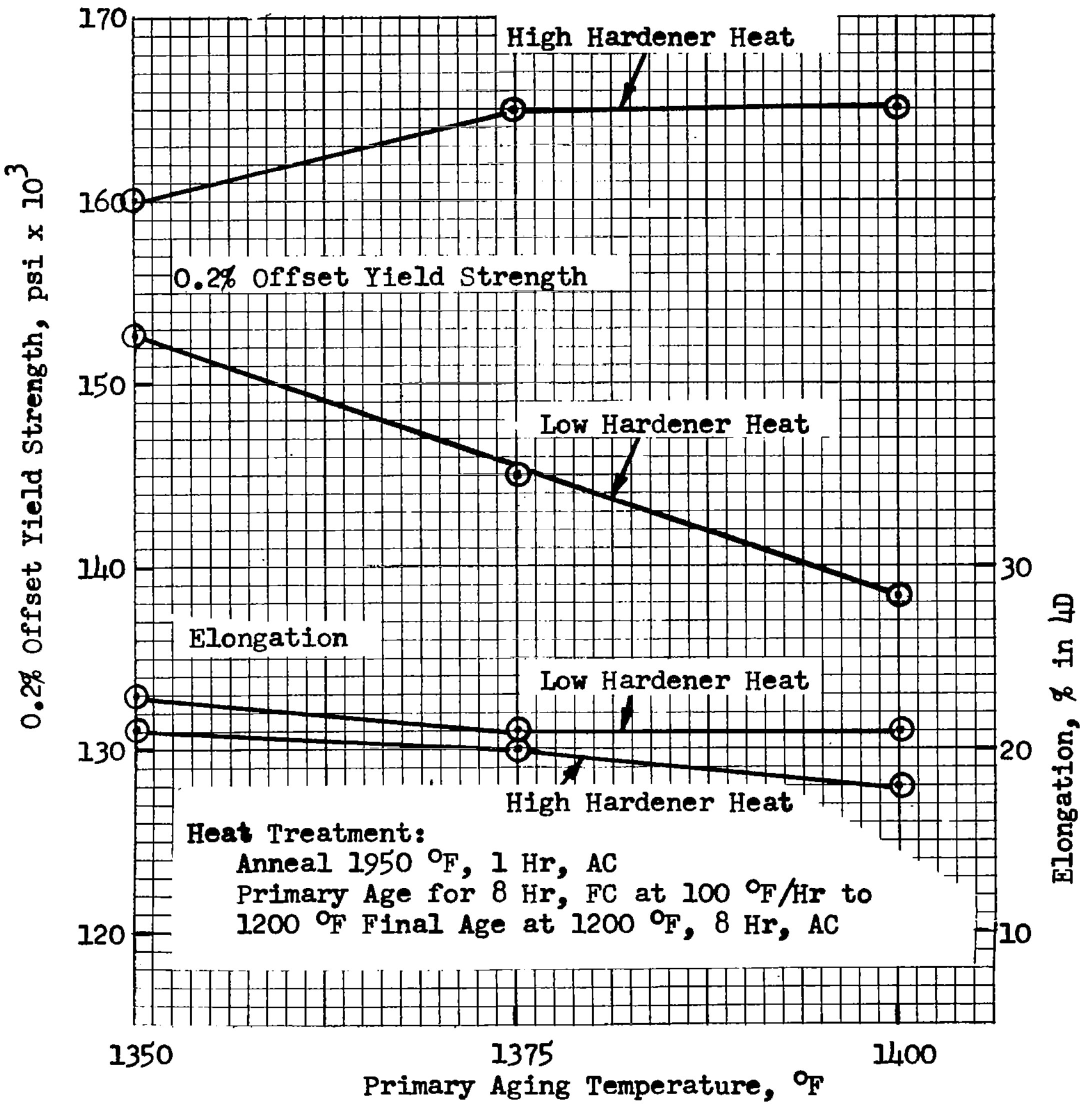

Figure I-16

Variation of Heat-Treated Properties of Sheet with Primary Aging Cycles

The treatments using the 1375°F and 1400°F primary aging cycles conferred the highest strength to the high hardener heats while the 1350°F primary age cycle conferred the highest strength to the low hardener heats. The low hardener heats also had better ductility.

Numerous heat-treatments now exist for Alloy 718. For example, optimum stress rupture properties are obtained with the 1750°F/1 hr + 1325°F/8 hr furnace cool to 1150°F treatment; however, other factors such as transverse ductility in massive sections and cold formability in thin sections have resulted in development of a heat-treatment utilizing a higher anneal at 1950°F. The problem is further complicated by the different chemistries adopted by several of the alloy producers, viz., hardener content levels. For example, one of the major sheet producers has studied the effects of aluminum and carbon upon Alloy 718 and found it desirable to keep these elements at low levels in tensile limited applications. The aluminum range recommended is 0.20% to 0.60%, the carbon is 0.08% maximum, and columbium is 4.75% to 5.25 or 5.50%. In contrast, a forging producer recommends a higher hardener content level. With the increase of hardener content, the aging temperature must be increased to derive maximum age-hardening response; however, high aging temperatures are not compatible with low hardener content heats because they may cause over-aging. From a user's standpoint, engine components utilize both low-hardener content sheet and high-hardener content forging in integrally welded assemblies, thus requiring the use of a compromise heat-treatment. Because the greatest concern is to provide adequate properties in the forgings without overaging the sheet, the Condition B treatment has been adopted for tensile-limited applications. This heat-treatment is acceptable for low-hardener heats; it is adequate but not optimum for high-hardener content heats.

E. PLATE

1. Thermal Treatment Effects Upon Warm-Worked Low-Aged Strength Response Plate

Alloy 718 plate (0.50-in. thick) was procured from two mill sources, "A" and "B", for the thrust chamber jacket.

Mechanical property results obtained in receiving inspection tests made by the material supplier are listed in Table I-XIX, and indicated high yield strengths (155.8 to 177.0 ksi) were obtained in Condition A. Mechanical property results obtained in parallel tests by Aerojet-General are listed in Table I-XX; the material properties exceeded material procurement specification minimums for Condition A, but properties in Condition B were marginal. However, subsequent tensile tests conducted by the fabricator of the thrust chamber jacket indicated that the Alloy 718 plate (0.50-in.) did not conform to the minimum requirements of 180 ksi ultimate strength, 150 ksi 0.2% offset yield strength, and 12% elongation. The low mechanical properties reported by the fabricator for plate in Heat Treatment Condition A are listed in Table I-XXI. The mill-annealed (1800°F/1 hr) plate had been stress-relieved five times at 1750°F and aged as in Condition A. The repeated stress-reliefs were applied to

TABLE I-XIX

MECHANICAL PROPERTIES OF ALLOY 718 PLATE FROM MILL SOURCE "A"
MATERIAL SUPPLIER RECEIVING INSPECTION

(Mill-Annealed and Aged per AGC Condition A by the Vendor)

	F_{tu} ksi*	F_{ty} (0.2%) ksi*	Elongation %*
	92.5	166.8	15.7
	192.2	177.0	13.3
	186.3	155.8	17.3
	184.0	162.1	14.2
	197.1	172.5	15.0
	189.6	164.3	14.5
	192.9	170.5	13.3
	188.2	163.7	13.0
	194.7	175.1	13.7
	191.2	173.2	13.0
Average	190.9	168.1	14.3

*Each value is an average of three tests.

TABLE I-XX

MECHANICAL PROPERTIES OF ALLOY 718 PLATE FROM MILL SOURCE "A" PARALLEL RECEIVING INSPECTION TESTS BY AEROJET-GENERAL

A. MILL-ANNEALED, THEN HEAT-TREATED TO AGC CONDITION A

	F_{tu} Strength (ksi)	F_{ty} 0.2% Strength (ksi)	Elongation (%)	Reduction in Area (%)	Hardness Rc
	218.5	170.1	19.8	33.5	41.0
	--	173.8	21.7	40.3	42.0
Average	218.5	172.0	20.8	36.9	41.5

B. MILL-ANNEALED, THEN HEAT-TREATED TO AGC CONDITION B

	F_{tu} Strength (ksi)	F_{ty} 0.2% Strength (ksi)	Elongation (%)	Reduction in Area (%)	Hardness Rc
	188.3	151.5	25.2	25.2	40
	190.2	153.3	26.0	26.0	40
	174.2	141.2	21.4	21.4	38
Average	184.2	148.7	24.2	24.2	39.3

TABLE I-XXI

MECHANICAL PROPERTIES OF ALLOY 718 PLATE FROM MILL SOURCE "A"

(Mill-Annealed, Stress-Relieved Five Times at 1750°F and Aged as in Condition A by the Fabricator)

Specimen	F_{tu} Strength ksi	F_{ty} (0.2%) Strength ksi	Elongation %	Hardness R_c
1	174.2	120.9	32.0	38
2	173.9	122.4	30.5	38
3	180.7	131.6	31.0	40
4	159.7	107.6	34.0	30
Average	172.1	120.6	31.9	37

facilitate fabrication of the jacket.

Therefore, an investigation was conducted to determine the cause for the low mechanical properties, and to study the effect of various thermal treatments upon the "as-received" material.

In this study, the microstructure was examined initially and test samples were sectioned from the "as-received" plate; these samples were heat-treated and evaluated for mechanical properties. The heat-treatments consisted of the following cycles:

Heat-Treatment Condition	Cycle
E	Mill-annealed, then stress relieved five times at 1750°F and aged as in Condition A by the vendor, then given Condition A heat treatment by Aerojet-General.
F	Mill-annealed, then stress relieved five times at 1750°F and aged as in Condition A by the vendor, then heat-treated to Condition B by Aerojet-General.
G	Mill-annealed, then heat-treated to Condition B.
H	Mill-annealed, then given Condition B heat-treatment except that the material was annealed for 3 hours instead of 1 hour.

The mechanical properties in Condition E and Condition F are listed in Table I-XXII and are lower than those in the mill-annealed and aged condition (Table I-XIX). Grain size results are listed in Table I-XXIII.

Metallographic examination revealed that Laves phase was present in the "as-received" material. Further, orthorhombic Ni_3Cb was present in material annealed at or below 1800°F. Both the Laves phase and orthorhombic Ni_3Cb contributed to the low strength of the repeatedly stress-relieved plate. (Figures No. I-17 through I-22)

As shown in Table I-XXIV, Condition G material had slightly higher yield strength than Condition E material (Table I-XXII). This is attributed to solutioning of the orthorhombic Ni_3Cb phase at 1950°F (Figures No. I-20 and No. I-21). Laves phase was not solutioned by the 1950°F anneal.

Material in Conditions G and H have comparable properties indicating no advantage for a three-hour instead of a one-hour anneal at 1950°F for Alloy 718 subsequently aged at 1350°F/1200°F for 20 hours.

The mechanical properties of plate from a second supplier, Source B, are listed in Table I-XXV. The mechanical properties are slightly higher than those for Mill Source A (Table I-XXIV). Orthorhombic Ni_3Cb was not

TABLE I-XXII

MECHANICAL PROPERTIES OF ALLOY 718 PLATE FROM MILL SOURCE "A"

A. CONDITION E: MILL-ANNEALED, STRESS-RELIEVED FIVE TIMES AT 1750°F AND AGED AS IN AGC CONDITION A BY THE VENDOR, THEN HEAT TREATED BY AEROJET TO AGC CONDITION A

	F_{tu} ksi	F_{ty} 0.2% ksi	Elongation %	Reduction of Area %	Hardness Rc
	179.7	135.6	26.5	33.8	38
	182.0	138.9	25.5	33.5	39
	181.3	141.2	26.5	38.8	39
	180.7	140.0	27.0	33.5	40
	184.6	153.1	21.0	31.8	41
	184.2	145.0	21.0	33.5	40
Average	182.1	142.3	24.6	34.2	39.5

B. CONDITION F: MILL-ANNEALED, STRESS-RELIEVED FIVE TIMES AT 1750°F AND AGED AS IN AGC CONDITION A BY THE VENDOR, THEN HEAT TREATED BY AEROJET TO AGC CONDITION B

	F_{tu} ksi	F_{ty} 0.2% ksi	Elongation %	Reduction of Area %	Hardness Rc
	178.9	146.7	28.5	37.0	40
	177.5	145.8	26.0	36.9	40
	181.1	147.9	27.0	36.9	41
	180.4	148.1	26.0	34.8	40
	184.1	149.9	25.0	39.0	39
	185.6	151.5	25.5	43.1	40
Average	181.3	148.3	26.3	38.0	40.0

TABLE I-XXIII

GRAIN SIZE OF ALLOY 718 PLATE FROM MILL SOURCE "A"

Condition	Grain Size
As received, mill-annealed.	6-7
Mill-annealed, stress-relieved 5 times at 1750°F, and aged as in AGC Condition A.	2-3 and 6
Mill-annealed and aged as in AGC Condition A followed by annealing and aging to Condition A	3-5

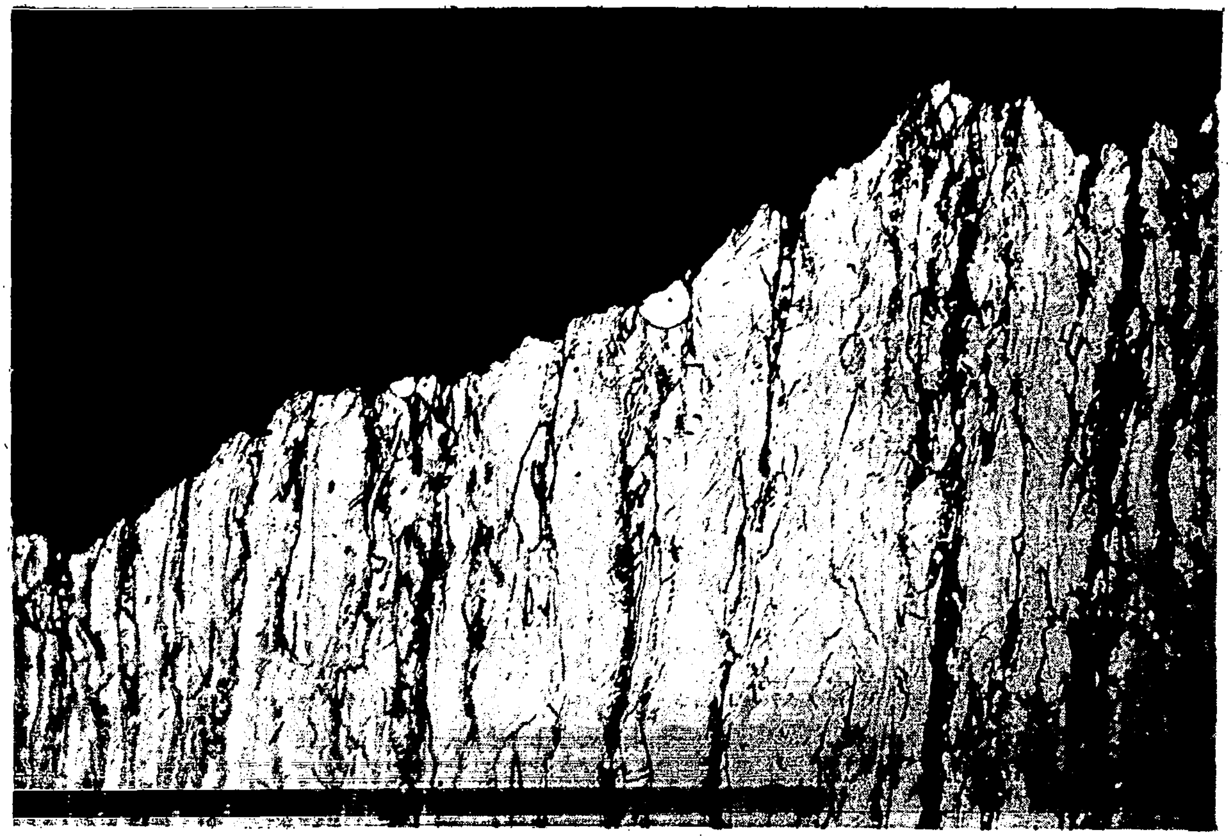

Magnification: 100X   Etchant: Chromic acid (electrolytic)

Note circular, white, etched Laves phase on fracture surface.

Figure I-17

Microstructure of Fracture Surface of Plate
from Mill Source "A" (Mill Annealed)

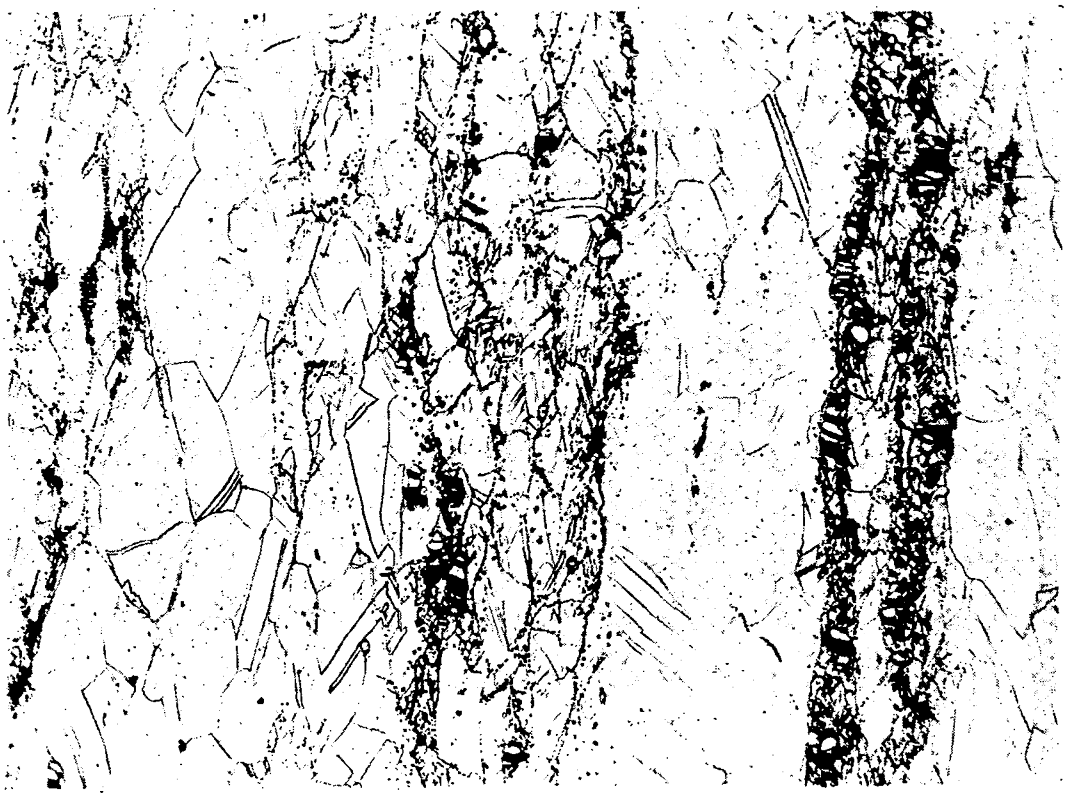

Magnification: 250X

Note the segregation banding in the Alloy 718 plate.

Figure I-18

Microstructure of Plate from Mill Source "A" (Mill Annealed)

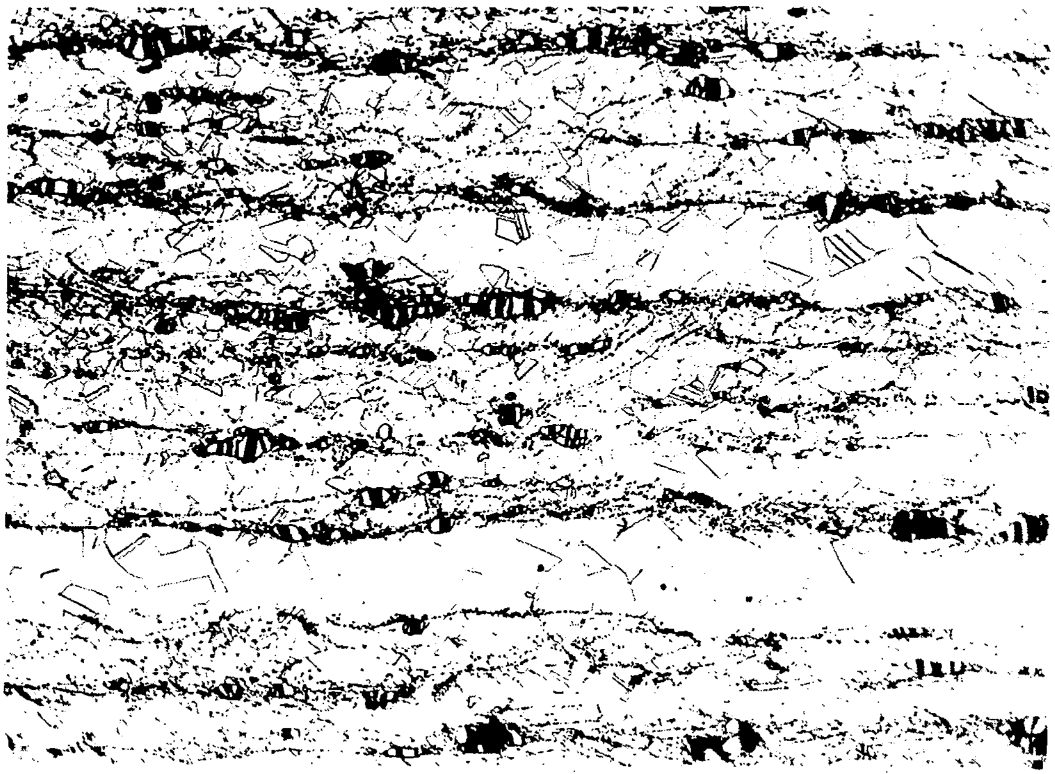

Magnification: 250X

Etchant: 50 HCL, 30 H_2O, 10 HNO_3, 20 HF

Figure I-19

Microstructure of Plate from Mill Source "A"
(Mill Annealed Plus Condition A Treatment)

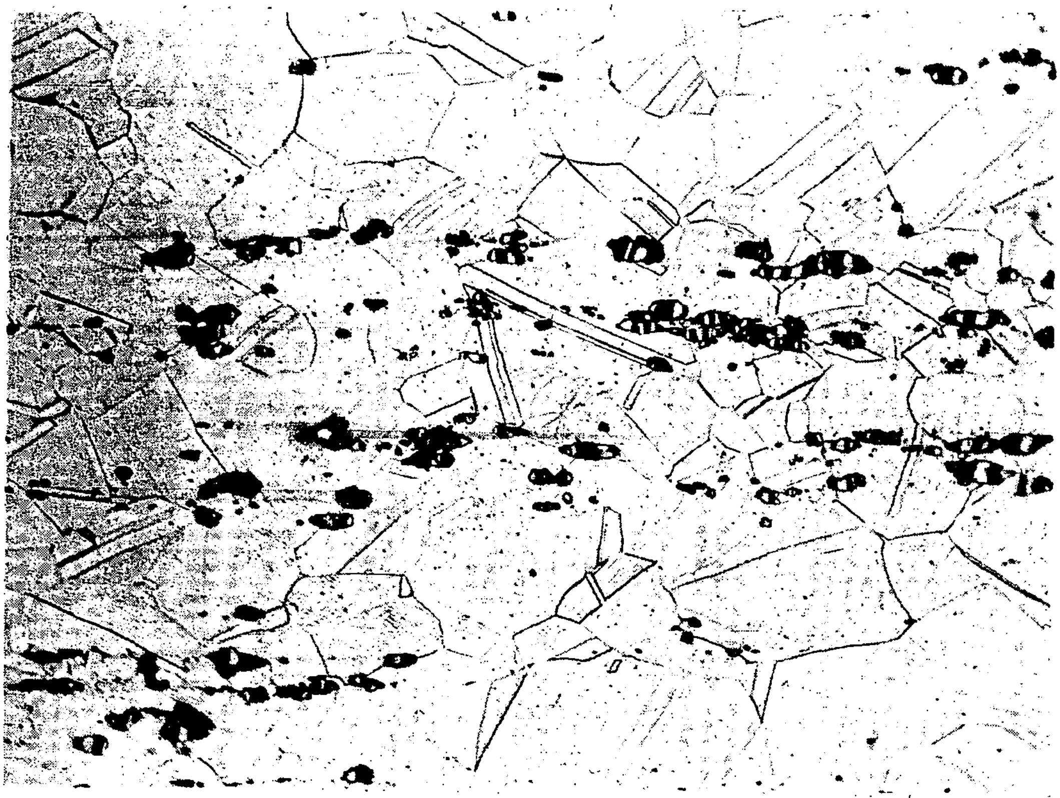

Magnification: 250X

Etchant: 50 HCL, 30 H_2O 10 HNO_3, 20 HF

Note that solutioning of orthorhombic Ni_3Cb was effected by the 1950°F reanneal; grain coarsening also resulted (compare with Figure I-22). Laves phase was not solutioned.

Figure I-20

Microstructure of Plate from Mill Source "A"
(Mill Annealed Plus Condition B Treatment)

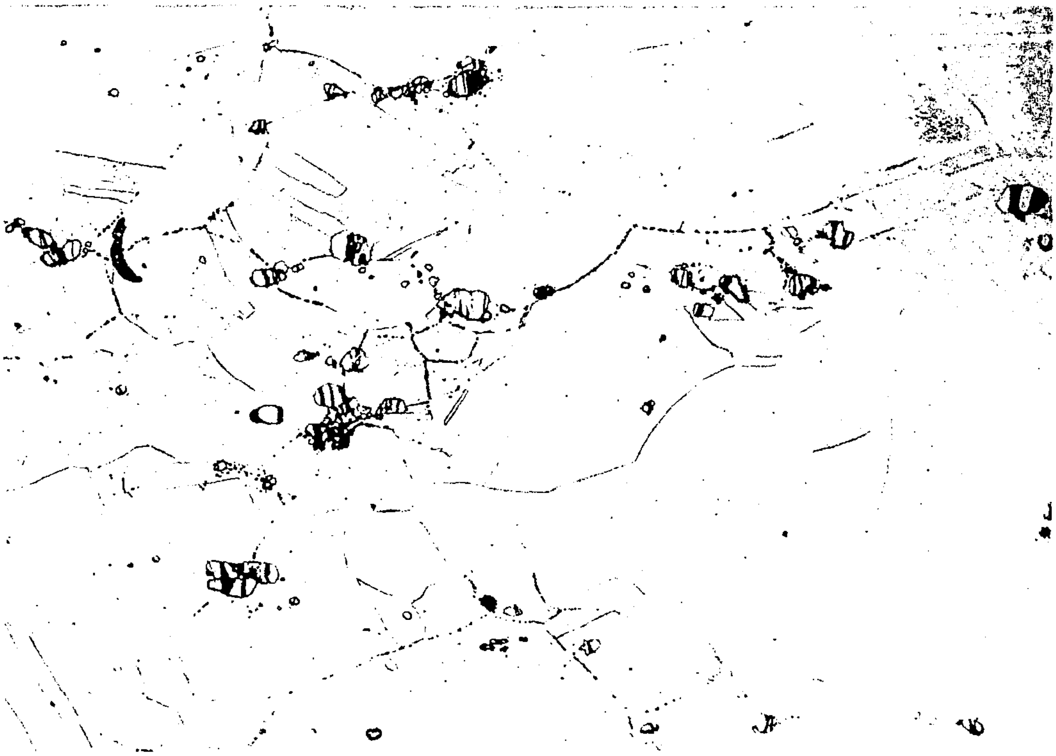

Magnification: 250X

Etchant: 50 HCL, 30 H_2O
10 HNO_3, 20 HF

Treatment modified with 3-hour anneal. Structure is similar to that shown in Figure I-23.

Figure I-21

Microstructure of Plate from Mill Source "A" (Mill Annealed Plus Condition B Treatment Modified with 3-Hr Anneal)

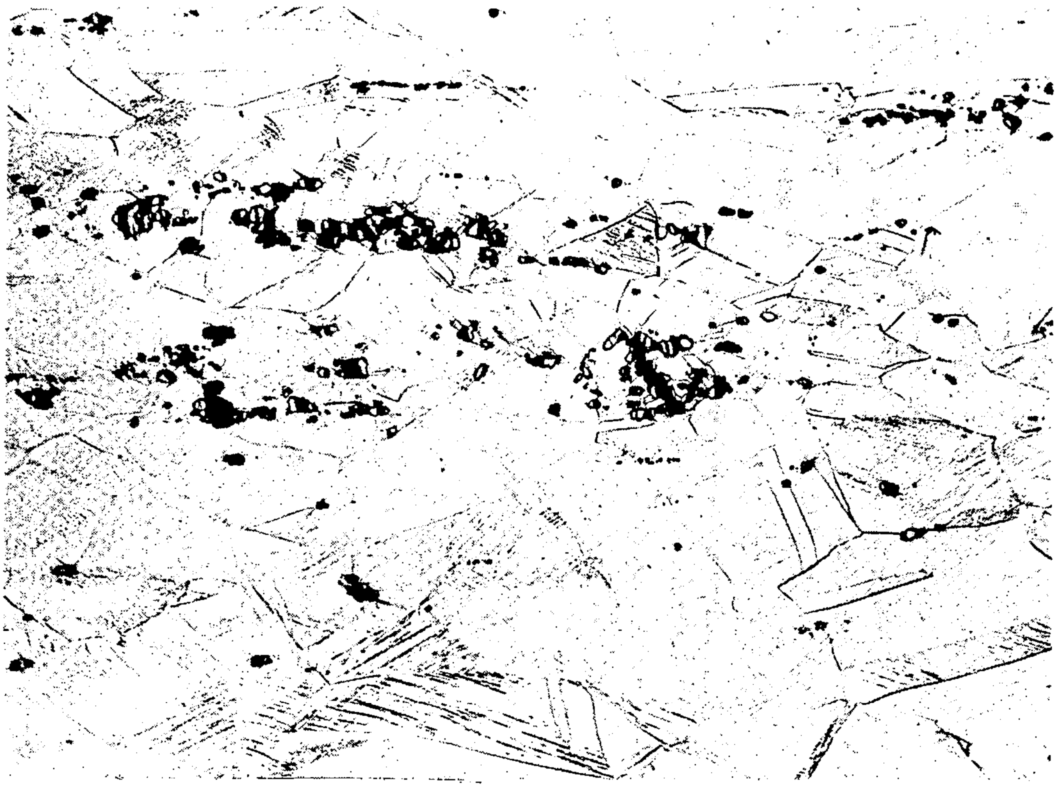

Magnification: 250X

Etchant: 50 HCL, 30 H_2O
20 HF, 10 HNO_3

Segregation of Laves phase is shown in this photomicrograph.

Figure I-22

Microstructure of Plate from Mill Source "B" (Mill Annealed Plus Condition B Treatment)

TABLE I-XXIV

MECHANICAL PROPERTIES OF ALLOY 718 PLATE FROM MILL SOURCE "A"

A. CONDITION G: MILL-ANNEALED ("AS-RECEIVED"), THEN HEAT TREATED TO AGC CONDITION B

	Ultimate Tensile Strength (ksi)	0.2% Yield Strength (ksi)	Elongation (%)	Reduction in Area (%)	Hardness Rc
	180.4	147.5	30.0	47.0	39
	179.6	138.3	27.0	40.1	40
	183.7	144.3	25.0	40.0	39
	185.7	150.9	30.0	47.7	39
	182.4	147.7	29.0	42.5	40
	182.0	144.8	27.0	34.8	39
	181.6	147.9	25.5	32.9	39
	180.0	147.0	20.0	27.5	39
	185.2	150.3	23.5	35.5	39
Average	182.3	146.5	26.3	38.7	39

B. CONDITION H: MILL-ANNEALED ("AS-RECEIVED"), SOLUTION-ANNEALED AT 1950°F FOR THREE HOURS AND AGED AS IN AGC CONDITION B

	Ultimate Tensile Strength (ksi)	0.2% Yield Strength (ksi)	Elongation (%)	Reduction in Area (%)	Hardness Rc
	184.7	151.3	30.0	47.4	40
	180.8	142.3	27.0	38.5	39
	185.3	149.9	27.5	44.1	39
	180.3	146.0	27.0	39.8	41
	180.0	148.3	28.0	43.7	41
	181.8	147.3	29.3	41.3	39
	179.8	145.6	25.0	31.5	41
	179.0	148.1	26.0	33.3	41
	182.2	148.3	24.5	39.0	39
Average	181.6	147.5	27.1	38.7	40

TABLE I-XXV

MECHANICAL PROPERTIES OF ALLOY 718 PLATE FROM MILL SOURCE "B"
(MILL-ANNEALED, THEN HEAT TREATED TO AGC CONDITION B)

	F_{tu} ksi	0.2% (ksi)	Elongation %	Reduction in Area %	Hardness Rc
	180.2	149.5	27.2	41.4	39
	187.6	155.1	29.5	46.0	38
	186.4	153.3	29.0	47.9	38
	187.2	151.1	29.5	45.6	39
	178.7	147.9	30.0	40.4	39
	187.7	157.9	26.0	47.7	40
	187.0	154.5	27.0	42.0	39
	185.9	150.7	28.0	41.7	41
Average	185.1	152.5	28.3	44.1	39.1

evident in this heat; however, Laves phase was observed (Figure No. I-22). The latter phase contributed to the marginal mechanical properties of Mill Source "B" material.

The segregation of Laves phase has most commonly been observed in single-vacuum-induction melted heats. Heats produced by double vacuum melting using the CEVM process in the remelt cycle have been shown (see Figure No. I-15) to produce a segregation-free alloy, this melting practice is now required in material procurement specifications.

A high temperature anneal at 1950°F has been shown to be effective in revealing warm work which obscured the true aged strengths of low-hardening-response plate. To preclude procurement of low-strength material which meets property requirements because of warm work, a high temperature annealing and aging capability test is included in material procurement specifications for cases where the material is furnished in the 1800°F annealed condition. Also, it was shown that stress relief can be performed at 1750°F and properties recovered by re-solutioning at 1950°F and conventional aging.

2. <u>Notch Toughness of As-Welded Heat Treated Plate</u>

Tests were conducted to determine the mechanical properties of welds (in the "as-welded" condition) in fully heat-treated Alloy 718.

One-half inch thick plate was heat treated to Condition B for maximum toughness, then TIG welded with Alloy 718 wire and machined into standard round R-3 tensile specimens. The specimens were tested at room temperature and -423°F.

Test results are summarized below:

a. As shown in Table I-XXVI, the as-welded yield strength at room temperature was 96,000 psi. This is reasonably good considering that the test bar represents an "as-cast" weld structure.

b. Notch-toughness evident at room temperature was retained at -423°F; this is indicated by notch tensile ratios above unity.

c. The test results indicate that Alloy 718 welds in the "as-welded" condition possess good notch-toughness at both room and liquid hydrogen temperatures. However, the strength is lower than that of aged welds and must be considered in the design. Further, the strength obtained in the tests are considered approximate values because of the variables of weld heat input and parent metal as well as weld quench effects which will vary with material thickness and weld tooling.

F. HIGH STRENGTH COLD WORKED AND AGED BOLT MATERIAL

Most of the bolts currently used in liquid rocket engines are fabri-

TABLE I-XXVI

NOTCH-TOUGHNESS OF AS-WELDED HEAT-TREATED PLATE
HEAT TREATED TO CONDITION B BEFORE WELDING

Test Temp °F	F_{tu} ksi	F_{ty} (0.2%) ksi	Elongation %	Reduction of Area %	Weld Hardness, Rc	Notch/ Ultimate Ratio
70	136.6	95.9	12.0	24.3	34.0	
70	136.9	96.4	11.5	25.6	37.0	
Average	136.8	96.2	11.8	25.0	35.5	
70	135.0*				26.0	
70	154.0*				27.0	
Average	144.5				26.5	1.06
-423	184.0	145.2	7.5	18.0	36.0	
-423	180.5	--	7.0	18.0	35.0	
-423	186.3	136.0	11.0	21.3	36.0	
Average	183.6	140.6	8.5	19.1	35.7	
-423	198.8*				28.0	
-423	191.3*				28.0	
-423	189.4*				27.5	
Average	193.2				27.8	1.06

*Round specimens with notches in the weld metal (K_t = 6.3) cated from cold-worked and aged A-286, which develop a yield strength of 160 to 180 ksi minimum. Alloy 718 in the cold-worked and aged condition appeared promising in more highly stressed bolted flanges, and the material was evaluated for bolting application at temperatures from -423°F to 600°F.

The test material consisted of two heats of forged bars supplied by a commercial bolt manufacturer to a minimum guaranteed yield strength of 250 ksi. The fabrication process is proprietary and the degree of cold work imparted to the bolt as well as the aging cycle is not known. As shown below, Heat A, consisting of 46 test bars, was split into two equal lots of 23 test bars; one lot was notched (5.9 to 7.0 stress concentration) while the second lot was reduced in diameter from 0.437-in. to 0.357-in. by machining. The original Heat B test bars were not modified.

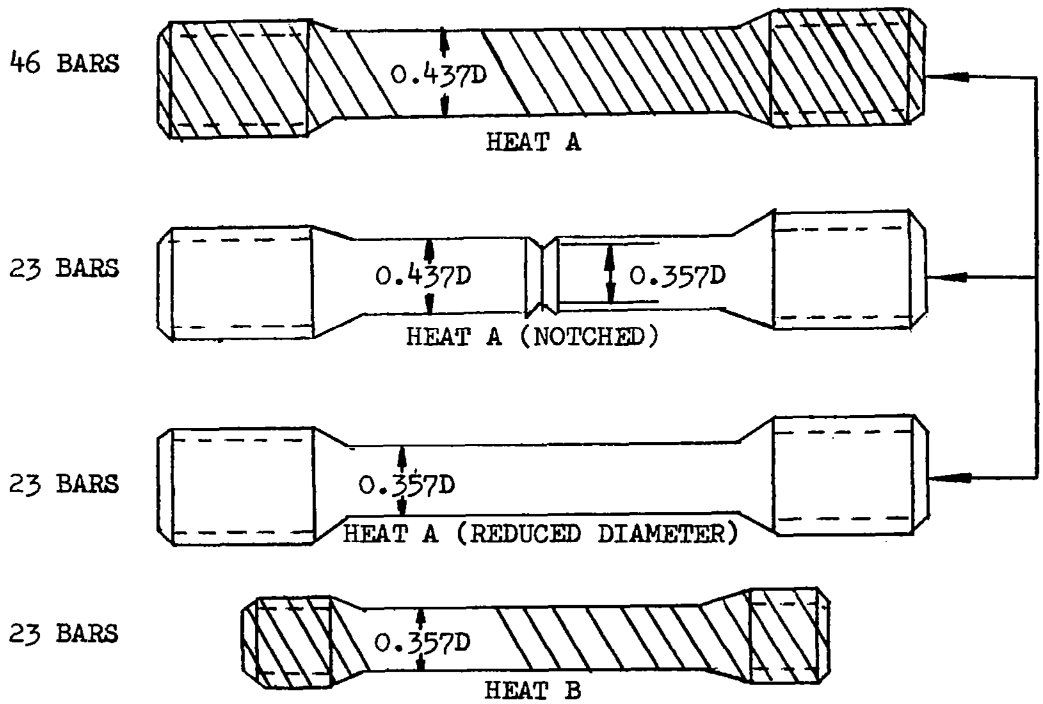

The bars were tested in accordance with Federal Test Method Standard No. 151 at a 0.004-in./in./min strain rate over the temperature range of -423°F to 600°F. The notched and unnotched tensile strength, the smooth bar 0.2% offset yield strength, elongation, reduction of area, and the notch/tensile and notch/yield ratios were determined.

Test results are listed in Table I-XXVII and shown in Figures No. I-23, No. I-24, and No. I-25. The ultimate, 0.2% yield strength, and elongation of the reduced and "as forged to size" test bars were essentially equivalent. Reduction of area for the "as forged" test bars were slightly higher than those for the reduced test bars; however, these bars represented two heats and some difference could be expected because of variable chemistry. Exposure of cold-worked and aged material at 400°F and 600°F resulted in some reduction of strength with little noticeable effect upon ductility. Lowering the test temperature to -320°F resulted in a substantial increase of strength and ductility. Based upon notch/tensile and notch/yield criteria, a slight degree of notch sensitivity was observed at -320°F at these strength levels. The strength further increased when the test temperature was lowered to -423°F while ductility was not reduced. At -423°F, the bolts were notch tough at a lower stress concentration of 5.9.

These data serve to illustrate that, based upon high strength, cold worked and aged Alloy 718 offers a potential for bolt application in cryogenic engines. The mechanical properties are influenced by degree of cold working and additional testing is required to obtain test data at different strength levels to provide accurate design minima.

G. LOCALIZED AGING OF ALLOY 718 PROPELLANT LINE

Local aging of Alloy 718 weld joint was investigated as a possible means of providing full-strength welds in the heat-treated alloy because it would not be possible to use conventional heat treatment furnaces for aging welded propellant lines.

To determine the effect of the temperature differential and the effect of a constant aging temperature upon strength and ductility, Alloy 718 sheet was heat treated to Condition B for optimum cryogenic properties, welded, machined into tensile specimens aged for 20 hours at temperatures between 1000°F and 1500°F, and tensile tested at room temperature. Specimens were also double-aged for 20 hr at the following temperatures for comparison purposes: per Condition B, 1450°F/1300°F, and 1250°F/1100°F.

Test results are listed in Table I-XXVIII. Highest aged strengths were obtained using the Condition B heat treatment, while aging at 1450°F/1300°F yielded next highest properties. Aging at 1300°F for 20 hr is the best single-temperature aging cycle (Figure No. I-26); properties are lower than those obtained using the dual aging cycles of Condition B and 1450°F/1300°F.

Additionally, a series of experiments was performed to determine the

TABLE I-XXVII

MECHANICAL PROPERTIES OF COLD WORKED AND AGED BOLT MATERIAL

A. HEAT A BARS REDUCED FROM 0.437-IN. TO 0.357-IN. DIAMETER

Test Temperature	F_{tu} ksi	F_{ty} (0.2%) ksi	Elongation in 1 in. (%)	Reduction of Area %
600°F	235.3	231.8	5.0	17.1
	234.3	229.8	5.7	16.6
	237.2	232.7	3.6*	12.0*
Average	235.6	231.4	5.3	16.8
400°F	242.2	238.2	5.0	18.7
	242.8	237.3	5.0	16.1
	245.3	239.8	2.9*	9.3*
Average	243.4	238.4	5.0	17.4
200°F	251.2	246.3	6.4	22.2
	253.7	247.3	5.7	15.1
	255.6	250.0	5.0	15.2
Average	253.5	247.8	5.7	17.5
RT	264.3	258.8	5.0	13.0
	263.2	254.7	5.7	16.6
	268.3	261.3	4.6	10.4
Average	265.2	258.2	5.1	13.3
-100°F	283.2	274.7	5.0	14.6
	282.2	272.2	5.7	18.2
	286.2	277.2	5.0	10.9
Average	283.8	274.7	5.2	14.5
-320°F	318.1	300.5	6.8	10.9
	313.7	297.7	8.9	17.1
	313.2	297.7	8.6	17.7
Average	315.0	298.6	8.1	15.2
-423°F	341.0	326.0	8.0	12.4
	334.5	319.5	10.0	22.3
	337.0	323.0	8.5	17.5
Average	337.1	322.8	8.8	17.4

*Value not used in determination of average

TABLE I-XXVII (CONT.)

MECHANICAL PROPERTIES OF COLD WORKED AND AGED BOLT MATERIAL

B. HEAT A BARS (NOTCHED)

Test Temperature	Notch Tensile Strength (in ksi)	Stress Concentration Factor K_t	Notch/Ult. Ratio	Notch/Yield Ratio
600°F	240.9	6.5		
	264.2	6.9		
	256.7	6.5		
Average	259.9		1.10	1.12
400°F	270.2	7.0		
	252.0	6.7		
	263.7	6.4		
Average	261.9		1.08	1.10
200°F	215.4	6.5		
	228.8	5.9		
	256.2	6.0		
Average	233.4		0.92	0.93
RT	258.1	6.0		
	239.3	6.1		
	232.9	6.7		
Average	243.4		0.92	0.94
-100°F	263.8	6.3		
	296.9	6.7		
	264.6	6.5		
Average	275.1		0.97	1.00
-320°F	247.3	7.0		
	258.3	6.5		
	278.7	6.5		
Average	261.4		0.83	0.88
-423°F	374.0	5.9		
	383.0	5.9		
	399.0	5.9		
Average	385.6		1.14	1.17

TABLE I-XXVII (CONT.)

MECHANICAL PROPERTIES OF COLD WORKED AND AGED BOLT MATERIAL

C. HEAT B BARS

Test Temperature	F_{tu} ksi	F_{ty} (0.2%) ksi	Elongation in 1 in. (%)	Reduction in Area (%)
600°F	230.3	227.3	4.3	24.1
	243.2	240.2	5.7	26.1
	242.2	239.8	5.7	25.1
Average	238.5	235.8	5.2	25.1
400°F	251.2	248.8	5.0	22.2
	220.3*	Failure occurred in threads		--
	248.3	244.8	5.7	23.6
Average	249.2	246.8	5.4	22.9
200°F	259.7	257.2	5.7	22.7
	256.7	253.7	3.5*	17.1*
	261.2	257.2	5.0	21.7
Average	259.2	256.0	5.4	22.2
RT	272.2	269.7	5.7	22.2
	260.2	254.7	6.4	25.6
	264.7	262.2	5.7	24.1
Average	265.7	262.2	5.9	23.9
-100°F	280.7	Failure occurred in threads		
	247.3	Failure occurred in threads		
	289.7	283.7	6.4	24.1
Average	285.2	283.7	6.4	24.1
-320°F	306.7	289.7	10.7	25.7
	319.2	303.7	Broke outside gage length	
	262.0	Failure occurred in threads		
Average	312.9	296.7	10.7	25.7
-423°F	338.0	330.0	10.0	24.2
	240.0	332.0	10.0	24.2
	339.8	--	11.5	25.2
Average	339.2	331.0	10.5	24.8

*Specific value not used in determination of the average

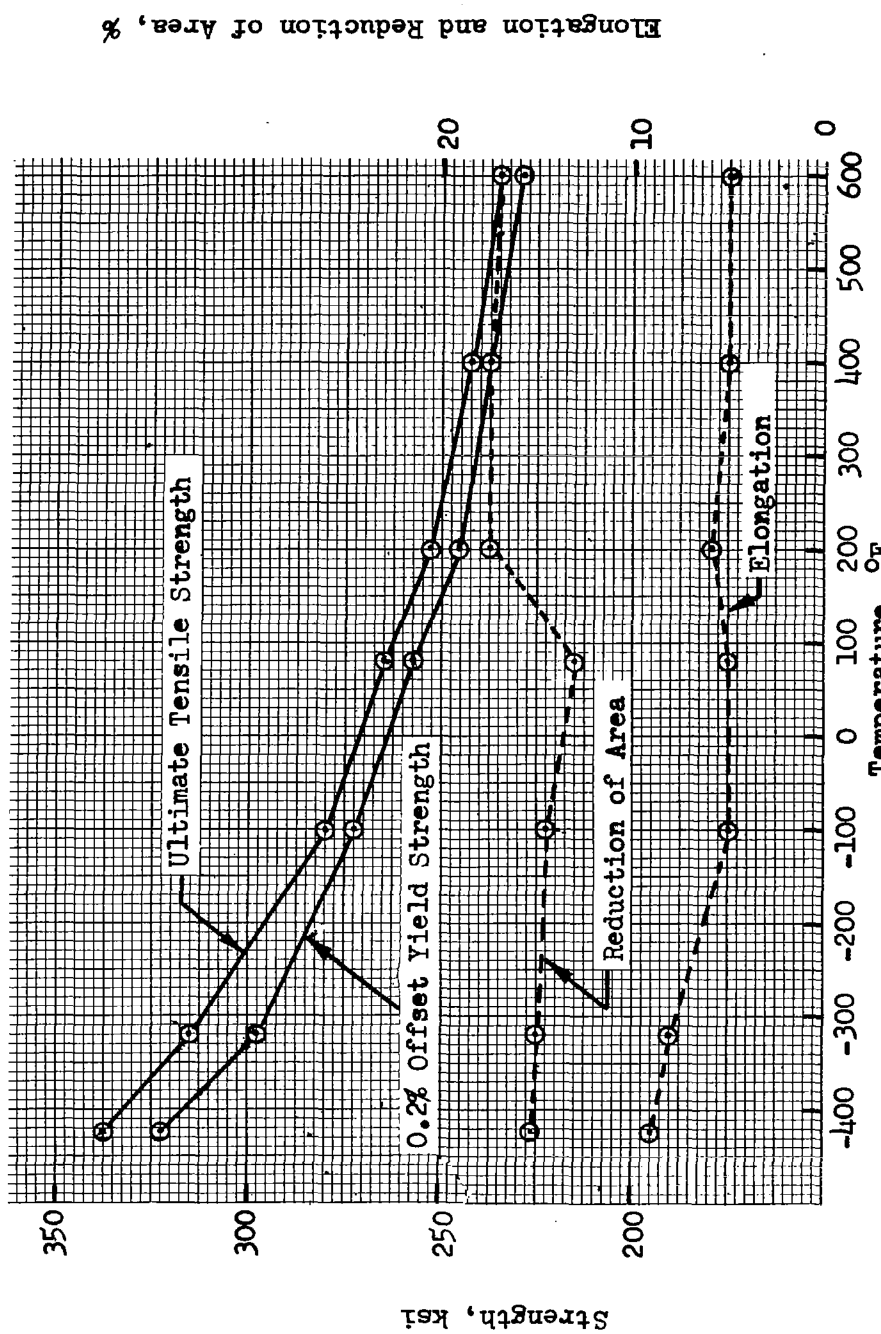

Figure I-23

Mechanical Properties of Bolt Material Vs. Temperature
(Heat A Bars Reduced from 0.437-In. to 0.357-In. Diameter)

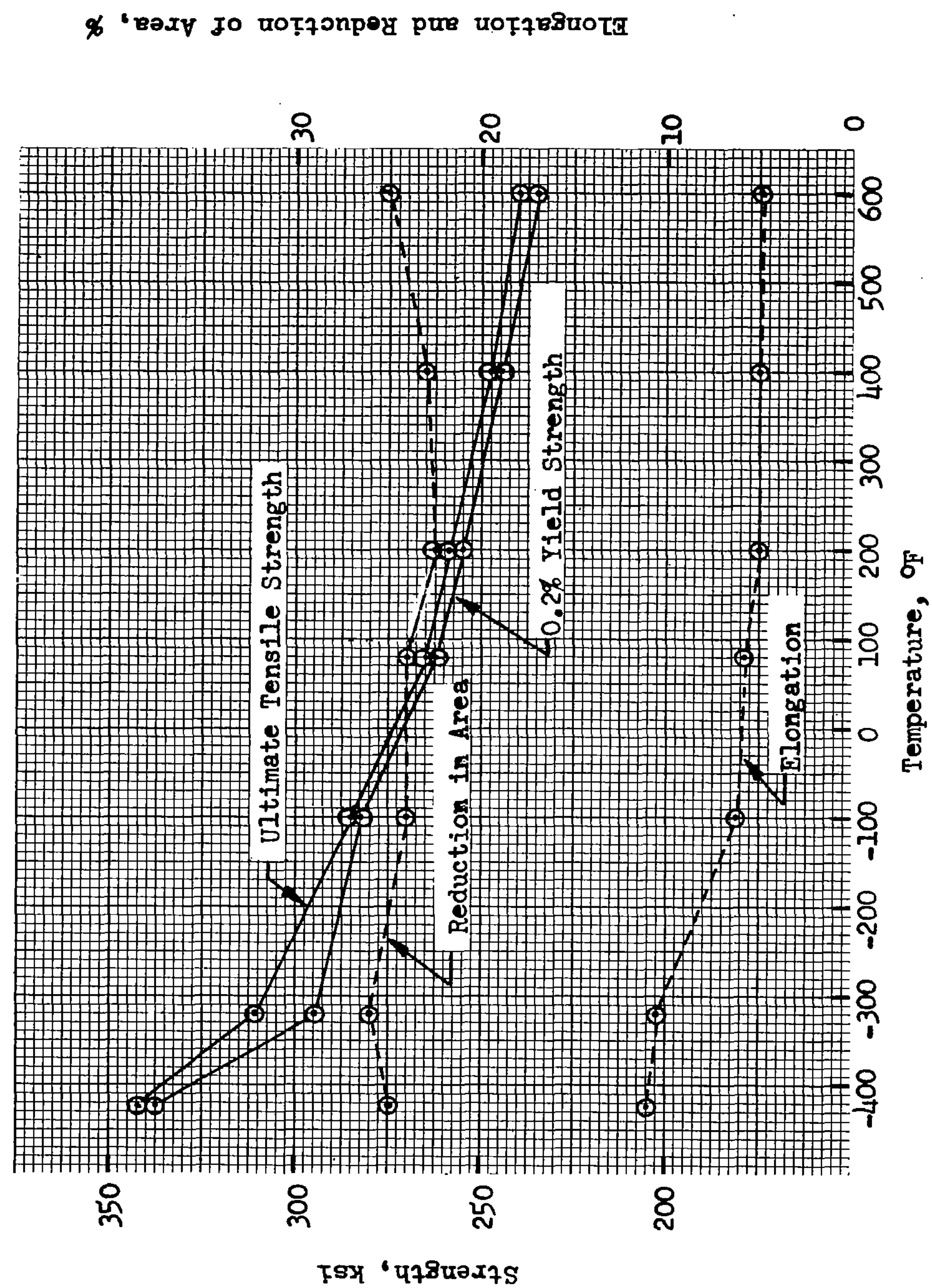

Figure I-24

Mechanical Properties of Bolt Material Vs. Temperature (Heat B Bars 0.357-In. Diameter)

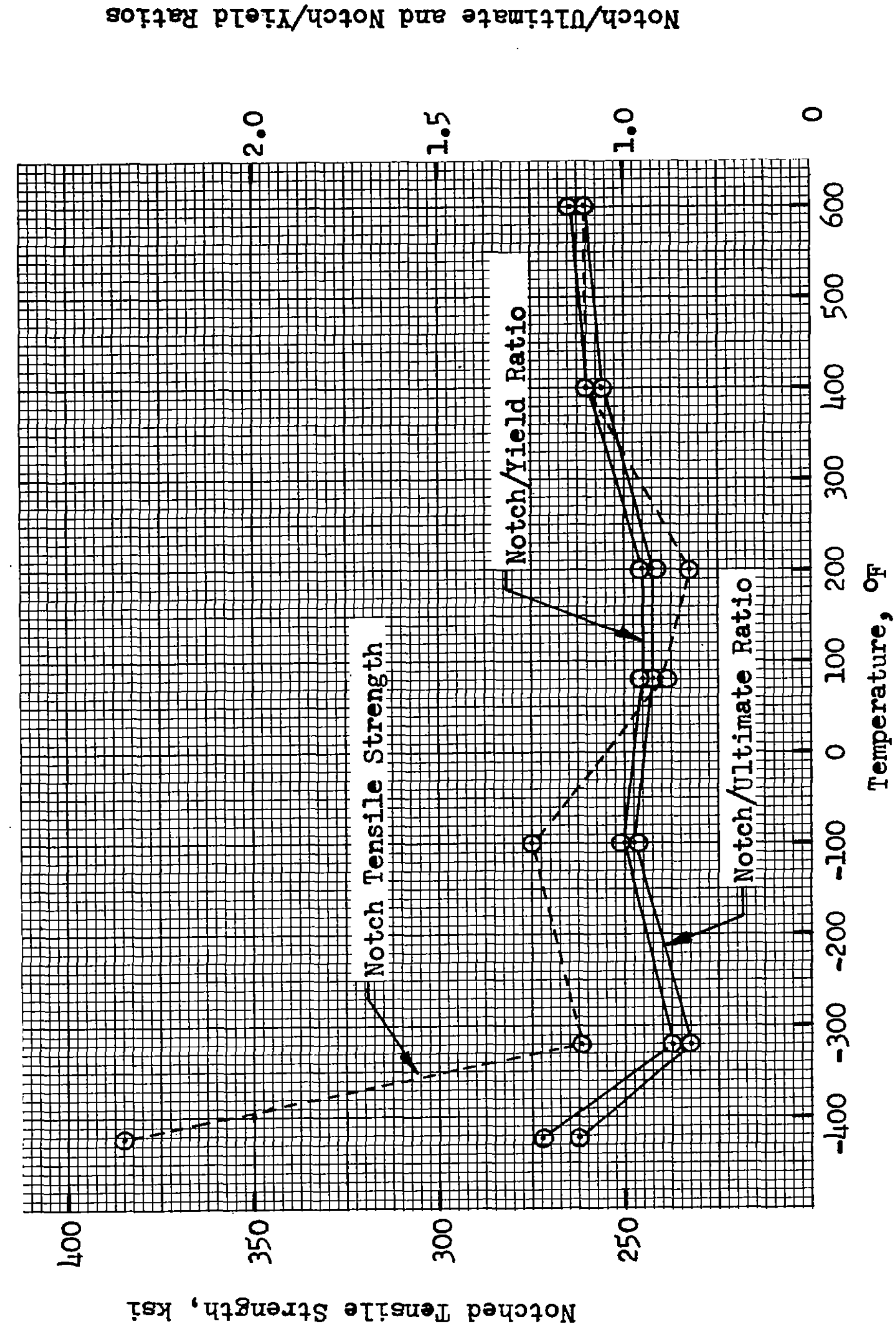

Figure I-25

Notch Tensile Strength, Notch Yield Ratio, and Notch Tensile Ratio of Bolt Material Vs. Temperature Heat A Notched Bars (0.0437-In. Diameter and Notched)

TABLE I-XXVIII

EFFECT OF POST-WELD AGING TEMPERATURE UPON THE ROOM TEMPERATURE MECHANICAL PROPERTIES OF WELDED ALLOY 718 SHEET*

Post-Weld Age Cycle	F_{tu} ksi	F_{ty} 0.2% Offset ksi	Elongation** % in 2 in.	Weld-Joint Efficiency (% of Parent-Metal) Yield Strength
1000°F/20 hr	120.8	86.8	3.5	
	122.5	90.0	4.5	
	126.2	88.4	4.5	
	121.5	84.8	4.0	
Average	122.8	87.5	4.1	55
1100°F/20 hr	127.1	103.3	3.5	
	123.5	103.1	3.0	
	135.4	103.5	4.0	
	120.1	104.4	4.5	
Average	126.5	103.6	3.8	65
1200°F/20 hr	150.8	109.6	15.5	
	149.2	125.9	4.5	
	143.2	118.3	4.5	
	148.2	118.3	7.5	
Average	147.9	118.0	8.0	74
1300°F/20 hr	168.8	132.6	13.0	
	174.8	134.1	18.0	
	171.8	132.6	16.0	
	170.5	134.0	14.0	
Average	171.5	133.3	15.3	84
1400°F/20 hr	164.0	128.6	8.5	
	170.4	127.4	12.0	
	172.7	126.5	14.5	
	166.7	126.7	11.0	
Average	168.5	127.3	11.5	80
1500°F/20 hr	155.0	98.2	14.5	
	151.8	97.5	13.0	
	152.5	96.2	14.0	
	148.5	95.8	12.0	
Average	152.0	96.9	13.4	61

TABLE I-XXVIII (CONT.)

Post-Weld Age Cycle	F_{tu} ksi	F_{ty} 0.2% Offset ksi	Elongation** % in 2 in.	Weld-Joint Efficiency (% of Parent-Metal) Yield Strength
As-Welded	116.1	72.2	5.5	
	124.2	83.1	4.5	
	124.2	79.5	6.0	
	124.8	82.4	5.5	
Average	122.3	79.3	5.3	50
Condition B	178.2	146.8	6.5	
(Annealed 1950°F,	177.5	144.2	7.0	
Aged 1350°F/8-10	173.1	147.4	4.0	
hr plus 1200°F				
for 20 hr Total)				
Average	176.3	146.1	5.8	92
1450°F/1300°F	180.9	138.0	7.5	
	181.4	138.0	7.5	
	180.6	139.7	7.5	
Average	181.0	138.6	7.5	87
1250°F/1100°F	163.8	122.2	15.0	
	152.0	122.4	6.0	
	157.7	129.6	2.5	
Average	157.8	124.7	8.0	78
Condition B	189.8	155.6	23.8	
(Parent Metal)	191.7	163.1	17.4	
Average	190.8	159.4	20.6	

* All samples were heat treated to Condition B, then welded and the welds ground flush before the post-weld aging cycle.

** All failures occurred in the welds.

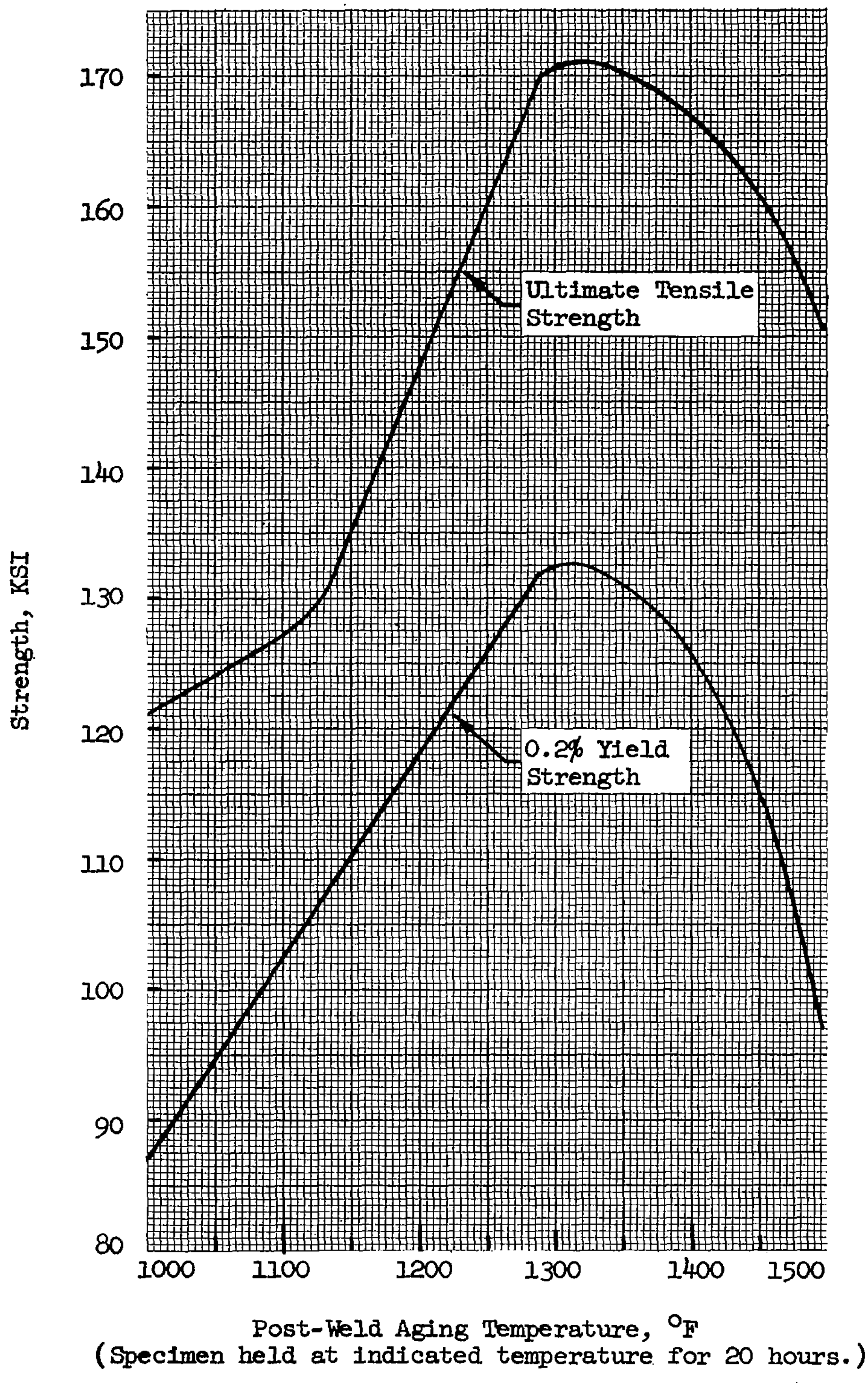

Figure I-26

Weld Joint Strength Vs. Post-Weld Aging Temperatures temperature differentials that would occur in propellant lines during local aging using a resistance heating device. An 18-in. long Alloy 718 tube (10-in. diameter, 0.156-in. wall thickness) simulating the propellant lines was used to develop the testing device for the local age study. The differential recorded in these tests was 150°F with the ends blocked and 200°F with the ends open. No insulation was placed in the tube near the weld area. Because there will be little convection inside the lines, the tube with the ends blocked more nearly represents the actual situation. Therefore, 150°F is the approximate differential expected during local aging if no insulation can be placed in the lines near the weld.

Based upon this study, the optimum aging cycle for locally aging Alloy 718 welded discharge lines is: 1450°F for 8 to 10 hr, cool to 1300°F and hold at 1300°F for a total aging time of 20 hr. This higher-Temperature aging cycle offsets the 150°F temperature gradient across the tube wall and provides optimum age-hardening response.

A tube of 10-in. diameter, 9-in. length, and 0.156-in. wall thickness was locally aged in the weld area at 1350°F/1200°F. This was done to prove the efficiency of the initial work. The inside of the tube was blocked on each side of the heater to simulate the conditions that will exist if insulation can be placed inside the line. At room temperature, weld joint efficiency was 94% based upon yield strength and weld elongation was 10% in a 0.75-in. gage length (Table I-XXIX).

The significant findings are as follows:

1. A double aging cycle of 1350°F for 8 to 10 hr. cooling to 1200°F, and holding at 1200°F for a total aging time of 20 hr (70°F wall-temperature differential) resulted in excellent weld response to aging.

2. A higher temperature double-aging cycle of 1450°F for 8 to 10 hr, cooling to 1300°F, and holding at 1300°F for a total aging time of 20 hr will give satisfactory aging response even if a higher temperature differential exists in the discharge line wall thickness.

H. THERMAL EXPANSION OF ALLOY 718

Applications of constructional materials, particularly in the turbopump assembly (TPA), required an accurate knowledge of their thermal expansion characteristics because of the temperature variation from -423°F to ambient, close fits, and assembly considerations.

Expansion-versus-temperature (-423°F to ambient temperature) readings were obtained on the Leitz dilatometer. To recheck original test data, as well as those reported by the literature, additional tests were performed by outside laboratories using similar testing techniques. The expansion-versus-temperature curve is shown in Figure I-27.

TABLE I-XXIX

WELDED ALLOY 718 TUBE LOCALLY AGED, AS IN CONDITION B

A. TEMPERATURE GRADIENT ALONG THE LENGTH OF THE TUBE OUTSIDE SURFACE

Hot Zone	1-1/4 in. From Weld, 1/4 in. From Heater	4-1/4 in. From Weld, 3-1/4 in. From Heater
1350°F	1210°F	610°F
1220°F	1090°F	550°F

B. TEMPERATURE GRADIENT THROUGH TUBE

Hot Zone, Outside Surface	Hot Zone, Inside Surface
1350°F	1280°F
1220°F	1150°F

NOTE: 1. Heat loss was minimized by blocking the tube at both ends, two inches from the heater. The insulation wrapped around the heater extended one inch on each side.

2. The heater was two inches wide.

C. ROOM-TEMPERATURE MECHANICAL PROPERTIES

	F_{tu} ksi	F_{ty} (0.2%) ksi	Elongation (%) 2-in. Gage Length	Elongation (%) 3/4-in. Gage Length	Hardness Rc
Welded and Locally	181.7	--	4.0	10.0	42.8
Aged per Condition B	180.1	147.4	4.0	10.7	39.4
	182.0	154.2	3.5	10.0	39.1
Average	181.3	150.8	3.8	10.2	40.4
Parent Metal	192.7	158.7	14.0		44.5
Condition B	196.0	164.7	14.5		44.0
	191.3	158.8	13.5		44.0
Average	193.3	160.7	14.0		44.2

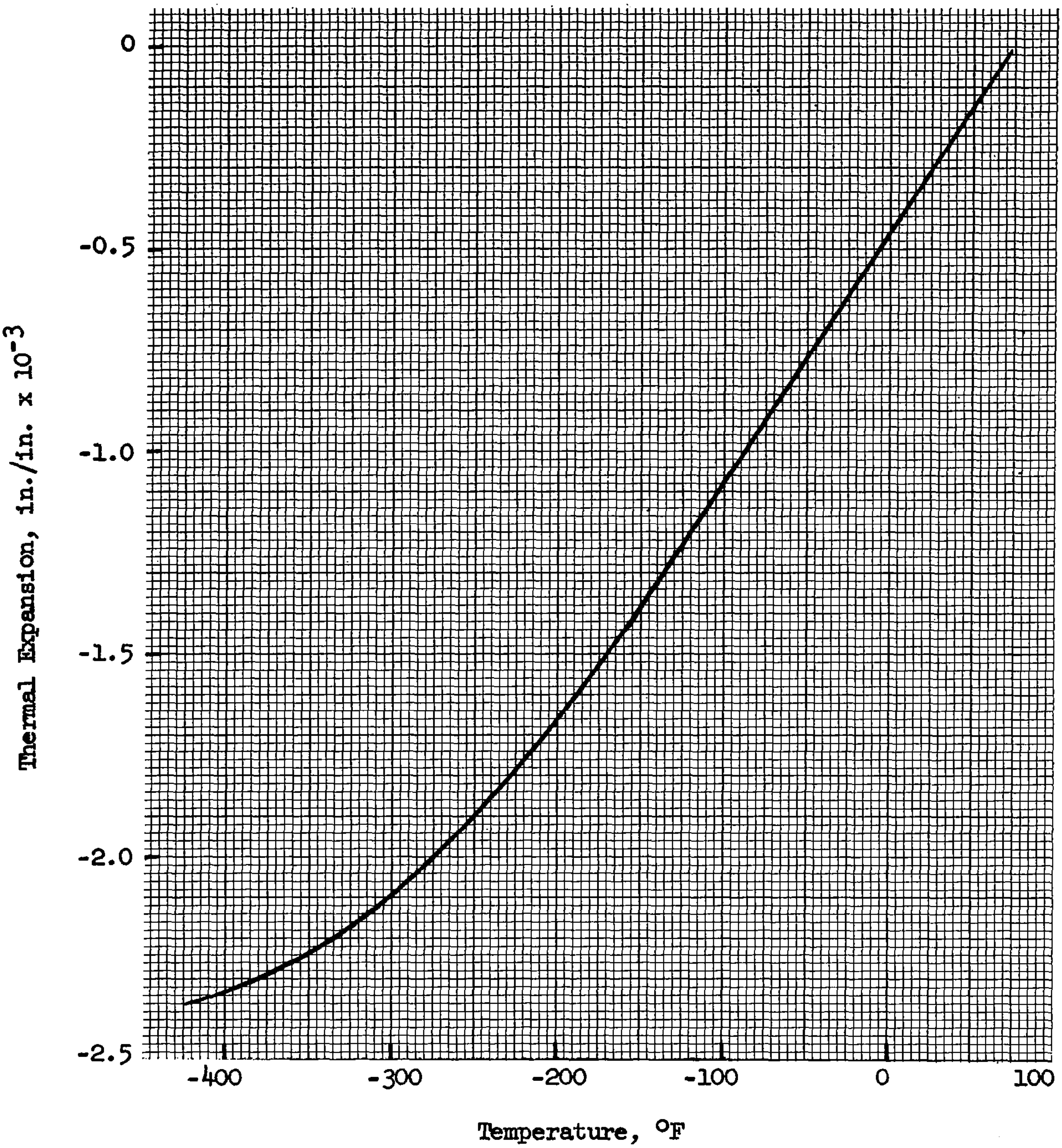

Figure I-27

Expansion Vs. Temperature for Alloy 718

II. CONCLUSIONS

Alloy 718, hardened principally by columbium, possesses unique metallurgical characteristics that give it many advantages over the other well-known nickel-chromium alloys that are hardened by additions of titanium and aluminum. These metallurgical characteristics are exceptionally high yield strength, ductility, and toughness up to 1350°F; good weldability in the age-hardened condition; and a slow rate of age-hardening which affords low annealed hardnesses.

This alloy is suitable for cryogenic service in liquid rocket engines at temperatures down to -423°F. The alloy has good notch-toughness and ductility in both the annealed and age-hardened conditions.

The Alloy 718 heat-treatment must be carefully controlled to obtain optimum tensile-limited and stress-rupture properties. The heat-treatment that produces optimum stress-rupture properties does not correspond with the heat-treatment that produces optimum tensile properties. Generally, annealing temperatures for stress-rupture applications must be 1750°F to 1800°F in the heat-treatment cycle, while the temperature for tensile-limited applications and for maximum cryogenic toughness is 1950°F. The optimum primary aging cycle in the heat-treatment process appears to be a function of hardener content, and high primary aging (1400°F) is required to develop maximum strength in high-hardener content heats. However, the 1400°F aging will overage low-hardener content heats.

The failure of large forgings to meet mechanical property requirements results from insufficient hot-working with resultant coarse grain structure and improper grain flow. A high degree of hot working appears to be necessary to refine the microstructure and produce good mechanical properties in large forgings.

Single-vacuum-induction melted Alloy 718 is not suitable for cryogenic applications. Excessive Laves phase segregation results when using this process. Double vacuum melting using the consumable-electrode-melting practice in the re-melting process produces an almost segregation-free product.

Warm work has been found to significantly strengthen flat-rolled plate and sheet and may, in some cases, mask the true age hardened strength of low-response-hardening plate. A high-temperature annealing at 1950°F in the heat-treatment cycle will eliminate the strain hardening and reveal the low-response hardening plate properties that would be obtained in repetitive stress-relief or full anneal fabrication cycles.

Alloy 718 can be welded using either Rene' 41 or Alloy 718 wire to produce high strength in TIG welded joints. The best weld properties are obtained by post-weld annealing and aging. Post-weld aging alone produces equivalent strength but the ductility is slightly lower. As-welded joints in Alloy 718 possess good cryogenic toughness.

Thin gage sheet possesses lower ductility than heavy gage sheet or plate.

Alloy 718 can be locally aged to produce properties almost equivalent to those of conventionally aged products.

Fatigue strength has been found to be quite good for Alloy 718. Higher fatigue strengths were obtained using a low-temperature anneal in the heat-treatment cycle, which results in a fine-grained structure.

III. RECOMMENDATIONS

Additional work should be performed to establish the cryogenic and elevated temperature fatigue properties, structural stability at elevated temperatures, oxidation resistance at high pressure and temperatures, cold-work and recrystallization characteristics, and weldability to low-density dissimilar metals and alloys. These data would be useful in determining additional future applications of Alloy 718 in advanced engine designs.

PART II. ELECTRON-BEAM WELDING OF ALLOY 718 AND ALLOY 718 TO RENE' 41 IN HEAVY SECTIONS

I. DISCUSSION

A. ELECTRON-BEAM WELDING ALLOY 718 TO RENE' 41

A weld development program was performed to determine the feasibility of joining heavy wall, hollow shaft forgings of Alloy 718 to Rene' 41, by the electron beam (EB) welding process. Two sets of 6-in. diameter forgings were procured for this weld development program. The M-1 fuel turbine shaft (Rene' 41) to disc stub shaft (Alloy 718) joint was designed to have 1-3/8-in. wall thickness. At the beginning of this program, there was no assurance that the existing EB welding capability would permit full penetration of the required 1-3/8-in. thick butt joint. To allow for this potential technological limitation, joints of the test specimens were designed to permit supplementing the electron beam weld with tungsten inert gas welding (TIG). The test specimen weld joints were machined to form a 1-3/8-in. flat face for EB welding and a 1-in. deep U-groove for TIG welding to complete the joint.

Alloy 718 back-up rings, 1/4-in. thick and 1/2-in. wide, were pressed into the forgings at the weld joint. These back-up rings served a twofold purpose: to hold the weld specimens in alignment and to prevent EB decay from burning through at the root of the weld. Such burn-through can cause defects at the root of the joint.

Photographs of the forgings as machined and welded along with a photomacrograph of an EB weld produced by a weld schedule developed for Alloy 718 and Rene' 41 plate is shown in Figure No. II-1. The same weld schedule was used in joining the Alloy 718 to Rene' 41 shaft forgings. The weld schedule was: 44 kv, 360 ma, 5.95 amp focus current, 24 ipm surface speed, and 3-in. gun-to-work distance.

Full EB weld penetration was obtained through the 1-3/8-in. joint thickness of materials used to develop the schedule as well as the weld test forgings. One Alloy 718 to Rene' 41 weldment was code marked "A", then inspected, heat-treated, re-inspected, machined into test specimens, and tested. The other weldment, code marked "B", was inspected, then the 1-in. U-groove weld was completed using the TIG welding process and Alloy 718 filler wire. Upon completion of weldment "B", it was inspected, heat-treated, and machined into test specimens and tested. Test data was obtained for EB and TIG welds at room and cryogenic temperatures for joints of Alloy 718 to Rene' 41 (see section entitled Mechanical Test Results). Figure No. II-2 shows a cross-sectional view of weldment "B" containing the combination of EB and TIG welds.

The Alloy 718 to Rene' 41 test weldments were initially welded using a 3-in. gun-to-work distance, which produced sound welds. Because of the EB gun diameter, the weld joint of the full-scale turbine shaft-to-disc joint was inaccessible when using the established 3-in. gun-to-work distance. Therefore, test specimens were welded using 30 kv welding equipment and a 10-in. gun-to-work distance, which would permit the necessary clearance for full-scale

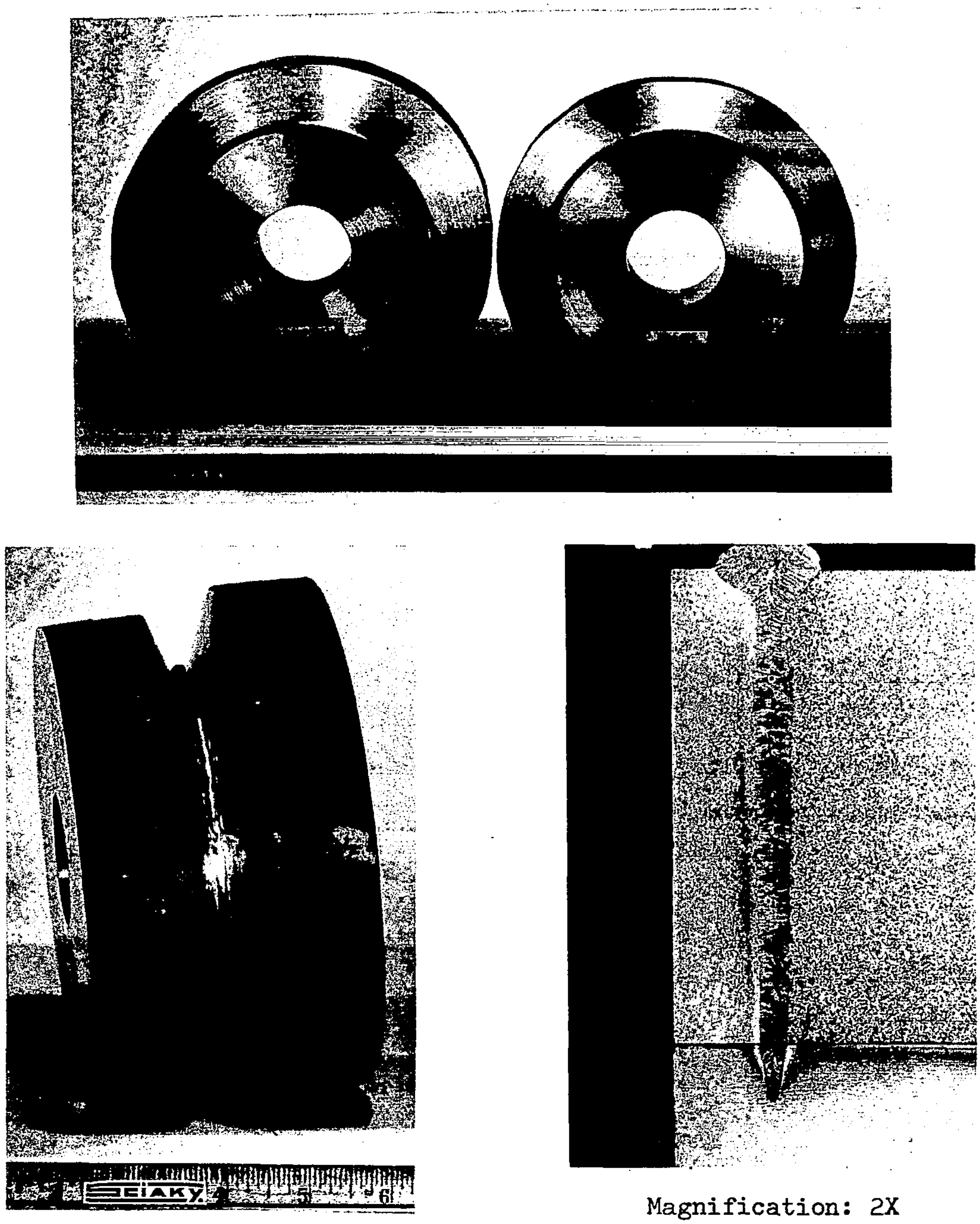

Magnification: 2X

Rene' 41 to Alloy 718

Figure II-1

Weld Test Discs Before and After Making an EB Circumferential Butt Weld and an Axial Section Through the Weld

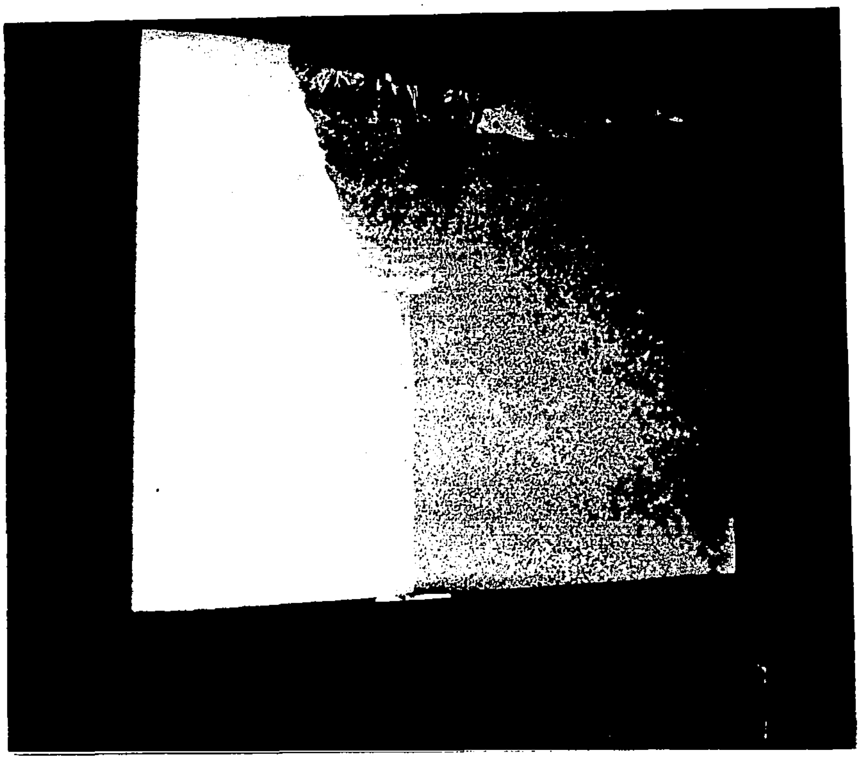

The electron-beam weld was made perpendicular to the axis of the forgings. Alloy 718 filler wire was used for the TIG weld portion.

Figure II-2

Cross-Sectional View of Weldment B

joints. The welds produced were extremely wide and contained defects (see Figure No. II-3). An acceptable weld schedule could not be obtained under these conditions; therefore, the weld joint was re-designed to contain a 70-degree angle from the axis center line of the forgings and weld tests were made. Figure No. II-4 shows a cross-sectional view of a sound EB weld produced by the beam impinging the surface at this angle.

The turbine shaft and disc weld joints were also machined to the 70 degree angle and welded. Two views of the welded Alloy 718 disc stub shaft to Rene' 41 shaft in the EB weld chamber are shown in Figure No. II-5. Successful angular welds are made; however, joint-preparation machining was extremely difficult because of the close tolerance requirements between mating members for EB welding. Therefore, an EB welding schedule using a 150 kv machine was developed and evaluated; the welds were oriented to the center line axis of the parts by using a 10-1/2-in. gun-to-work distance. The weld schedule was: gun-to-work distance 10-1/2-in., beam current 35 ma, voltage 140 kv, and surface speed 16 ipm. The weld beam was focused on a tungsten target to obtain minimum beam diameter prior to welding the joint. The cross-section of a full penetration EB Alloy 718 to Rene' 41 weldment is shown in Figure No. II-6. The microstructure of the EB weld fusion zones produced by a high voltage EB welder (150 kv) is described under Metallography (Section III).

All failures of electron-beam-welded Alloy 718 to Rene' 41 test specimens occurred in the Rene' 41 parent metal.

B. OXIDIZER TURBINE ASSEMBLY

The size of the M-1 turbopump components preclude the use of conventional fir-tree blade-to-disc attachments. The added hub thickness necessary for such attachment and concomitant increase in stress could not be tolerated for the large-diameter turbine.

Various approaches for joining turbine blades to discs were explored utilizing the EB welding process. The initial design involved EB welding the blades into inner and outer shrouds, followed by the bladed subassembly to the periphery of the turbine disc. Test specimens were machined using 1/4-in.-thick Alloy 718 plates to represent the shrouds and 1-in. outside diameter by 0.060-in. wall tubing to represent the blades. Holes were machined into the shroud plates to accept the tubes for welding into the test specimens. Round tubing was used to simulate the blades to allow simple rotation of the circular specimen joint during EB welding. Elaborate tracing devices would have been required to track the actual blade contours for the purpose of welding the blade-to-shroud joints.

The test specimens shown in Figure No. II-7 were welded using the following schedule: gun-to-work distance, 2-in.; beam current, 30 ma; voltage, 31 kv; focus current, 5.3 amp; filament current, 16 amp; speed, 60 ipm; filament type, 250 ma; and filament-to-cathode distance, 0.365-in. The EB welds

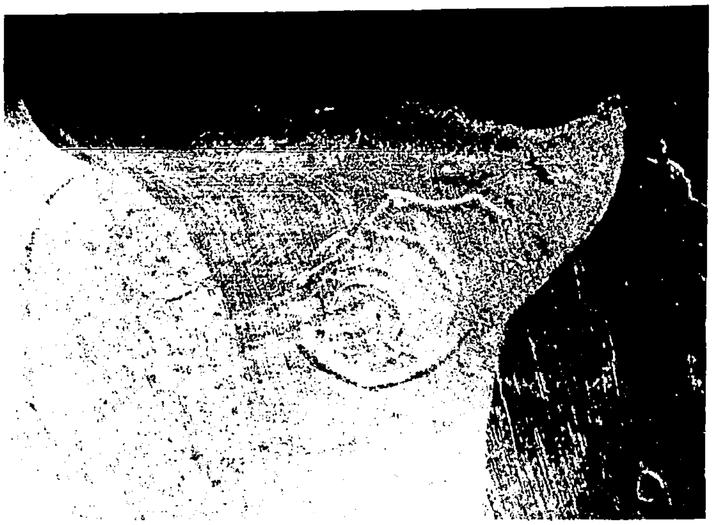

Magnification: 8X

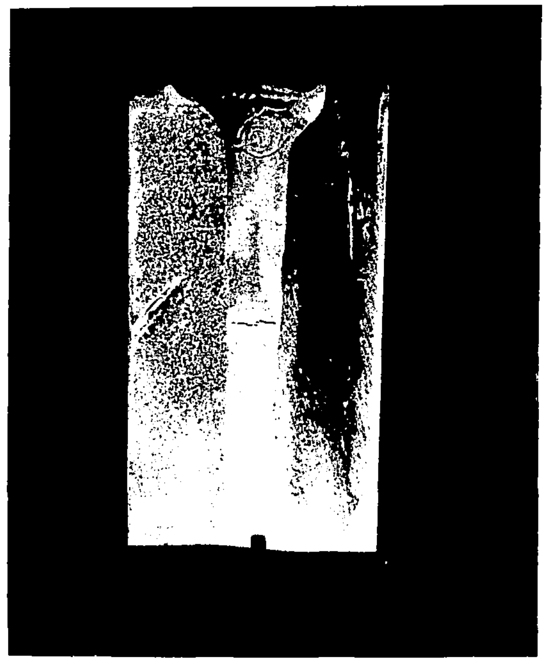

Magnification: 2X

The photograph on the left shows a sub-surface crack in the Alloy 718 just to the left of the "nailhead" shaped weld nugget. The photograph on the right shows a crack in the weld and the "nailhead" effect of the extremely wide weld nugget, which is attributed to the 10-in. focal length between the EB gun and the work piece when welding with 30 kv welding equipment.

Figure II-3

Cross-Sectional View of Defective Electron-Beam Welds of Alloy 718 to Rene' 41

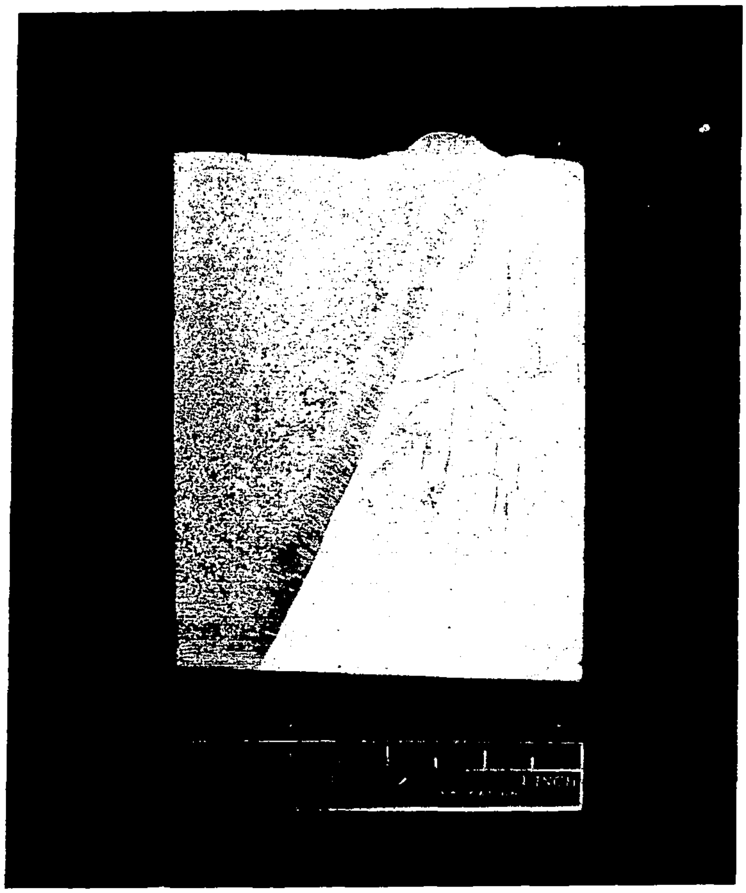

The weld beam was focused at a 70-degree angle from the axis of the center line of the shaft forging, with the gun held at a distance of 3-in. from the weld joint. No beam deflection was encountered.

Figure II-4

Cross-Sectional View of Angled Electron-Beam Weld of Alloy 718 to Rene' 41

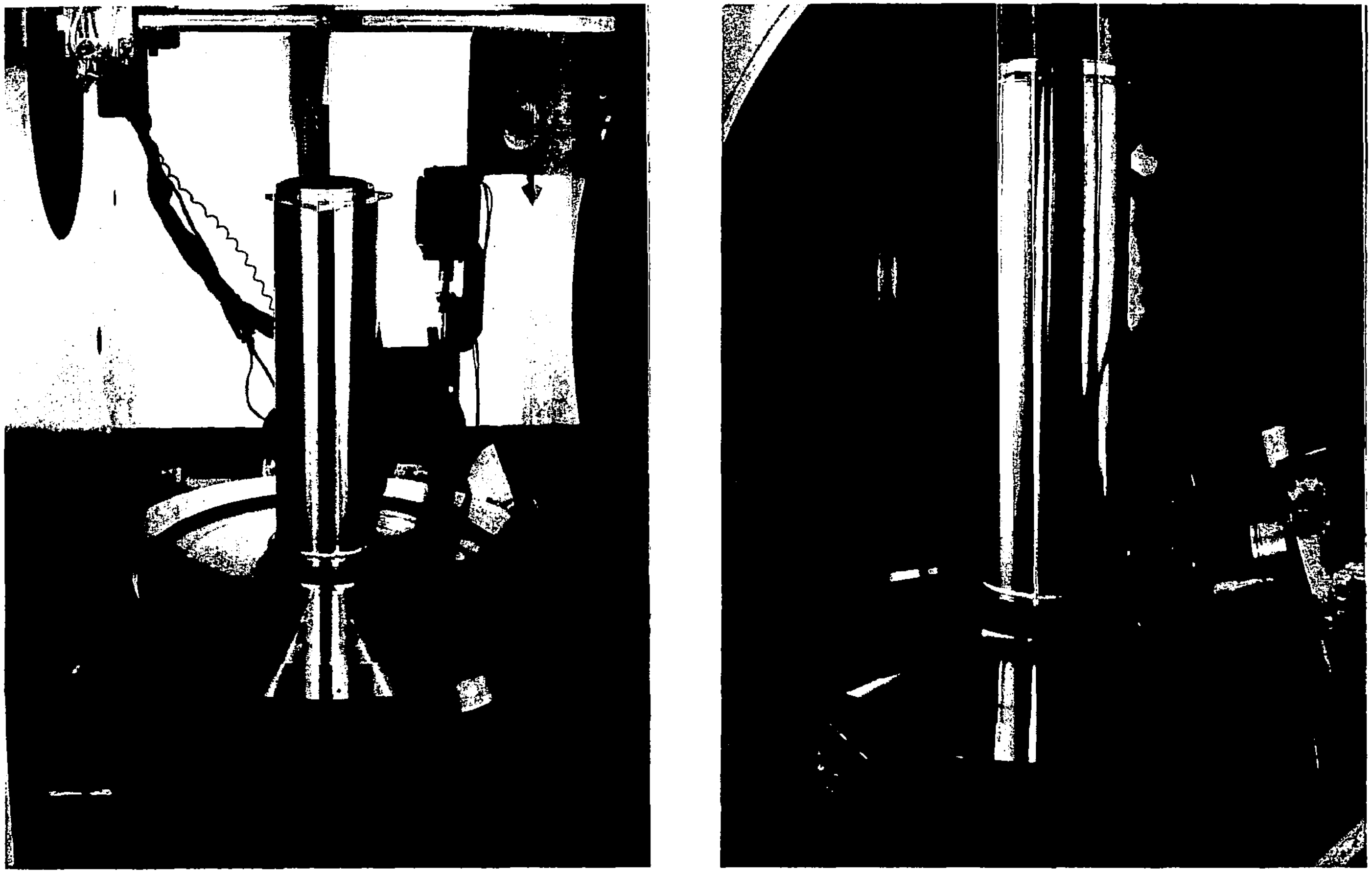

Figure II-5

First-Stage Model I Fuel Turbine Rotor Weldment
Mounted in the Electron-Beam Weld Chamber

At the left is the Alloy 718 disc and Rene' 41 shaft on the rotation fixture. At the right is a close-up view of the EB gun, positioned at 70-degrees to the shaft axis, after making the circumferential butt weld.

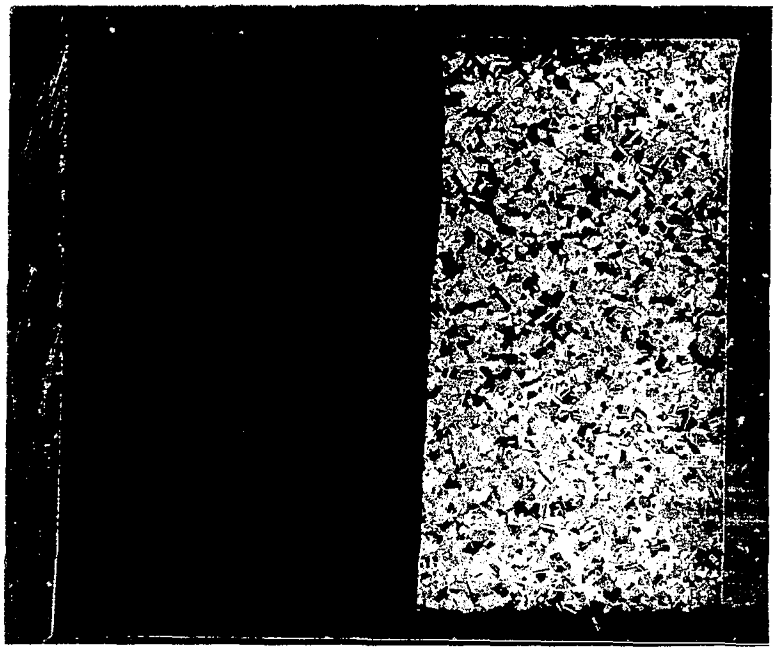

Magnification: 5X

Figure II-6

Cross-Sectional View of an Electron-Beam Weld of
Alloy 718 (on right) to Rene' 41 Produced by a High-Voltage Machine

Magnification: 1.5X

Electron-Beam Weld Joint (Alloy 718 Plate to AISI 347 Tube). Depth of weld penetration is directly proportional to the gap width as indicated by comparing the penetration depth of the weld on the left with the weld on the right. No gap is seen on the left weld, while the right weld shows a 0.006-in. gap.

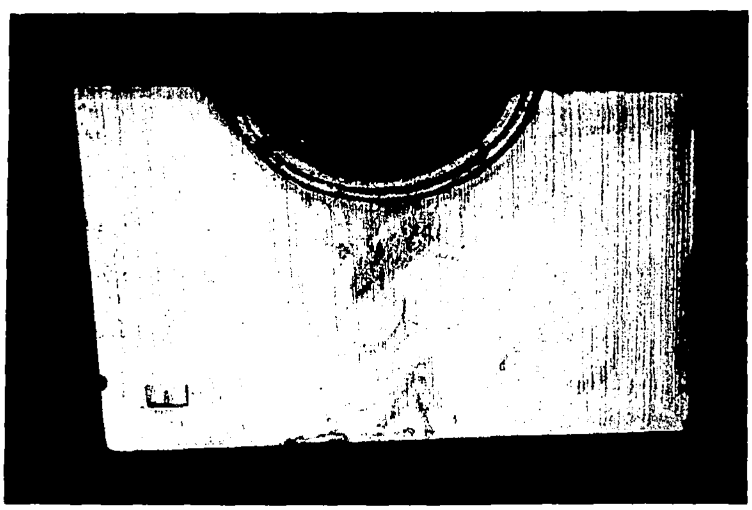

Magnification: 1.5X

The same specimens show the weld bead resulting from the electron-beam impingement which produced the weld seen in the top photograph.

Figure II-7

Simulated EB Welded Blade-to-Shroud Joints Utilizing Tubular Test Specimens and Circular Weld were sound but displayed variations in depth of penetration because maximum shrinkage occurred at the start of the weld leaving a total 0.006-in. gap on the opposite side. This complication, together with the difficulty of tracking an airfoil-contour blade joint, required the investigation of other joint designs.

A new approach was used. Instead of the individual airfoil profile peripheral weld, the blades were inserted into the slotted shroud or rim with an internal plug and electron-beam welded around the periphery of the disc. A simulation of this welded design, welded from one and both sides, is illustrated on Figure II-8. The single pass weld schedule was: gun-to-work distance, 2-in.; beam current, 325 ma; voltage, 50 kv; focus current, 6.1 amp; filament current, 55 amp; speed, 30 ipm; filament type, 500 ma; and filament-to-cathode distance, 0.374-in. The schedule for the double-pass weld was the same except that the speed was increased to 40 ipm to decrease penetration.

The results of the welded test specimens were satisfactory and the blade-to-disc joints were further simplified. Airfoil-shaped slots of the blade-end contour and thickness were machined into simulated discs. This procedure eliminated the inner shroud and plug and also correctly positioned the blade for welding. The specimens were identical to those shown in Figure No. II-8, except that the shroud and plug are part of the disc.

Because of the configurations of the previously welded blade-to-disc specimens and the short tube lengths, the mechanical properties of the joint could not be obtained. To determine the strength of this type of joint, T-shaped test specimens were designed and welded as shown in Figure No. II-9. Two T-specimens were welded from one side and one specimen from both sides, fusing the blade end to the disc block. T-shaped test specimens were also machined and EB welded to simulate the blade-to-shroud joints, thus simulating the shrouded turbine wheel for test purposes. The grooves in the blocks were machined 3/8-in. deep to enable the weld nugget to be placed through the blade shank and permit loading of the weld in shear. One T-specimen was welded penetrating the specimen from one side and one specimen was welded from both sides.

Various design approaches were also evaluated for joining blades to the outer shrouds of the shrouded turbine wheel. The first approach was to weld the blade-to-shroud joint by tracing the joint with the electron beam. As previously described, the welded test specimens contained inconsistent weld penetration at the joints and would require costly tracing equipment; therefore, this approach was discarded.

The next approach was to use a double shroud ring, the outer ring being 0.182-in. thick and the inner ring 0.090-in. thick. The inner ring was slotted to receive the blade and was then EB butt welded to the outer ring to complete the blade-to-shroud joint. The inner shroud ring eroded during welding as shown in the upper view of Figure No. II-10. Excessive distortion of the shroud also occurred because of an off-center weld as shown in the lower view of Figure No. II-10.

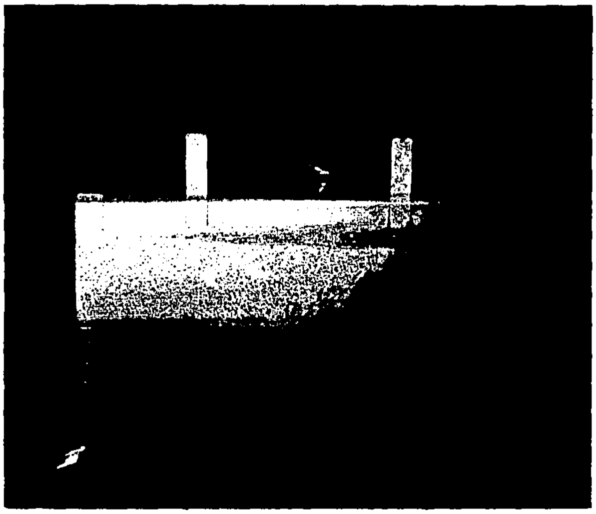

Magnification: 1.2X

Simulated blade-to-disc joint welded from one side by the electron-beam process. Material is Alloy 718.

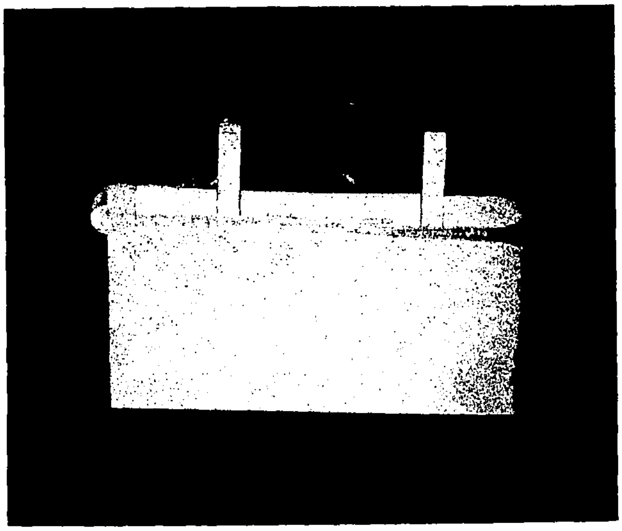

Magnification: 1.2X

Simulated blade-to-disc joint electron-beam welded from both sides and supplemented with a nickel brazing alloy. Base material is Alloy 718; the brazing alloy conforms to AMS-4777 (LMW).

Figure II-8

Simplified Revised Blade-to-Disc Electron-Beam Welded Joint

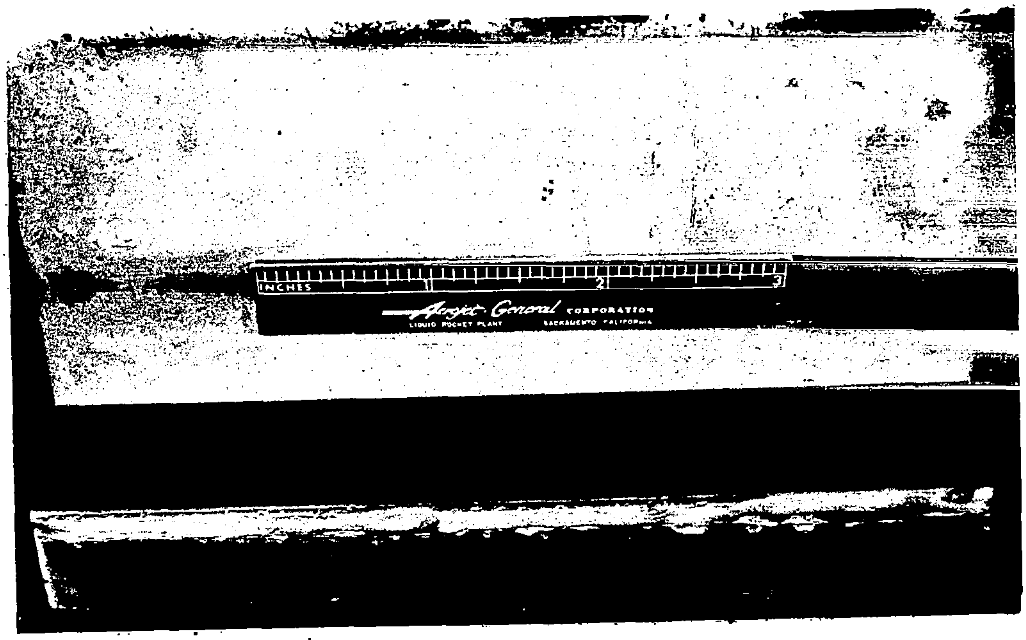

A view of a weldment showing the side of weld beam impingement.

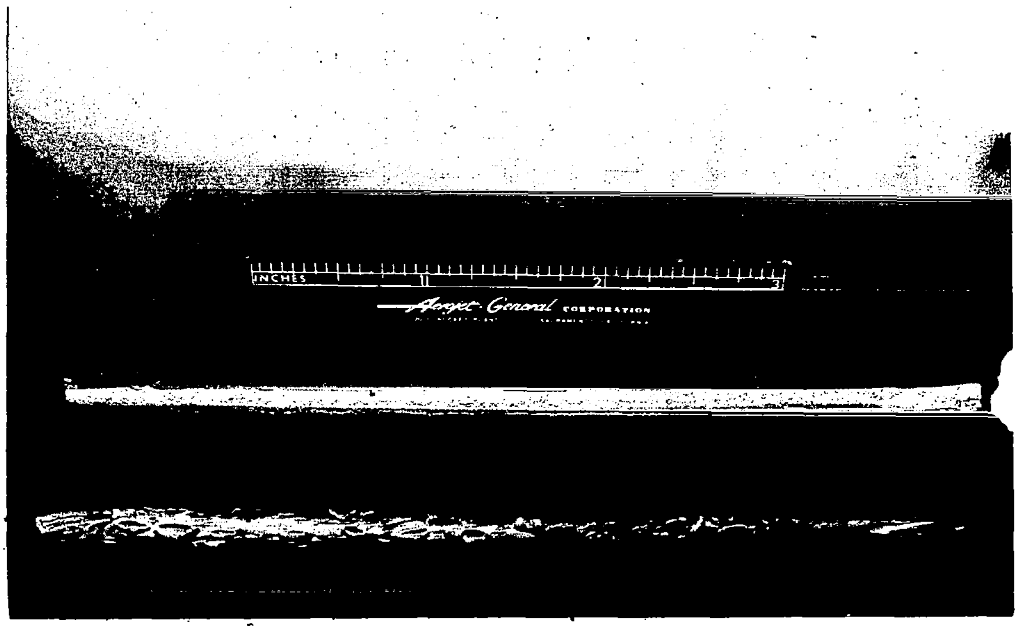

A view of a weldment showing the weld side and also the braze fillet. A braze fillet is incorporated in the welded blade design to eliminate the notch effect at the weld point.

Figure II-9

T-Shaped Electron-Beam Weld Test Specimen

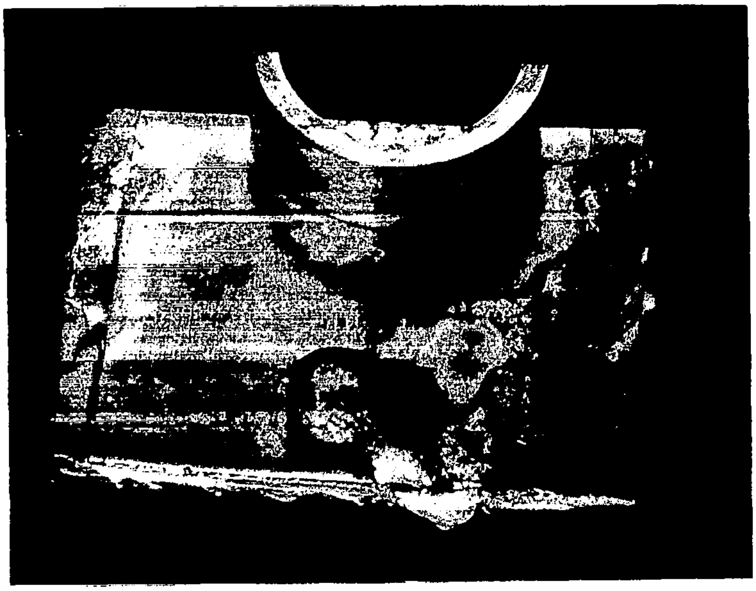

Magnification: 1.5X

View of the outer blade-to-shroud joint. The thin member (0.090-in. thick) eroded during electron-beam welding. All material is Alloy 718.

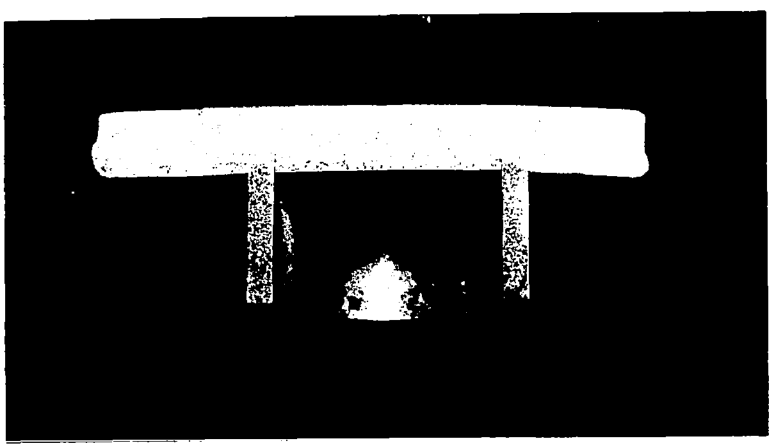

Magnification: 1.5X

Cross-sectional view showing full weld penetration. The welding was performed from both sides.

Figure II-10

Simulated Electron-Beam Joint of Blade to Outer Shroud

These deficiencies were overcome by machining slots in a 1/4-in.-thick shroud to receive the blade and inserting the hollow blade. Plugs were inserted in the ends of the hollow blades at the joint area to prevent EB deflection and to maintain constant cross-sectional areas to prevent weld burn-through. The blade-to-shroud joints shown in Figure No. II-11 present no welding problems and require a minimum amount of tooling to fabricate the parts.

The above electron-beam weld schedules used to weld the blade-to-disc and blade-to-shroud simulated joints were also used for the T-specimens.

A simulated turbine blade assembly with actual production blades was welded to evaluate the welds. A typical assembly is shown in Figure No. II-12. The welded specimen was cross-sectioned through the blades and the welded joints (see Figure No. II-13). After evaluating the simulated weld specimens, production hardware was welded using the weld procedures developed for the test specimens.

The oxidizer reversing vane assembly consists of an inner and an outer shroud and 98 hollow fabricated sheet metal vanes. Slots were machined in the shrouds to receive the vanes. The vanes were assembled in the shrouds and plugs were placed in both ends to facilitate electron-beam welding. The part was rotated in the horizontal plane under the electron-beam gun. Four weld passes, one from each side of each shroud, were required to completely weld the part. The finish-machined reversing vane assembly with the shrouds slotted after welding is shown in Figure No. II-14. The arrows indicate the location of the EB welds where the beam penetrated into the shrouds.

The oxidizer turbine rotor disc assemblies were EB welded in the same manner (i.e., circular welds in the horizontal plane). As previously described, the disc-to-blade joints had slots machined into the disc rim to receive the blades thereby making the blade plugs an integral part of the disc. Separate plugs were required at the blade-to-shroud joints. Braze fillets were made at both the disc and shroud joint areas to provide dampening and to eliminate the notch effect.

Several braze alloys were investigated including Nioro (82% Au, 18% Ni), nickel braze alloy AMS 4777, and Wall Colomonoy AMS 4777 (LMW). The latter alloy displayed the best wet and flow characteristics forming uniform fillets and penetrating the joint gaps. The brazing was done at 1925°F ± 25°F for 10 minutes in vacuum. This also provided solution treatment of the Alloy 718. Aging was in accordance with AGC Condition B. The aged hardness of specimens was R_c 39-41 and represents age response normally obtained for the same material solution treated for one hour at 1925°F.

Completed first-stage and second-stage oxidizer pump turbine rotors are shown in Figure No. II-15. Two smaller turbine rotor assemblies of the Titan II first-stage and second-stage engines are also shown for size comparison. The areas where EB welds join the blades to the disc and shroud are

Top view of Alloy 718 tube welded to shroud joint. The tube was plugged to prevent beam deflection and to maintain a constant cross-section area.

Bottom view of the same joint shows no evidence of erosion or weld burnthrough.

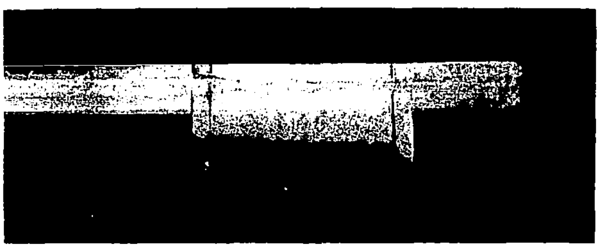

Cross-sectional view of the same specimen shows the weld nugget through the center of the shroud.

All Magnification: 1.5X

Figure II-11

Electron-Beam Weld of Simulated Final Blade-to-Shroud Joint Design

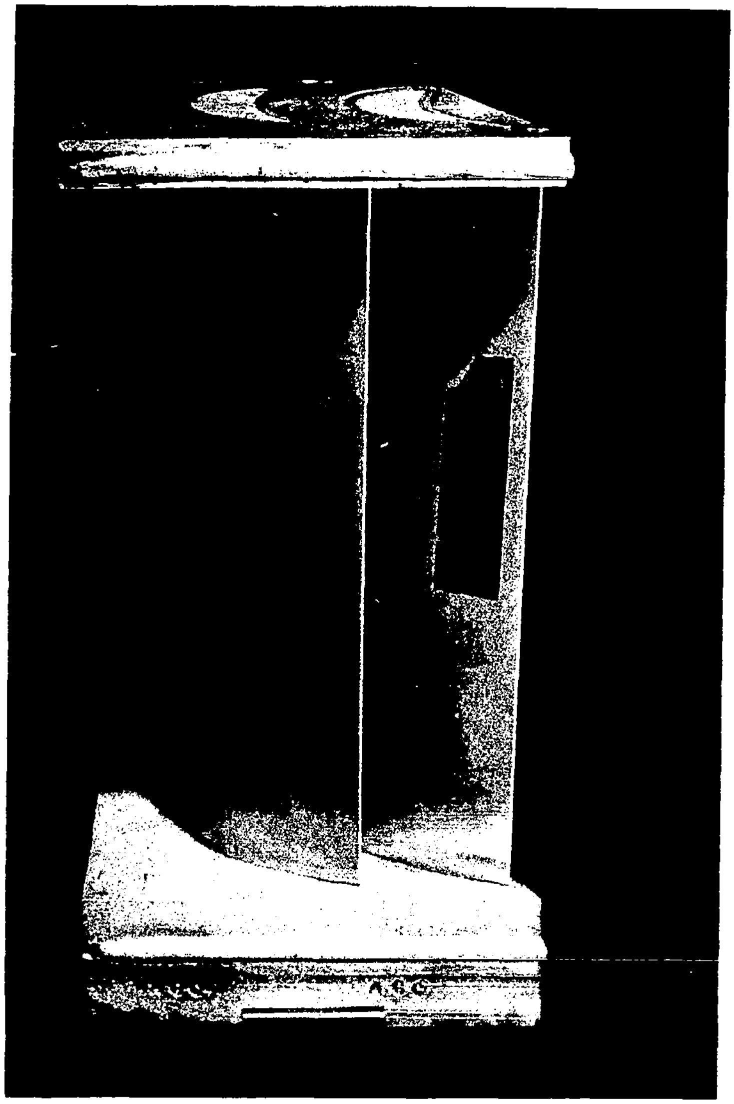

Magnification: 3/4X

The electron-beam welds were made from both sides of the disc and shroud joints.

Figure II-12

Electron-Beam Welded Turbine Disc-to-Blade and Blade-to-Shroud Weld Specimen

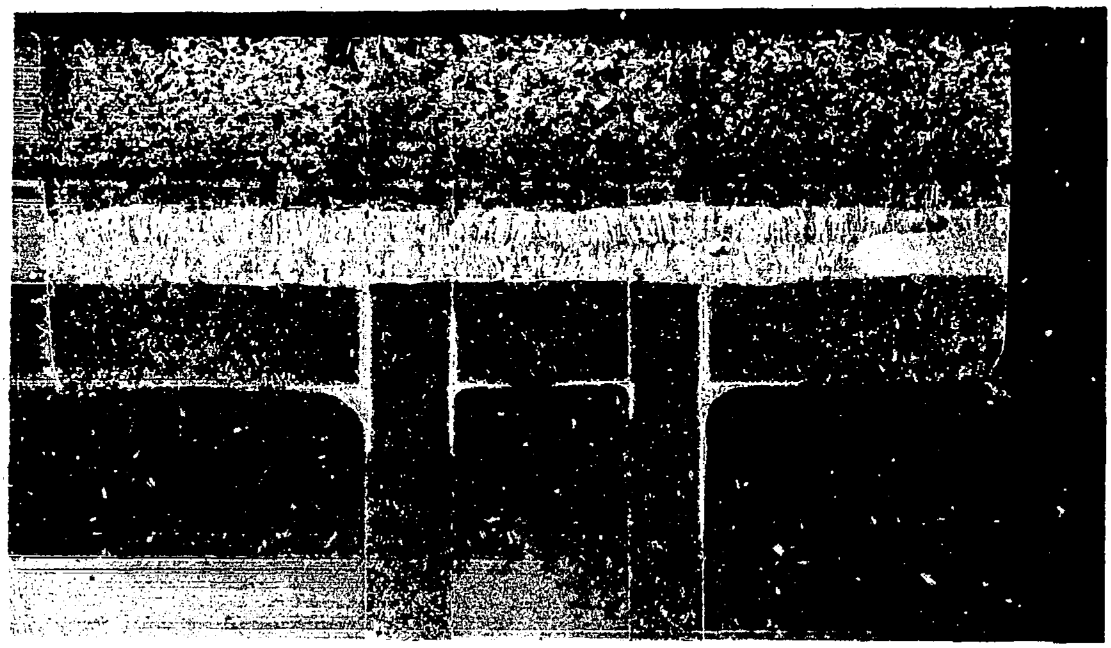

Magnification 6X

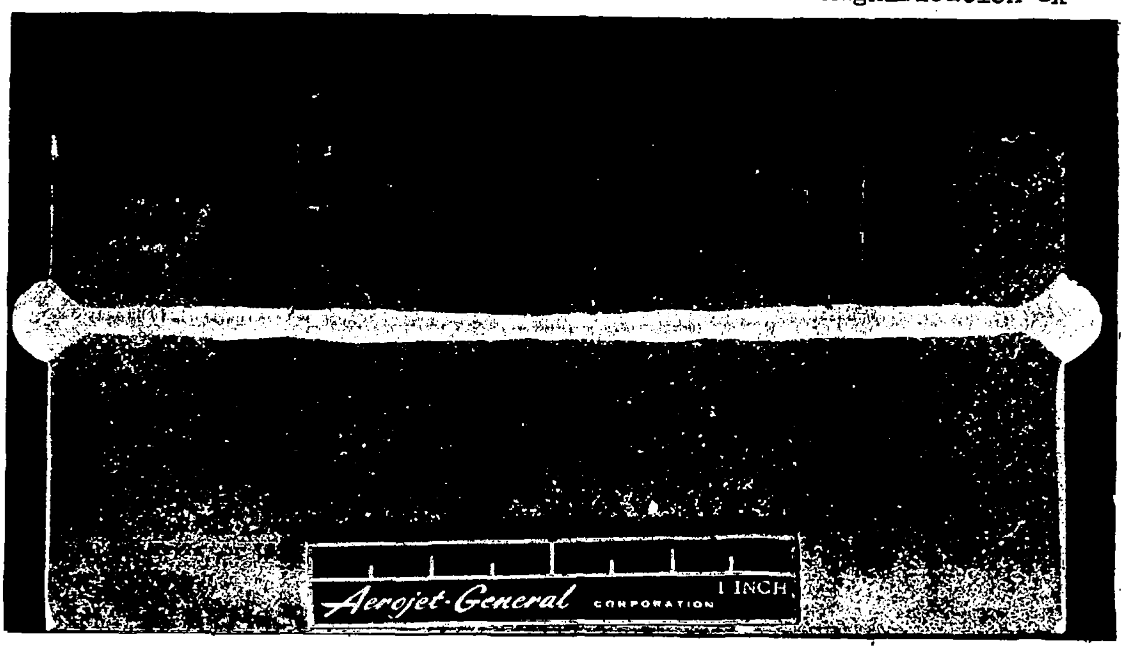

The top view is a section through the shroud near the trailing edge of the blade. The specimen was brazed prior to sectioning.

Figure II-13

Cross-Sectional Views of Blade-to-Shroud and
Blade-to-Disc Electron-Beam Welds

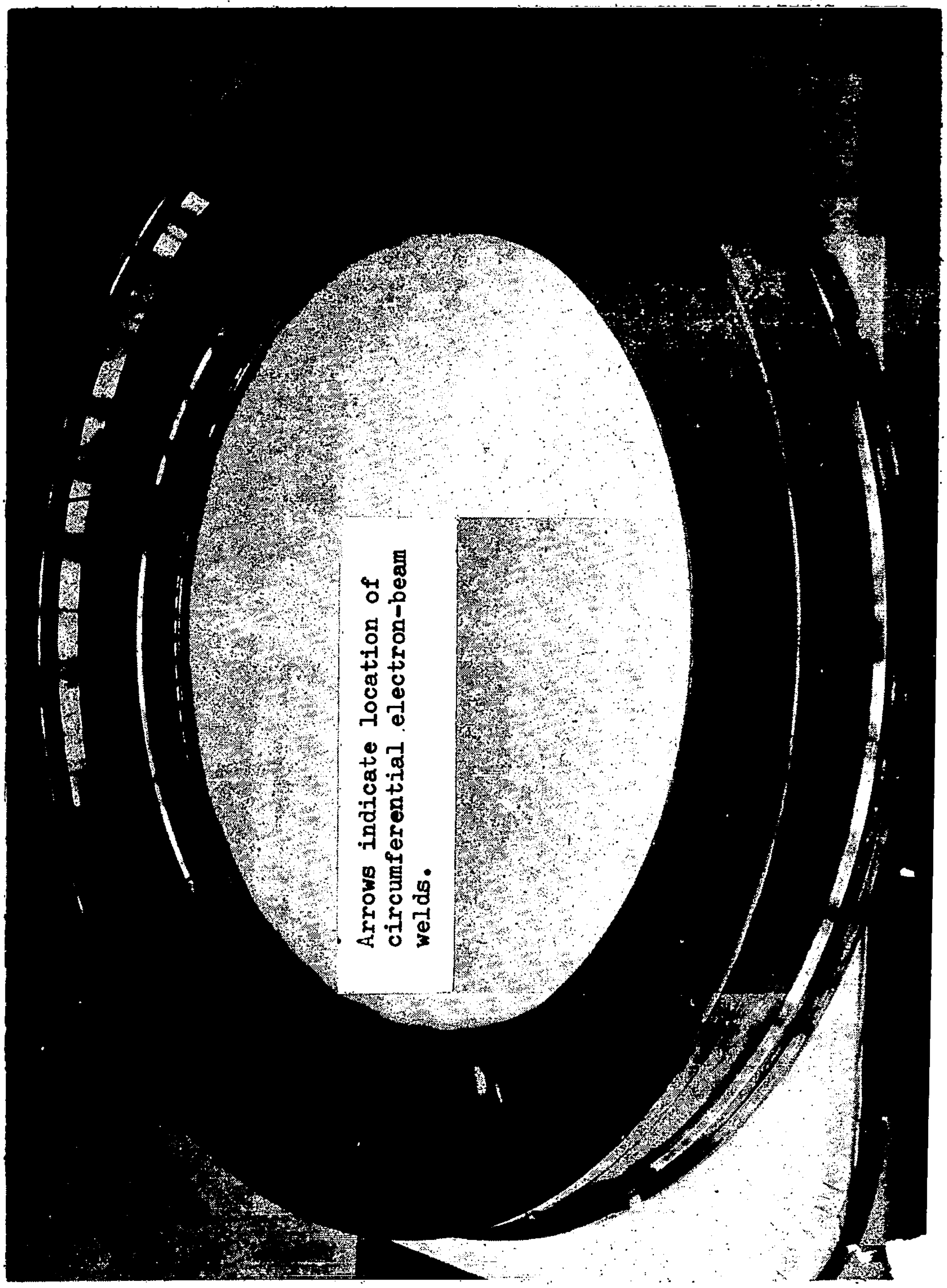

Figure II-14

Oxidizer Reversing Vane Assembly (Approximately 1/4 Scale)

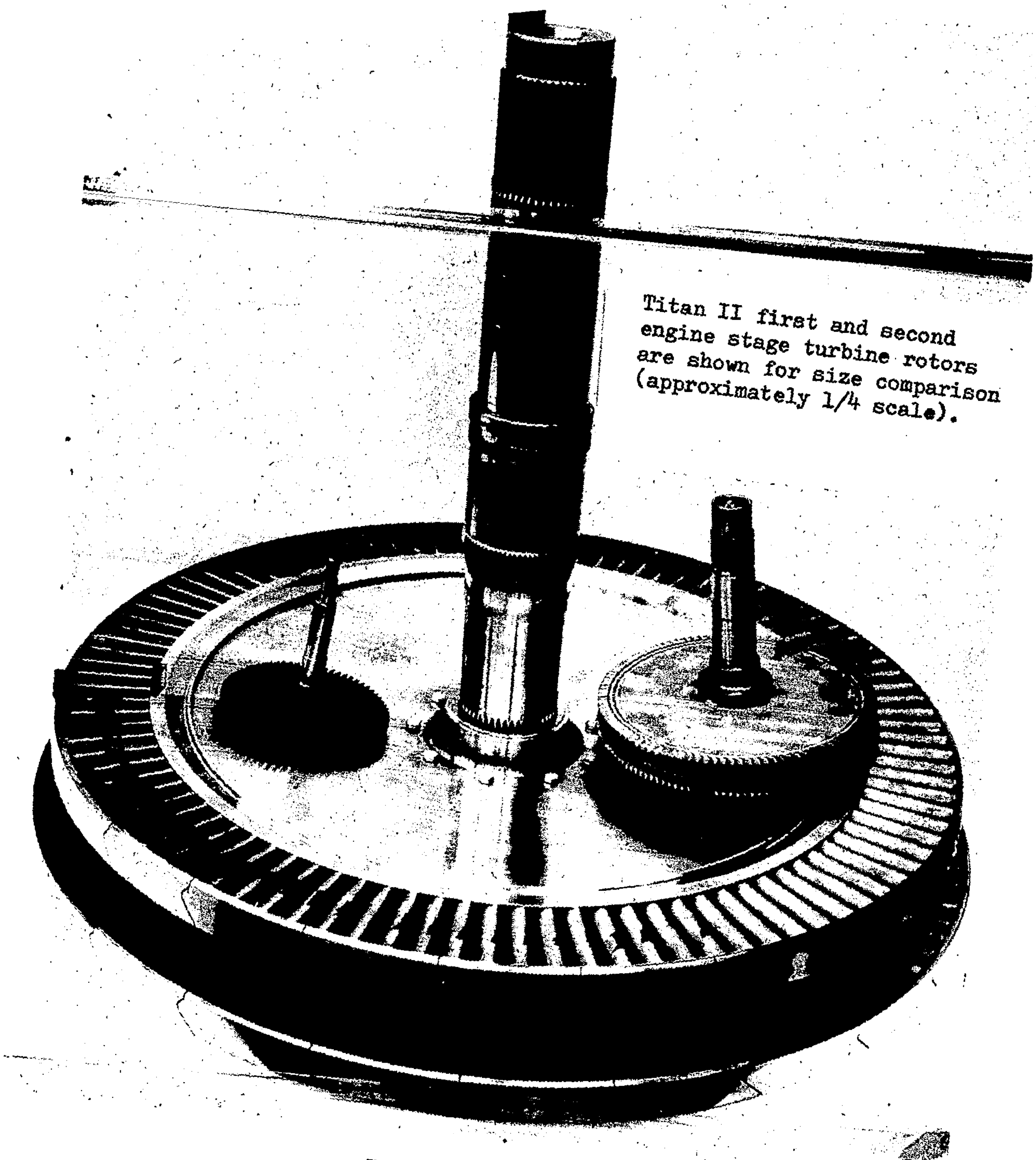

Figure II-15
M-1 First-Stage and Second-Stage Electron-Beam Welded Oxidizer Turbine Rotors

indicated by arrows.

C. FUEL TURBINE ASSEMBLY

The fuel turbine assembly was EB welded in a manner similar to that described for the oxidizer assembly. However, chevron-shaped platforms were integrally forged on both ends of the Alloy 718 blades. Therefore, the slotted disc-hub procedure used with the oxidizer discs was not used with the fuel turbine.

Two blade-to-disc segments simulating the fuel turbine disc assemblies were electron-beam welded. The segments consisted of six of the platformed blades welded to the disc sections from both sides to equalize weld shrinkage. A sketch of the weld test specimen is shown in Figure No. II-16.

Round specimens (1/2-in. diameter) were machined from the bladed segments and heat treated prior to final machining of Standard R_3 (Federal Standard 151a) test specimens. The weld joints were centered in the reduced areas of the test specimens. Tests were conducted at -320°F, room temperature, 800°F, 1200°F, and 1350°F. Specimens tested at cryogenic and elevated temperatures were allowed to soak for 15 min prior to testing. The results of these tests are discussed in the section under Mechanical Testing.

A completely EB welded second-stage turbine rotor is shown in Figure No. II-17. The weld (shown by the arrow) was made from both sides of the disc to maintain uniform weld shrinkage the full depth of the weld joint. To obtain uniform close tolerances at the blade-to-disc joints, the blades were nested in the weld fixture, and the blade platforms were machined to fit the turbine-disc contour. After machining, the fixtured blades and disc were thoroughly cleaned and assembled for welding. The turbine disc assembly was EB welded by rotating the part horizontally at 10 ipm under the weld gun, which was positioned 10-in. from the joint. The assembly was continuously tack welded on one side using 140-kv acceleration voltage and 6-ma beam current. The part was then reversed and the opposite side of the joint welded. The electron-beam current was increased to 35 ma for the penetration-fusion passes.

The Model I first-stage fuel turbine disc assembly consisted of an electron-beam welded Alloy 718 disc welded to a Rene' 41 shaft. Turbine blades were then integrally machined into the disc. The design of the Model II differed from the Model I disc assembly. The Model II first-stage blades were electron-beam welded to the turbine disc in the same manner as that used for the second-stage disc assembly. The same machining and welding procedures were applied. However, every other blade outer shroud platform was TIG welded together and a Rene' 41 stub shaft was welded to the disc (see Figure No. II-18). The arrow in the upper left of Figure No. II-18 indicates a TIG weld joining the outer blade platforms. The EB weld joining the blades to the periphery of the disc is shown by the white arrow. The EB weld build-up at the blade joints has been removed.

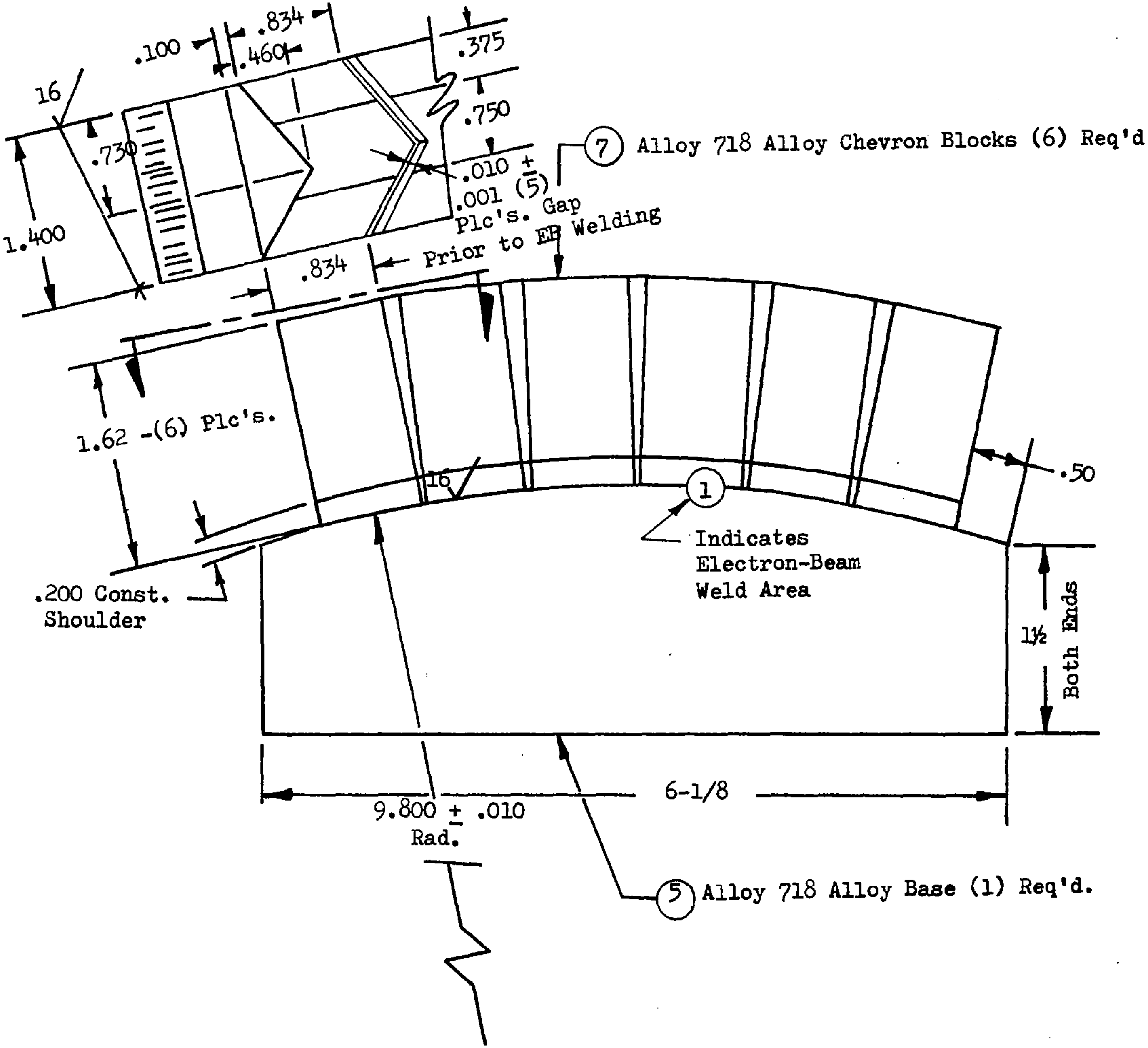

Figure II-16

Fuel Turbine Blade-to-Disc Test Specimen

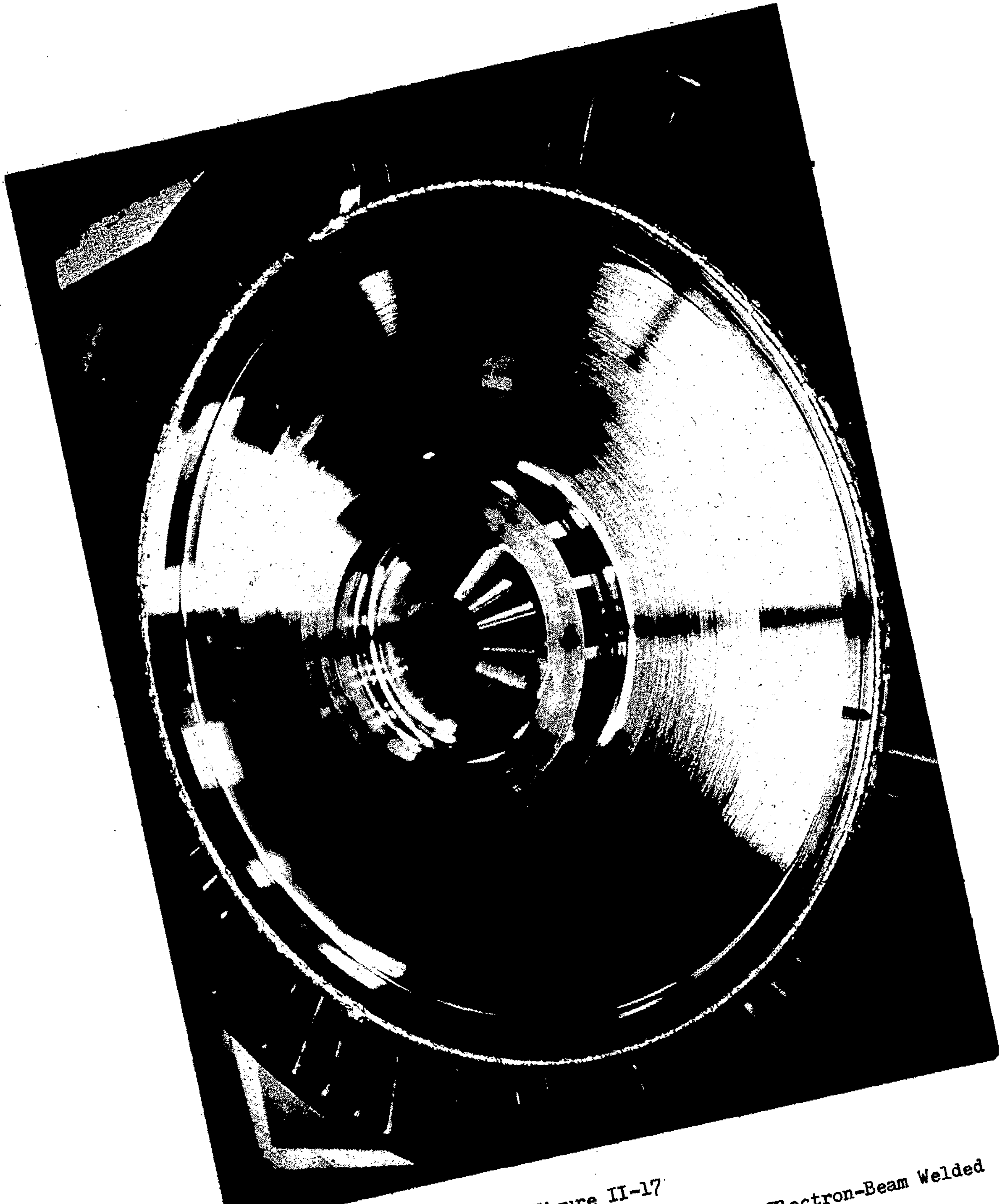

Figure II-17

Disc Assembly Electron-Beam Welded

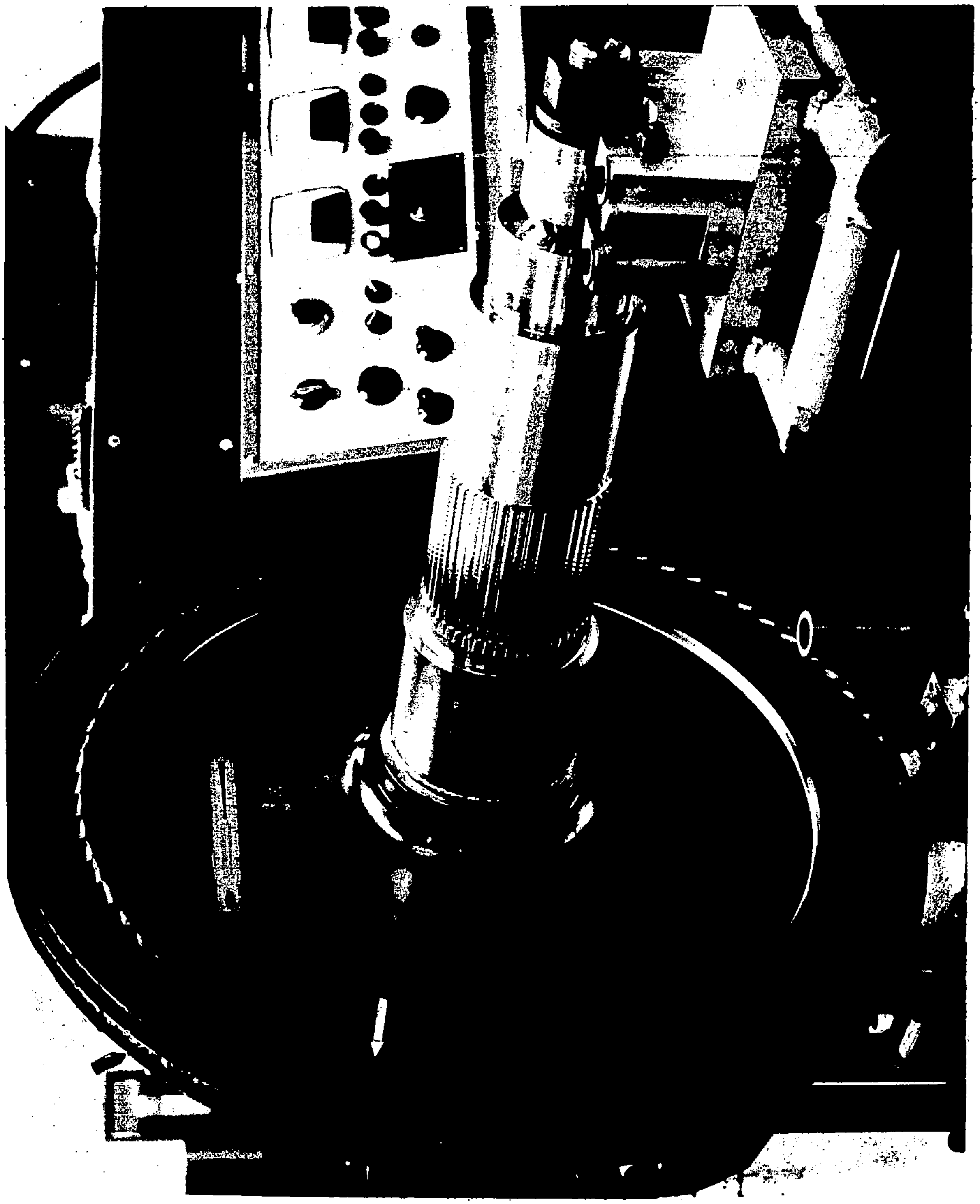

Figure II-18

M-1 First-Stage Model II Fuel Turbine Rotor
Disc Assembly Electron-Beam Welded

The Alloy 718 disc to Rene' 41 shaft weld is shown by an arrow on the shaft. The unit is located in the electron-beam weld fixture that is used to rotate the part while welding the disc-to-shaft joint. Alignment of the shaft to the disc was maintained by a step-type back-up ring on the shaft and a through bolt to hold the parts in position. The weld schedule to join the disc to the stub shaft for the tack weld was: acceleration voltage, 140 kv; travel speed, 16 ipm; gun-to-work distance, 10.5-in. and beam current, 6 ma. The beam current was increased to 35 ma for the penetration-fusion pass.

Weld shrinkage experienced was 0.009-in. lineal shrinkage of the disc-to-shaft weld joint and 0.018-in. diametral shrinkage on the blade-to-disc weld.

D. FUEL PUMP ROTOR WELDING

The M-1 fuel pump rotor shaft is made up of four large alloy 718 forgings joined by TIG welding. This welding is described in Part III of this report. The EB welding of this unit was also evaluated as an alternative method for possible improvement of weld quality and cost reduction.

A series of bead-on-plate welds were made on 1.3-in. thick Alloy 718 plate to establish an optimum EB weld schedule for joining flat plates and ring forgings. Figure No. II-19 shows a cross-section of the weld test plate containing five weld nuggets produced with slight modifications to the weld schedule. Weld No. 1 failed to penetrate the test plate using the weld schedule shown. The welding speed was reduced from 60 ipm to 50 ipm for Weld No. 2. Weld back-up strips were not used until complete weld penetration was obtained. To attain this on Weld No. 2, a weld back-up strip was used with the same weld schedule that was used to make Weld No. 3. The focus current was increased from 6.73 amp to 6.83 amp to make Weld No. 4. This slight modification to the weld schedule slightly reduced the depth of weld penetration and widened the nugget and weld "nail head." Weld No. 5 was produced with a reduction of weld focus current to 6.63 amp. This modification produced a narrow weld nugget and "nail head." It also increased the weld depth of penetration into the weld back-up strip. Another weld was made with the focus current reduced to 6.53 amp. The depth of weld penetration decreased and the nugget width increased from Weld No. 5. This verified that the schedule used to produce Weld No. 5 was optimum. The energy expended to produce Weld No. 5 was approximately 19,200 joules/in.

A photomacrograph and a photomicrograph of Weld No. 4 of Figure No. II-19 are shown in Figure No. II-20. Minute cracks existed in the parent metal below the weld nugget "nail head" as shown in the view to the right.

During EB welding, there is a possibility of the beam being extinguished by one of several causes (e.g. power malfunction, metal vapor deposition in EB gun, and outgassing), thereby resulting in a weld crater in the joint. A weld-repair method was established using a 1.3-in.-thick butt joint. The first weld was initiated at the end of the specimen and made 2.5-in. long, then the power was shut off. A second weld was initiated at the same point as the

Figure II-19

Weld Test Block Showing the Effect of Varying Specific Parameters

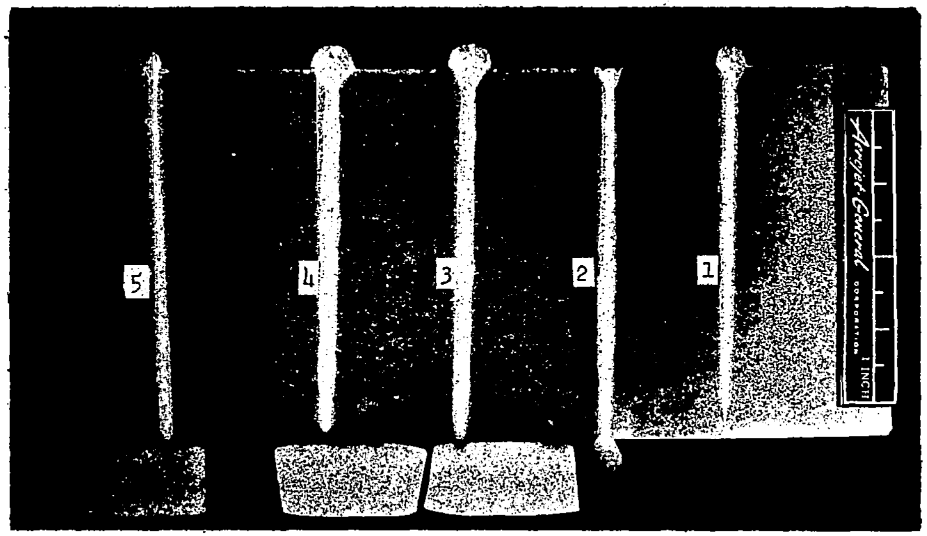

Welds No. 1 to 5 demonstrate the effect of minor electron-beam weld schedule changes on the nugget configuration. The test block is 1.3-in. thick. The schedules used are shown below.

Weld No.	Gun to Work Dist. (in.)	Beam Current (ma)	Voltage (kv)	Focus Current (amp)	Filament Current (amp)	Speed IPM	Filament Type (ma)	Filament to Cathode (in.)	Anode to Cathode (in.)
1	2	320	50	6.73	55	60	500	.374	.050
2	2	320	50	6.73	55	50	500	.374	.050
3	2	320	50	6.73	55	50	500	.374	.050
4	2	320	50	6.83	55	50	500	.374	.050
5	2	320	50	6.63	55	50	500	.374	.050

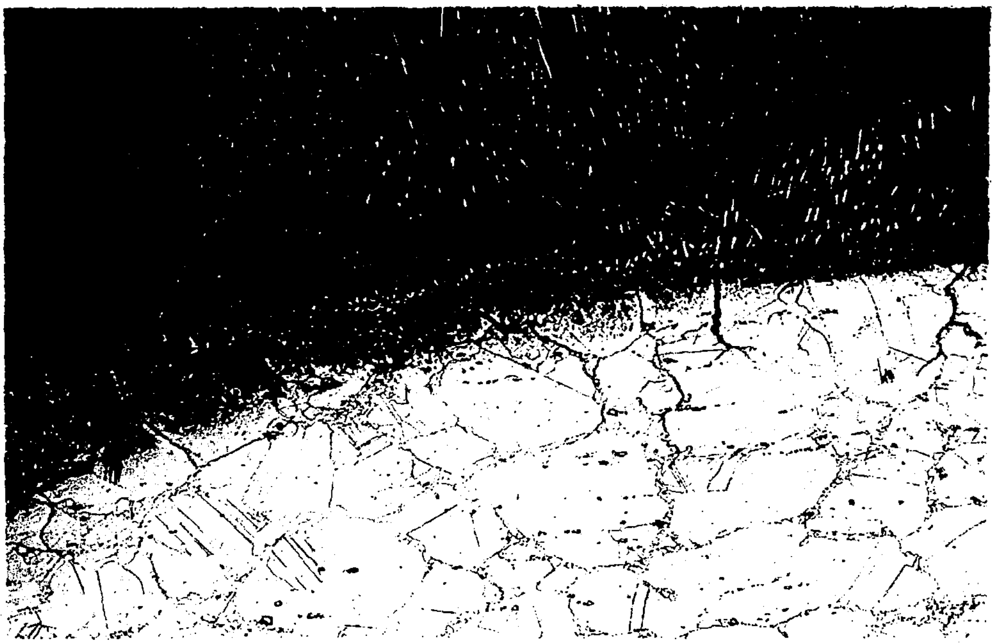

Magnification: 100X

The photomicrograph was taken of the specimen below. Micro-cracks are present below the nail head approximately 0.090 below the joint surface.

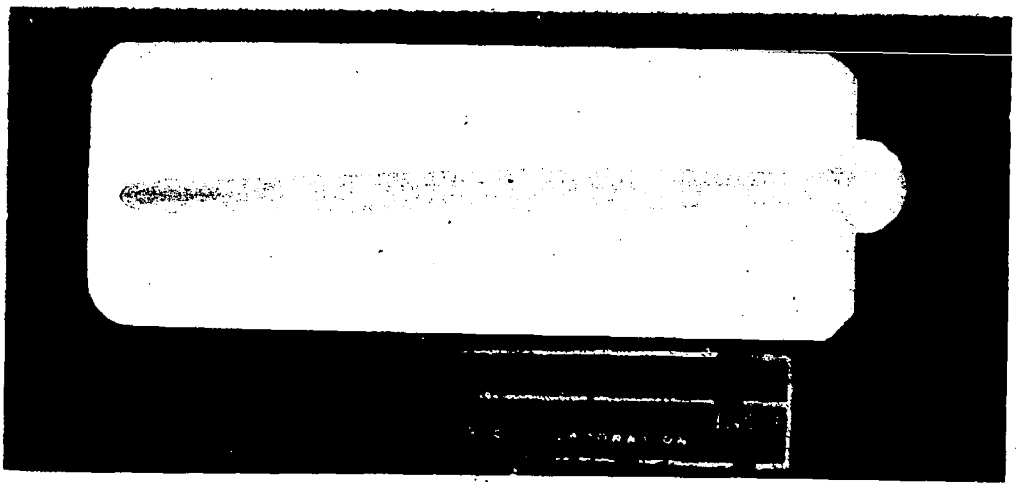

A photomacrograph of an electron-beam bead-on-plate weld having insufficient weld penetration and a wider weld nugget than is desired for electron-beam welding of Alloy 718.

Figure II-20

The Weld Contour and Microstructure of Weld No. 4
(See Figure No. II-19)

first and was 3.25-in. long. A third weld was started at the same location as the first two and welded the full length of the joint. The specimen was welded using the schedule shown in Figure II-20 for Weld No. 5. No changes were made to the schedule for the re-welding passes.

The weld-repaired areas in the plane of the weld nugget are shown in Figure No. II-21. The arrows indicate the areas where the beam was extinguished. Shown in Figure No. II-22 are the types of minute spherical voids found in the weld-repaired area. Acceptance of such voids would have to be evaluated with regard for the particular hardware and service involved.

Several sets of ring forgings of different configurations were electron-beam welded using the optimum weld schedules previously described (Weld No. 5). Figure No. II-23 shows two sets of welded ring forgings. A loose back-up ring was used for the specimen to the left. An integral step-type back-up lip machined in the forging face was used for the butt joint of the specimen on the right. Several TIG tack fillet welds at the back-up rings were used to hold the parts in alignment for electron-beam welding. Two sets of weld restraint test forgings were also EB welded to simulate stresses anticipated in the welding of the fuel pump rotor. The welding face of one forging of each set contained a step-type lip for alignment and electron-beam decay purposes, as shown in Figure No. II-24.

During the EB welding of the ring forging specimens, it was discovered that small globules of weld splatter adhered to the fixture rolls and to the ring forging bearing surfaces, thereby interfering with rotation of the parts. The slippage problem caused by the weld splatter was resolved by covering the fixture rolls with masking tape (see Figure No. II-25). The forging bearing areas were also masked; however, this is not shown in the photograph. The presence of masking tape did not affect the welding function in the vacuum chamber. The photograph shows a welded restraint weldment positioned in the electron-beam weld chamber (a portion of the gun is visible). The weldment was suspended by four rolls and rotated by the drive roll at the lower left of the specimen. Thrust bearings were used at the forging faces to maintain proper joint alignment under the gun.

The EB welded ring forgings shown in Figure No. II-23 were cross-sectioned and the welds examined. A cross-sectional view of a weld is shown in Figure No. II-26. The narrow weld nugget "spike" and "nail head" are indicative of an optimum electron-beam welding schedule. This is necessary to minimize the microcracks under the "nail head" in weldments of Alloy 718 in this heavy thickness (1.3-in.).

The enlarged views of this electron-beam weld are shown in Figures No. II-27 and II-28. Microcracks generally occurred to approximately 0.090-in. below the beam impingement surface of the part. The "spike" of the weld is free of any defects. Design criteria for heavy thickness EB welded hardware can eliminate this zone of potential cracking. This can be accomplished by excess stock removal of 0.100-in. from the beam impingement surface or by the use

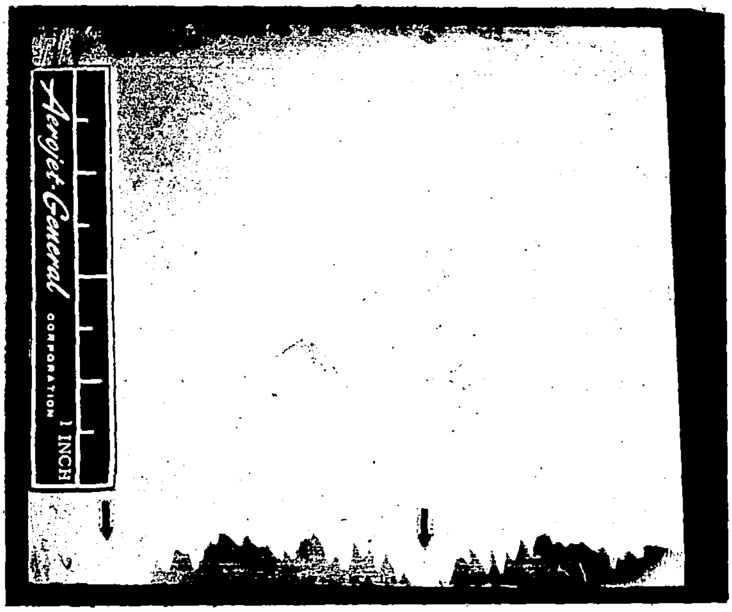

Minute spherical voids are scattered in the repaired area. The voids vary in sizes from 0.003 to 0.009-in. diameter. At the extreme left of the photo the weld was rewelded twice shown by the arrow. Between the arrows is an area which was re-welded once. The area on the right was welded in one pass.

Figure II-21

Simulated Weld Repair in an Alloy 718 Butt Weld

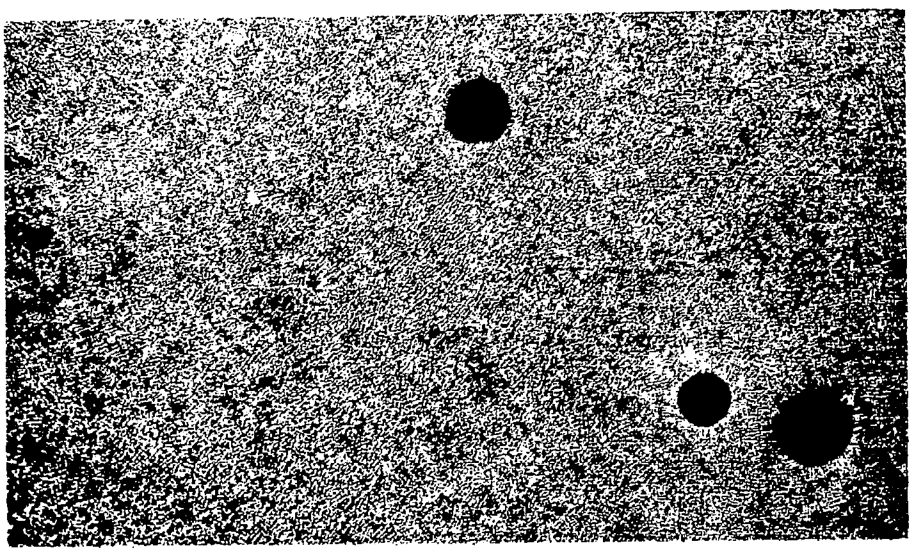

An enlarged view of the spherical voids in the electron-beam weld repaired area. The voids ranged from 0.003 to 0.009-in. diameter.

Figure II-22

Spherical Voids in Repair-Welded Alloy 718

Figure II-23

Electron-Beam Welded Alloy 718 Ring Forgings

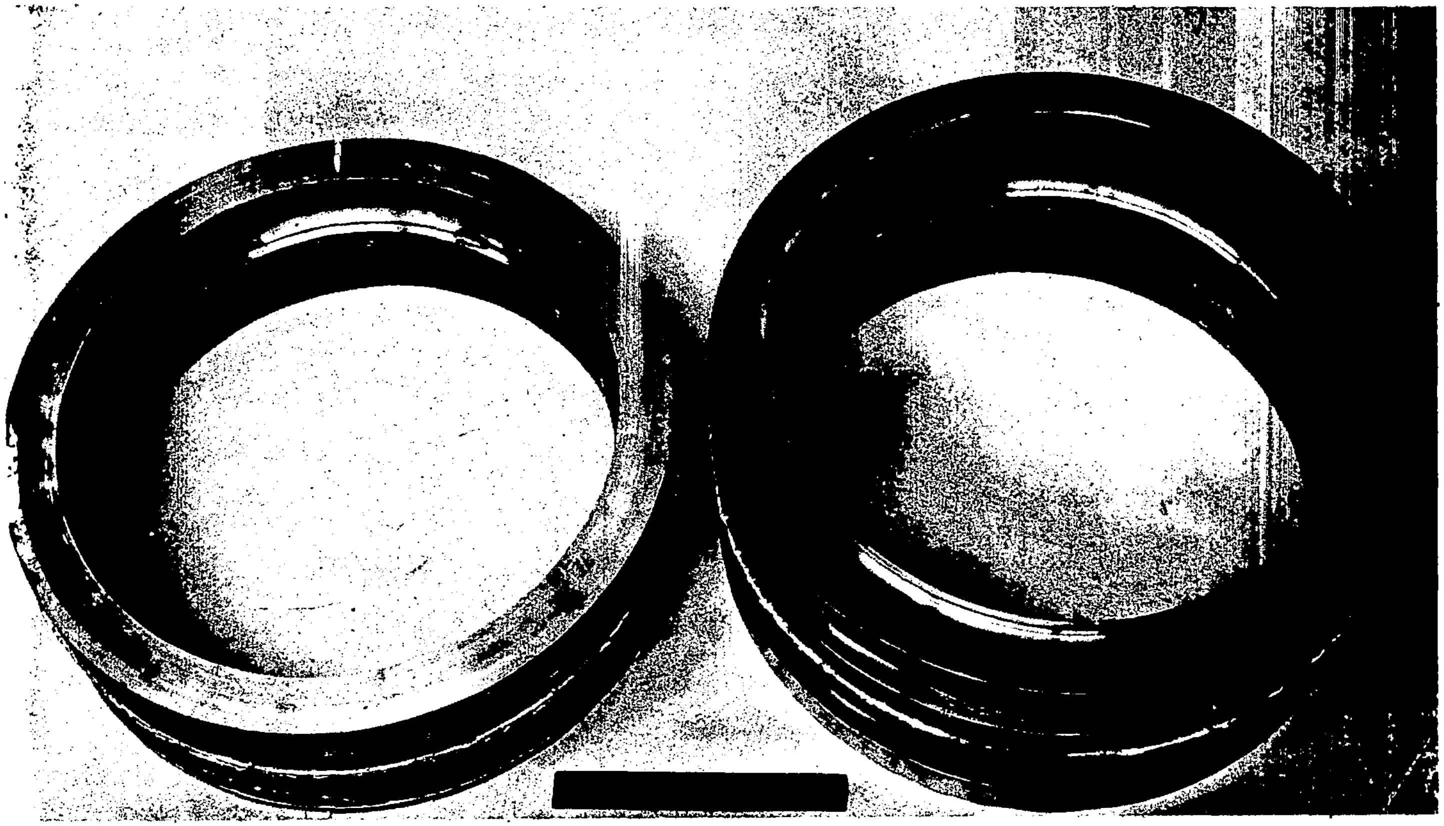

A separate backup ring was used on the left assembly and a machined step backup on the right assembly.

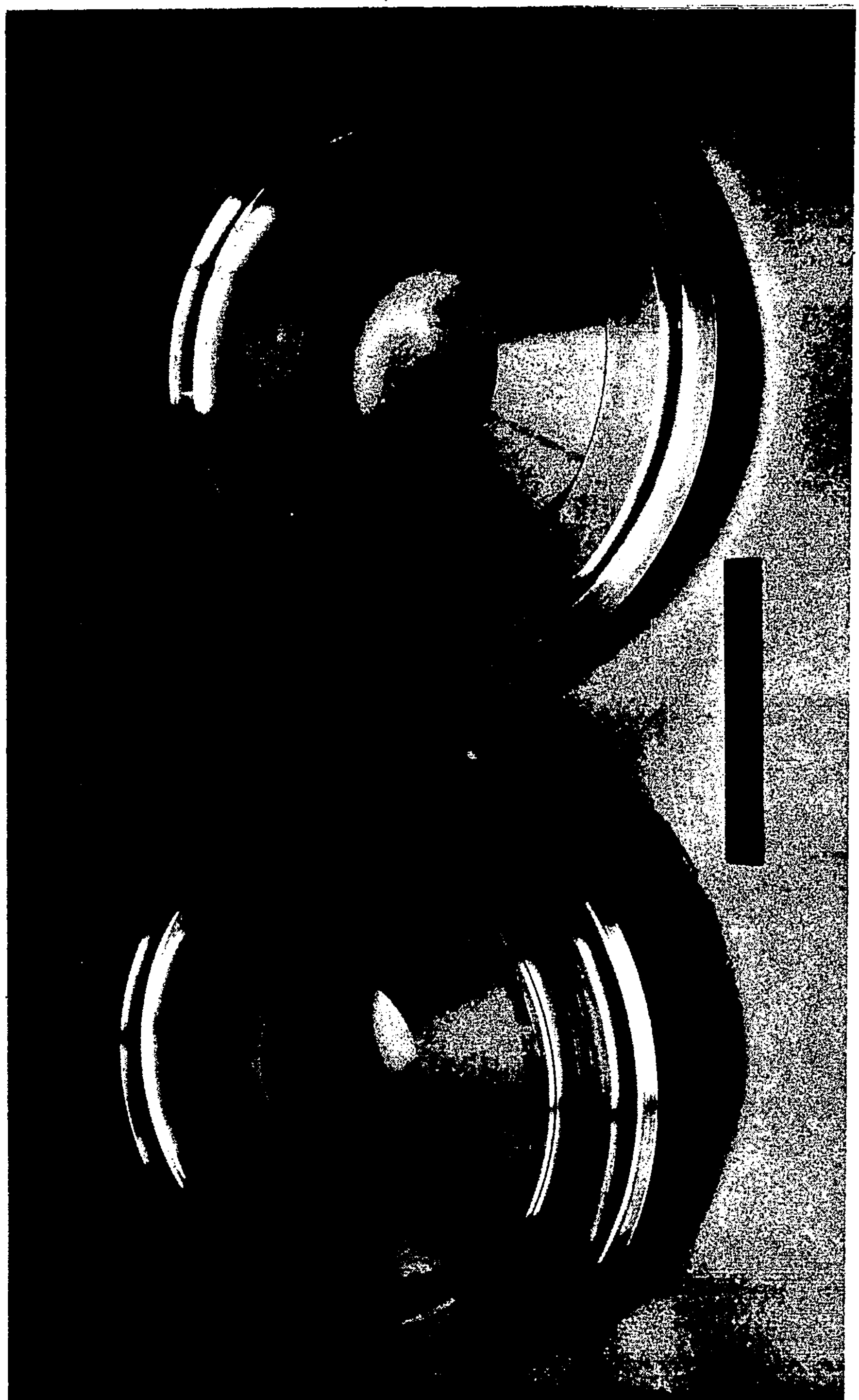

Figure II-24

Weld Restraint Test Forgings Showing the Machined Back-Up Step

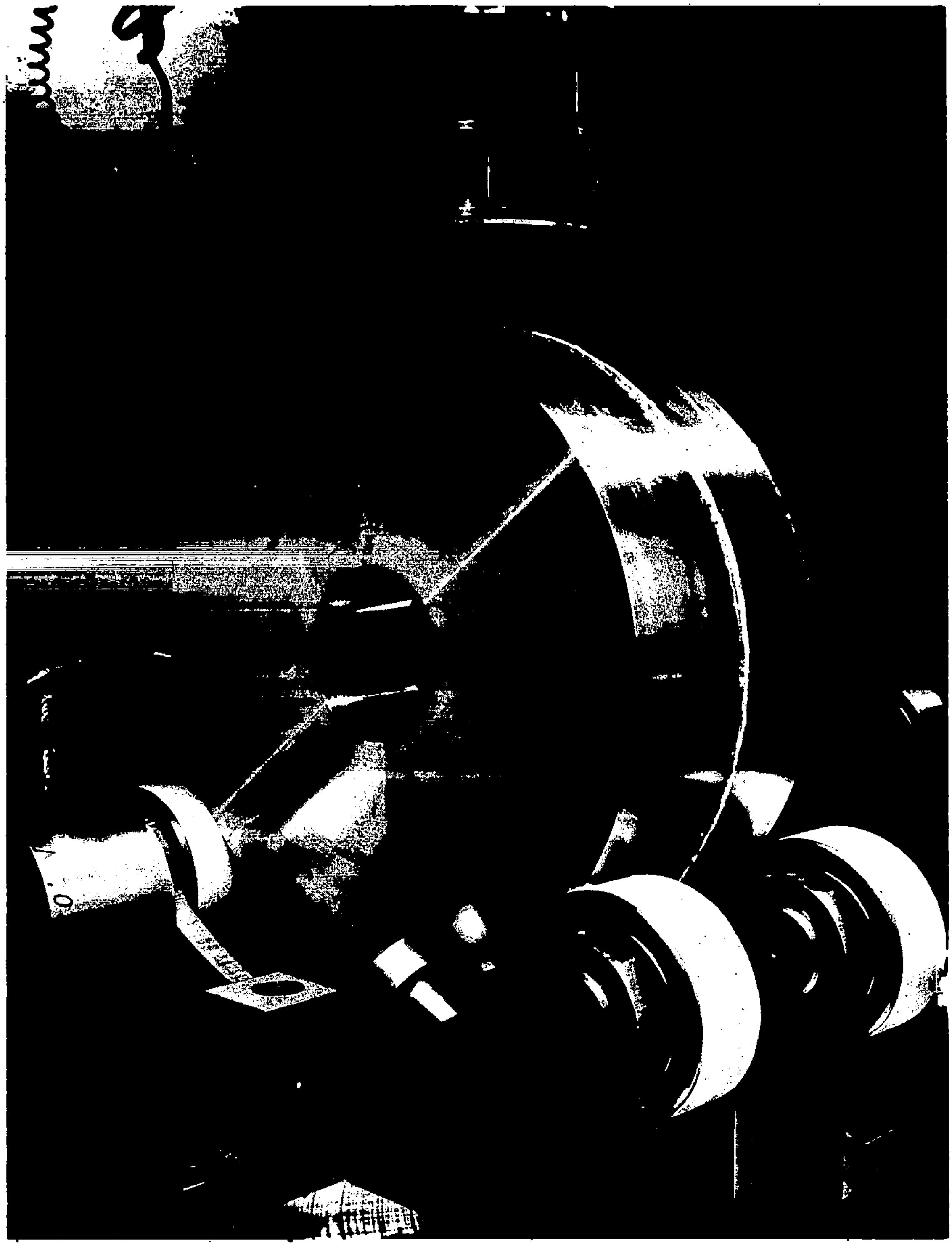

Figure II-25

Weld Restraint Forging in Electron-Beam Weld Chamber

Magnification: 5X

The weld bead build-up and back-up ring were machined off to facilitate non-destructive testing.

Figure II-26

A Cross-Sectional View of an Electron-Beam Butt Weld Joining Two Alloy 718 Ring Forgings

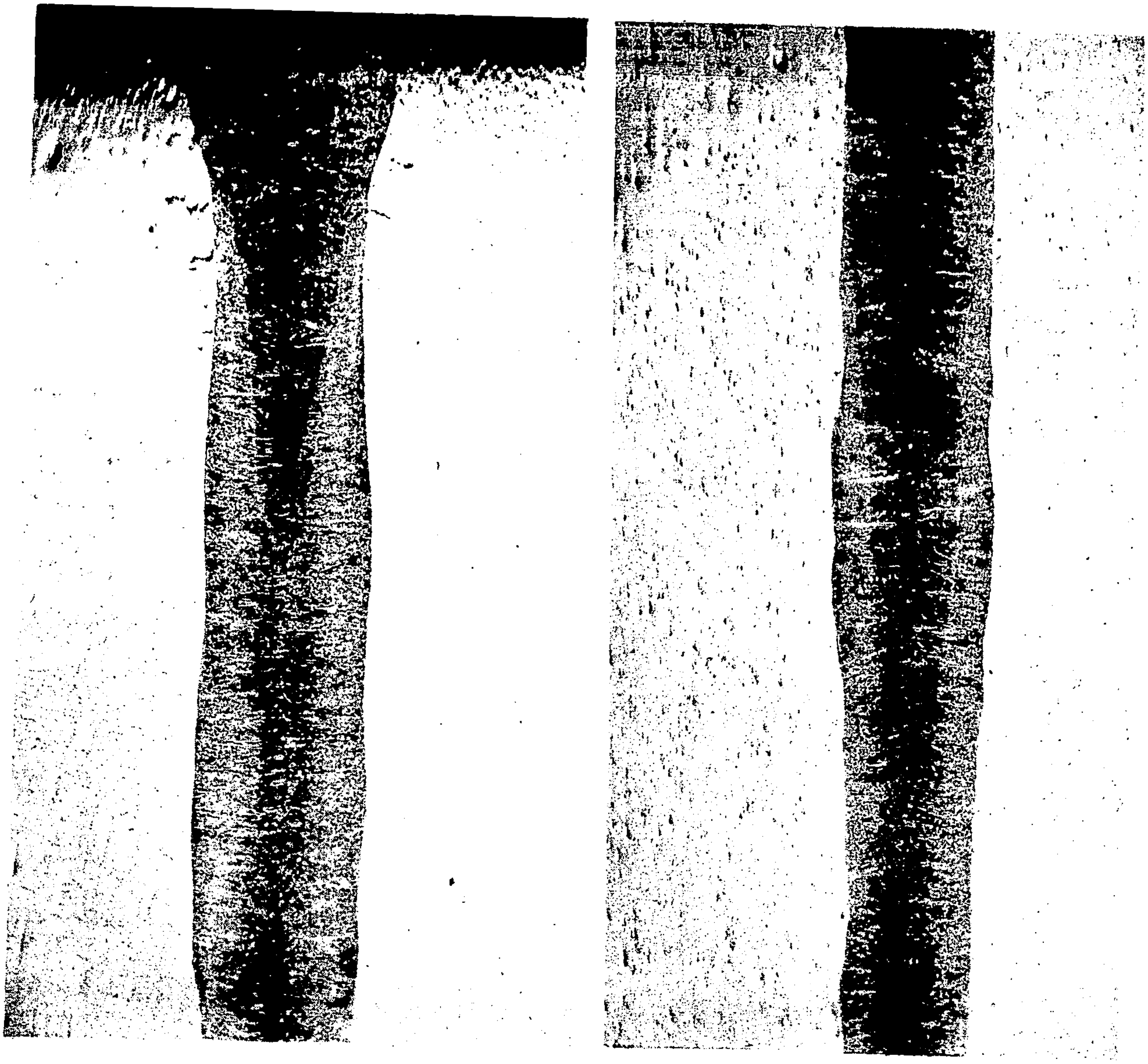

Magnifications: 15X

Above are enlarged views of the weld shown in Figure II-26. The view to the left shows the electron-beam weld nugget "nail head" and a portion of the weld "spike". The lower portion of the weld is shown on the right.

Figure II-27

Macrostructure of Electron-Beam Butt Weld in Alloy 718

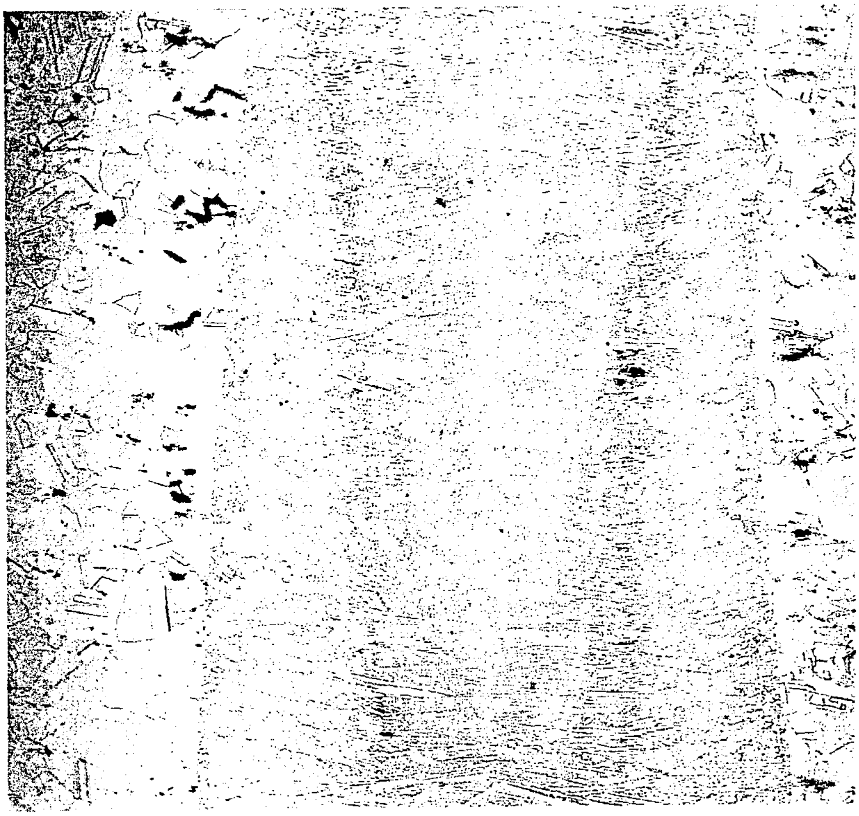

Magnification: 50X

This photomicrograph is taken under the "nail head" of the left view of Figure II-27. The microfissures are located 0.090-in. below the outer surface of the part.

Figure II-28

Microfissures in Electron-Beam Butt Weld in Alloy 718 of "scab" stock where post-weld machining from the part is impractical. "Scab" stock refers to material similar to a back-up strip or ring, but is positioned on the beam impingement side of the weld.

II. MECHANICAL TEST RESULTS

A. ALLOY 718 EB WELDED TO RENE' 41

Microtensile test specimens were removed from the Alloy 718 and Rene'41 forging weldment parent material after heat treatment to obtain parent material mechanical properties. The dual alloy weldment was heat treated to Condition B because optimum properties were desired for the Alloy 718 portion of the weldment. The stub-shaft portion operates at cryogenic temperatures while the disc-hub is approximately 1100°F. The forging supplier also performed ambient tensile tests for Alloy 718, heat treated to Condition A. Also ambient and 1400°F test results for the Rene' 41 forgings were provided. These test results including -320°F tests, are shown in Table II-I.

The Rene' 41 ambient properties show good correlation in comparing the standard Rene' 41 heat treatment, used by the supplier, to the results after heat treating to the Alloy 718 Condition B. The slight loss in strength and increase in ductility of the Alloy 718 forging from Condition B, as compared to Condition A, is attributed to loss in some warm work and possible grain growth in the latter 1950°F solution anneal.

Electron-beam welds of Weldments A and B (previously described in Part II, Section I, A) were tested with standard R3 (Federal Standard 151a) specimens to evaluate the Alloy 718 to Rene' 41 welds. Weldment B had the outer U-groove filled by the TIG process after the electron-beam joint was made. The properties of the TIG welded portion are given in Part III of this report.

The EB weld tensile test results are given in Table II-II for ambient, -320°F, and -423°F test temperatures. A strain rate of 0.005-in./in. min was used in all tests.

Although cryogenic tests were conducted for the EB welds at -423°F only for Weldment A and -320°F only for Weldment B, the data are directly comparable because the same heats of materials were used and the heat treatment as well as the weld schedules were identical. This was necessary as a result of the limited number of test specimens that were available from each weldment.

The dissimilar metal weld joint gave nearly 100% joint efficiency considering the Rene' 41 age response to the 718 heat treatment. All failures occurred in the Rene' 41 parent metal.

B. ALLOY 718 EB WELDED TO ALLOY 718

Electron-beam welded Alloy 718 test specimens joining the chevron-

TABLE II-I

RESULTS OF RENE' 41 AND ALLOY 718 PARENT METAL TESTS

Specimen Number	Temp of Test	Ftu ksi	Fty 0.2% Offset ksi	Elongation (%)	Reduction of Area (%)
A. RENE' 41 SUPPLIER TEST RESULTS (AMS 5712)					
--	RT	188	139.2	12.6	13.1
--	1400°F	159	123.3	9.4	11.6
B. ALLOY 718 SUPPLIER TEST RESULTS (AGC CONDITION A)					
--	RT	193	155	23	39
C. RENE' 41 AGC TEST RESULTS (AGC CONDITION B)					
1	RT	176.5	144.3	10.5	26.5
2	RT	190.1	138.3	16.2	19.3
3	RT	171.9	130.0	13.3	25.5
Average		179.5	137.5	13.3	23.8
4	-320°F	208.1	167.3	12.9	28.4
5	-320°F	195.1	162.9	7.7	25.4
6	-320°F	198.4	161.5	9.0	24.9
Average		200.5	163.9	9.9	26.2
D. ALLOY 718 AGC TEST RESULTS (AGC CONDITION B)					
1	RT	177.0	151.0	31.4	36.4
2	RT	174.8	150.0	29.2	44.2
3	RT	174.5	149.7	25.2	43.3
Average		175.4	150.2	28.6	41.3
4	-320°F	209.4	160.4	31.2	27.0
5	-320°F	210.5	182.4	31.0	38.6
6	-320°F	217.0	182.5	28.9	43.0
Average		212.3	175.1	30.4	36.2

TABLE II-II

RENE' 41 AND ALLOY 718 WELDED BY ELECTRON-BEAM PROCESS
(HEAT TREATED TO CONDITION B AFTER WELDING)

WELDMENT A

1. Tests at Room Temperature

Smooth Specimen Number	Ftu ksi	Fty 0.2% Offset ksi	Elongation (% in 4 dia.)	Reduction in Area (%)	Remarks
A-6	171.9	130.1	8.5	11.6	All failures occurred in the Rene' 41 parent metal
A-15	163.4	132.8	5.5	9.2	
A-16	163.5	130.7	5.5	7.0	
A-18	170.3	135.5	7.5	10.2	
A-22	171.8	143.3	4.5	6.4	
Average	168.2	134.1	6.3	8.9	

Notched Specimen Number		
A-3	198.2	$K_t = 4.9$
A-8	208.3	$K_t = 4.4$
A-9	204.8	$K_t = 4.2$
A-10	229.4	$K_t = 4.4$
A-24	239.4	$K_t = 4.2$
Average	216.0	

At room temperature the average notched-to-smooth tensile ratio is 1.28.

2. Tests at a Temperature of -423°F

Smooth Specimen Number					
A-4	191.8	173.4	3.0	4.8	All failures occurred in the Rene' 41 parent metal
A-5	196.5	181.7	3.5	4.7	
A-3	199.4	173.2	6.0	5.4	
A-14	196.8	178.5	3.0	4.7	
A-17	198.6	176.1	2.0	3.2	
A-19	195.3	176.7	3.0	3.0	
Average	196.4	176.6	3.4	4.3	

Notched Specimen Number		
A-1	238.8	$K_t = 4.4$
A-2	257.2	$K_t = 4.8$
A-7	246.8	$K_t = 4.2$
A-11	239.4	$K_t = 4.6$
A-12	245.4	$K_t = 4.6$

TABLE II-II (CONT.)

RENE' 41 AND ALLOY 718 WELDED BY ELECTRON-BEAM PROCESS (HEAT TREATED TO CONDITION B AFTER WELDING)

WELDMENT A

2. Tests at a Temperature of -423°F (Cont.)

Notched Specimen Number	Ftu ksi	Fty 0.2% Offset ksi	Elongation (% in 4 dia.)	Reduction in Area (%)	Remarks
Average	245.5				

At -423°F the average notched-to-smooth tensile ratio is 1.25.

WELDMENT B

1. Tests at Room Temperature

Smooth Specimen Number	Ftu ksi	Fty 0.2% Offset ksi	Elongation (% in 4 dia.)	Reduction in Area (%)	Remarks
B-13	158.7	2127.3	5.0	9.4	All failures occurred in the Rene' 41 parent metal
B-22	159.8	128.2	6.5	9.3	
B-27	153.4	123.3	5.5	7.7	
Average	157.3	126.3	5.6	8.8	

Notched Specimen Number	Ftu ksi	Fty 0.2% Offset ksi	Elongation (% in 4 dia.)	Reduction in Area (%)	Remarks
B-7	223.7			$K_t = 5.9$	
B-14	223.5			$K_t = 4.8$	
B-30	218.2			$K_t = 5.3$	
B-31	217.5			$K_t = 5.6$	
B-39	223.0			$K_t = 5.2$	
Average	221.2				

At room temperature the average notched-to-smooth tensile ratio is 1.41.

TABLE II-II (Cont.)

RENE' 41 AND ALLOY 718 WELDED BY ELECTRON-BEAM PROCESS (HEAT TREATED TO CONDITION B AFTER WELDING)

WELDMENT B (CONT.)

2. Tests at a Temperature of -320°F

Smooth Specimen Number	Ftu ksi	0.2% Fty Offset ksi	Elongation (% in 4 dia.)	Reduction in Area (%)	Remarks
B-16	181.1	159.8	2.5	3.2	All failures
B-23	183.8	160.6	3.0	4.7	occurred in
B-26	179.5	163.7	4.0	3.9	the Rene'41
B-32	173.2	153.8	3.0	3.2	parent metal
B-33	168.8	157.6	2.0	1.6	
Average	177.3	159.1	2.9	3.3	

Notched Specimen Number	Ftu ksi	
B-8	262.3	$K_t = 6.3$
B-15	260.6	$K_t = 6.3$
B-20	261.7	$K_t = 5.7$
B-31*	207.1*	$K_t = 5.6$
B-21	305.6	$K_t = 5.9$
Average	272.5	

At -320°F the average notched-to-smooth tensile ratio is 1.54.

*Defect in specimen - Not included in average shaped, platformed, blade-to-disc segments simulating the fuel turbine rotor assembly (see Figure No. II-16) were machined into standard R3 tensile bars. Tests were conducted at -320°F, ambient, 800°F, 1200°F, and 1350°F to obtain mechanical properties of the Alloy 718 weld joints. The test results are shown in Table II-III, and 100% joint efficiency was realized in all tests at all temperatures when given the Condition B heat treatment after welding with the exception of one test at -320°F.

Alloy 718 test specimens, (approximately 7/8-in. wide) were machined from the T-welded specimens discussed previously and shown in Figure No. II-9. These weldments were designed to permit loading the welds in both tension and shear. The ambient temperature test results of the Condition B heat treated specimens are shown in Table II-IV. Excellent strength was demonstrated as evidenced by the parent metal failure. Photographs of the T-weld specimens both before and after fracture are shown in Figures No. II-29 and No. II-30. The blade shanks were 0.125-in. thick to assure failure of the weld in shear.

III. METALLOGRAPHY

Electron-beam welds joining Alloy 718 to Rene' 41 were made in several joint configurations as previously described. Equipment of 30 kv, 60 kv, and 150 kv were used to make the welds.

The initial welds were produced with 60 kv equipment and are shown in Figures No. II-1 and No. II-2. A typical weld joining the same combinations of alloys with a 150 kv machine and a 10.5-in. gun-to-work distance is shown in Figure No. II-6. Microstructures of these EB weld fusion zones are shown in Figure No. II-31. The fine grain structure of the weld metal deposit is typical of the high quality obtainable in joining such heavy thicknesses with the electron-beam process. Joint efficiencies of 100% can be readily attained.

Serious weld cracking resulted from attempting to use a low voltage (30 kv) machine with a large gun-to-work distance (10-in.) to weld the thick Alloy 718/Rene' 41 joint. The photomacrographs (Figures No. II-3 and No. II-32 show the resulting large "nail head" and wide weld "spike" with weld and fusion some cracks. The weld cracking was eliminated and microfissures greatly reduced by using the higher voltage equipment.

Alloy 718, EB welded to itself, is shown in Figures No. II-26, No. II-27, and No. II-28. A 60 kv unit was used to produce this weld of 1.5-in. thickness. The weld schedule used resulted in welds with a high depth-to-width ratio. The weld nugget "spike" is fairly uniform and sound. Microfissures were present just below the "nail head" and varied from 0.002-in. to 0.006-in. in length. This condition is difficult to completely eliminate; however, with optimum weld schedules for these heavy thicknesses, the microfissures have been limited to an area of less than 0.090-in. below the beam impingement surface. Wherever possible, designs are such that approximately 1/8-in. of this surface is machined away.

TABLE II-III

MECHANICAL PROPERTIES OF ELECTRON-BEAM WELDED ALLOY 718 FORGINGS, HEAT TREATED PER CONDITION B AFTER WELDING

Specimen No.	Temp of Test	Ftu (ksi)	Fty 0.2% (ksi)	Elongation (% in 4D)	Reduction of Area (%)	Remarks
6*	-320°F	184.2	177.9	3.5	14.4	Incomplete weld penetration
7	-320°F	226.8	179.9	14.5	18.7	Failed adjacent to weld
8	-320°F	229.3	179.6	21.0	24.4	Failed 3/16 in. from weld in parent metal
9	-320°F	217.2	179.2	8.0	16.8	Failed in weld
22	-320°F	226.6	180.1	15.5	17.5	Failed 1/8-in. from weld in parent metal
Average		225.0	179.7	14.8	19.4	
1	RT	176.5	154.7	12.0	23.1	All failures occurred 1/8-5/32-in. from welds in parent metal
2	RT	175.7	154.1	11.5	22.7	
3	RT	178.3	155.8	15.5	34.9	
4	RT	178.6	157.1	14.5	22.4	
5	RT	178.5	154.3	13.0	23.0	
Average		177.5	155.2	13.3	25.2	
Specification Minimum						
	RT	175.0	145.0	12.0%		

*Defect in specimen - Not included in average

TABLE II-III (CONT.)

Specimen No.	Temp of Test	Ftu (ksi)	Fty 0.2% (ksi)	Elongation (% in 4D)	Reduction of Area (%)	Remarks
10	800°F	149.9	134.4	13.5	36.5	All failures occurred 1/8 - 1/4-in. from welds in parent metal
11	800°F	150.3	132.9	18.0	35.5	
12	800°F	148.7	133.5	16.0	36.6	
13	800°F	148.3	133.2	16.0	36.4	
Average		149.2	133.4	15.9	36.2	
14	1200°F	143.1	130.2	15.5	33.8	Failures occurred 1/8 - 1/4-in. from weld in parent metal
15	1200°F	144.0	125.8	16.5	35.5	
16	1200°F	144.0	--	14.0	40.4	Extensometer slipped
17	1200°F	140.8	--	14.0	27.0	Extensometer slipped
Average		142.9	128.0	15.0	34.2	
Specification Minimum	1200°F	140.0	120.0	10.0	--	
18	1350°F	122.3	103.7	11.0	11.4	All failures occurred 1/8 - 5/16-in. from welds in parent metal
19	1350°F	119.2	106.4	11.0	17.9	
20	1350°F	123.1	103.6	11.0	15.2	
21	1350°F	121.2	106.5	10.0	19.6	
Average		121.4	105.0	10.8	16.0	

TABLE II-IV

MECHANICAL PROPERTIES OF ELECTRON-BEAM WELDED ALLOY 718
T-SPECIMENS TESTED AT ROOM TEMPERATURE

Specimen No.	Ftu (ksi)	Location of Failure
4. Weld in tension (EB welded from one side and brazed).		
A	171.8	P.M.* in blade at braze fillet
B	174.8	P.M. in blade
D	173.7	P.M. in blade
Average	173.4	
5. Weld in tension (EB welded from both sides and brazed).		
A	172.0	P.M. in blade
B	173.4	P.M. in blade
D	177.1	P.M. in blade
Average	174.1	
9. Weld in tension (EB welded from one side; no braze).		
A	181.4	P.M. in blade
B	177.8	P.M. in blade
D	173.4	P.M. in blade
Average	177.5	
11. Weld in shear (EB welded from one side and brazed).		
A	170.5	Weld sheared
B	171.8	Weld sheared
D	162.7	Weld sheared
Average	168.3	

*P.M. - Parent Metal

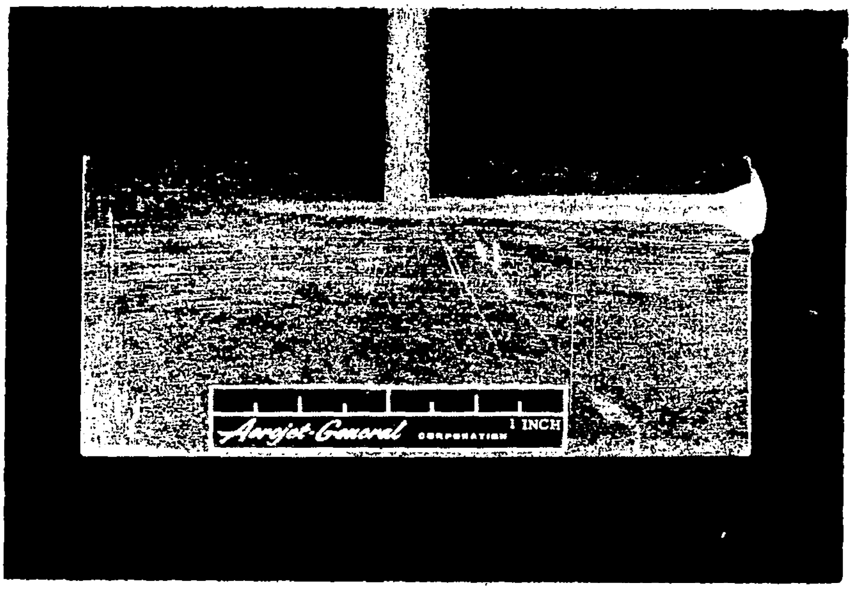

This cross-section of a T-weld specimen shows the weld nugget from one side joining the blade to the disc.

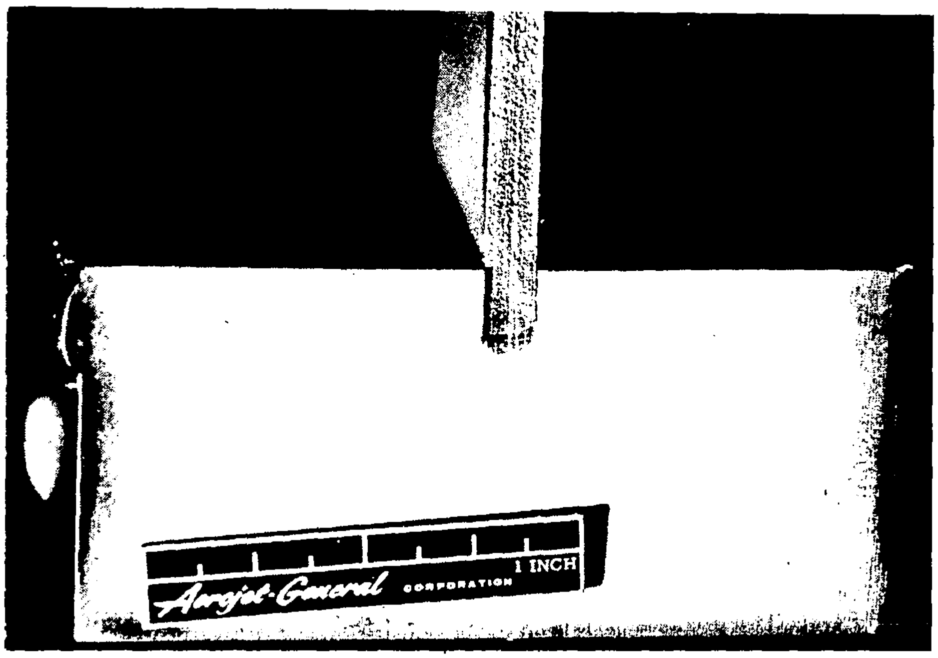

The end view of a test specimen is shown above after testing. Parent metal failure of the blade shank is not in view. The blade shank yielding can be observed.

Figure II-29

Electron-Beam Welded Alloy 718 Tensile Specimen

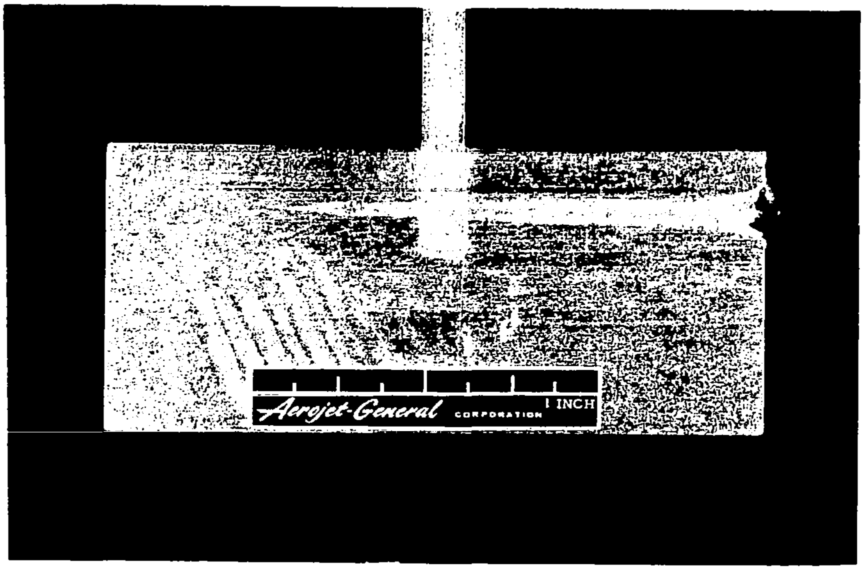

Cross-section view of a T-weld specimen showing the weld nugget through the blade. The weld specimen has braze on the right side at the simulated blade-to-disc joint.

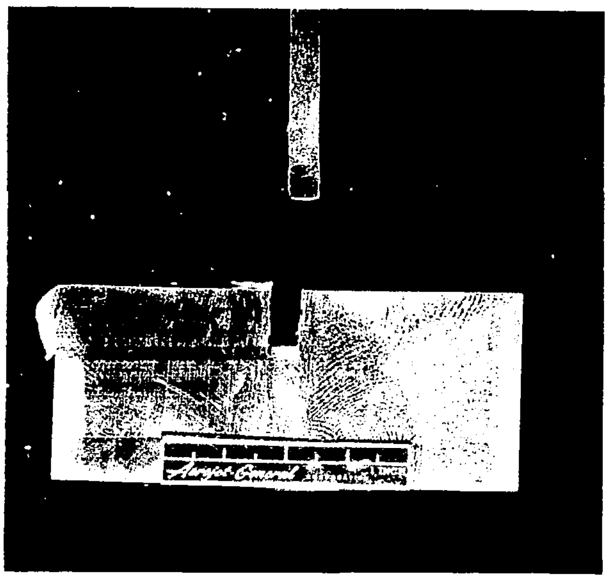

Typical weld shear failure of the test specimen shown above.

Figure II-30

Electron-Beam Welded Alloy 718 Tensile Shear Specimen

Figure II-31

Microstructure of Electron-Beam Weld Fusion Zones

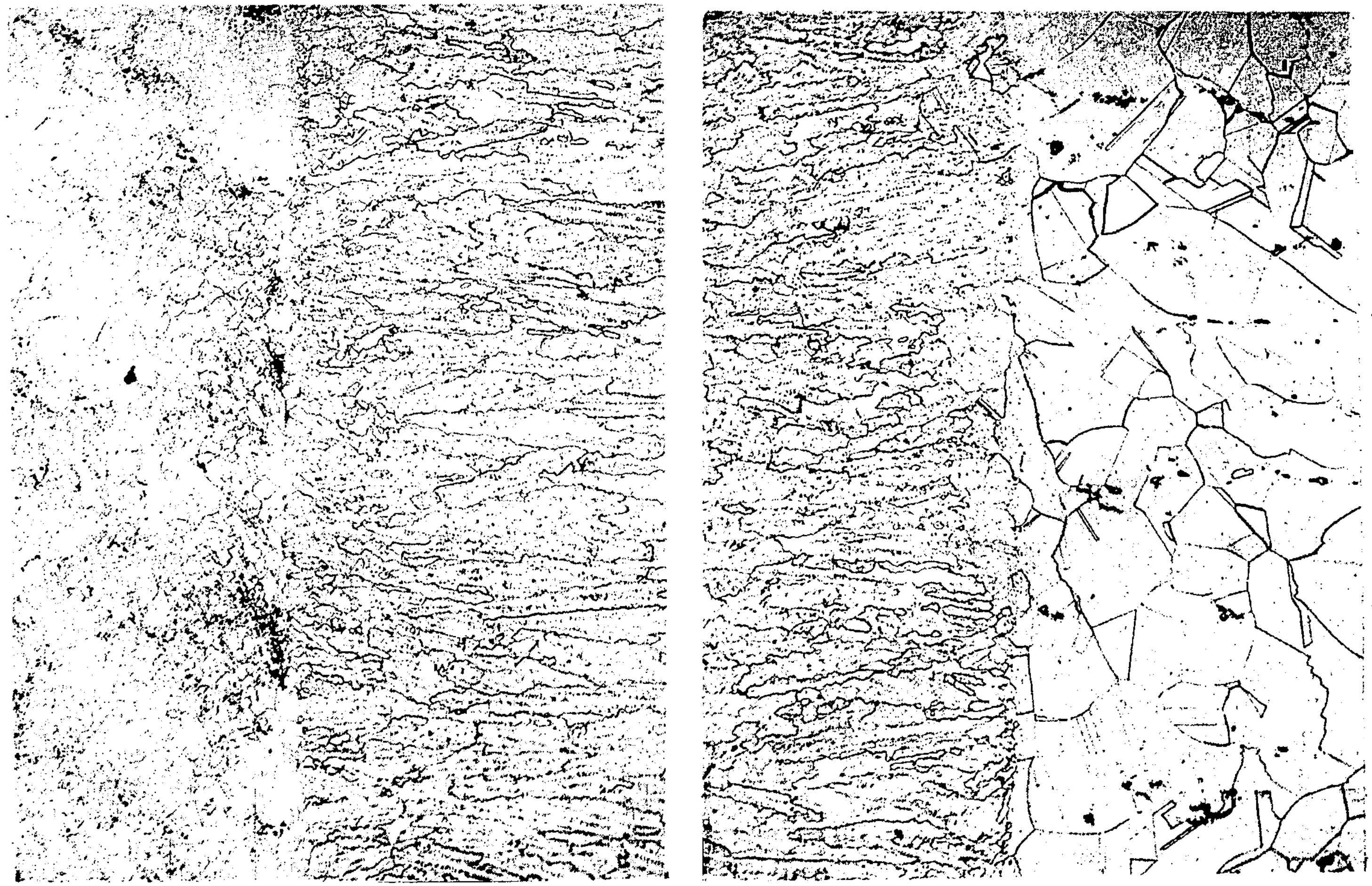

Magnification: 100X   Magnification: 100X

Rene' 41 is on the left and Alloy 718 on the right. The weld was made with a 150 kv machine.

Magnification: 250X

The weld was produced with 30 kv welding equipment and 10-in. gun-to-work distance on test specimens. Micro-cracking was almost eliminated by using 150 kv equipment at 10.5-in. gun-to-work distance or 60 kv equipment and 2-in. gun-to-work distance on re-designed joints.

Figure II-32

Microfissure in Alloy 718 Parent Metal Adjacent to "Nail Head" Portion of Electron-Beam Weld

IV. CONCLUSIONS

High quality butt welds in heavy sections of Alloy 718 and Alloy 718 to Rene' 41 can be produced by the electron-beam welding process. Control must be exercised to obtain good fit-up, cleanliness, and proper weld parameters to minimize the width of the weld nugget.

Weld joint efficiencies of 100% can be attained in the solution-treated and aged weldments.

Lighter-weight bladed turbopump components can be fabricated by taking advantage of the unique design potential afforded by the incorporation of the EB welding process.

V. RECOMMENDATIONS

Weld back-up material, 0.250-in. thick, is recommended for butt joints that are over 1-in. thick because of fluctuations in the depth of EB weld penetration. The back-up material must be of the same composition as the alloy that is being joined to prevent undesirable dilution of the weld nugget.

Parts should be designed to permit removal of 0.100-in. minimum surface stock from the weld-bead side of the joint. This will remove the area of micro-fissures generally found in thick joints adjacent to the "nail head" portion of the weld nugget. If such machining is not possible, a "scab" strip can be placed on the weld impingement side of the joint. Machining or grinding off the strip after welding will eliminate the "nail head" area.

Electron-beam weld schedules must be established to provide the highest weld nugget depth-to-width ratio for optimum joints in heavy section thicknesses. This will minimize weld shrinkage and microfissures under the weld nugget nail head.

Electron-beam weldability tests should be performed using the Alloy 718 heats that will be used for production weldments prior to welding production parts.

PART III. TUNGSTEN INERT GAS WELDING OF ALLOY 718 AND ALLOY 718 TO RENE' 41 IN HEAVY SECTIONS

I. DISCUSSION

A. TUNGSTEN INERT GAS WELDING (TIG) ALLOY 718 TO RENE' 41

Two sets of forgings of Alloy 718 and Rene' 41 were welded by the electron-beam process. These weldments (Weldments A and B) were described in Part II of this report. Weldment A contained only the electron-beam (EB) weld while the Weldment B joint was completed by the tungsten inert gas weld (TIG) process to fill the 1-in.-deep U-groove with Alloy 718 filler wire. This joint, prior to TIG welding, was described in Part II and shown in Figure II-1.

The electron-beam bead buildup at the bottom of the U-groove was removed by machining and dye-penetrant inspected. Thirty-four weld passes using stringer heads and minimum heat input were required to complete the joint. The machine settings for the first 16 weld passes were: 285 amp, 10.5 v, 40 imp feed (1/16-in.-diameter wire), 9 ipm surface speed. A gas mixture of 75% helium and 25% argon was used at the torch with a flow rate of 45 cu ft/hr. A weld torch trailing shield was used with an argon flow of 15 cu ft/hr. The remaining 18 weld passes were applied using the same parameters except the current was increased to 295 amp and the wire feed increased to 51 ipm. An interpass temperature of 200°F maximum was maintained.

Dye penetrant inspection was performed on each weld pass and occasional crater cracks were ground out, reinspected, and the weld cleaned with a rotary stainless steel wire brush and swabbing with MEK prior to depositing the next weld bead. Great care was taken to prevent surface contamination.

The completed weld was radiographically inspected, heat treated to Condition C. (The higher primary age 1400°F, was used in the early stages of this work prior to the establishment of the Aerojet-General standard heat treatments for Alloy 718 as represented by the previously referenced Conditions A and B). Nondestructive test inspection was again performed after solution treating and aging.

B. TUNGSTEN INERT GAS (TIG) WELDING OF ALLOY 718

A number of Alloy 718 ring forgings were welded to establish automatic TIG welding and inspection procedures for use on the M-1 fuel pump rotor weldments. Weld joint designs incorporating U-grooves, were used throughout this program. The grooves 1-1/8-in. thick, were machined to contain a 0.050-in. flat node, 0.125-in. radius, and 10-degree side angle on each of the mating forging faces. A consumable weld insert was used to make the smooth penetration root weld pass. Contour machined inserts were mated to the flat nodes machined in the forgings to hold proper joint alignment. The inserts were machined 0.002-in. larger than the inside diameters of the ring forgings. To assemble the components for welding, it was necessary to preheat the forgings 200° to 300°F for assembly purposes. Positive contact of the insert and the ring forgings was maintained during the welding of the root pass to permit uniform melting of the insert and a resulting uniform deposit. All detail parts were thoroughly cleaned by swabbing with Freon then handled with white lint-free gloves during assembling and welding. High purity argon and helium were used for weld and back-up gasses. Purging was begun with argon and then changed to helium because it produced a more uniform wetting and final contour of the consumable insert. Purging adequacy was assured by monitoring the oxygen content of the purge gas. The purge gas pressure was controlled during welding of the root pass by using a manometer reading of 0.1 to 0.2-in. of water during welding. Controlling the internal purge gas pressure was also necessary to assure uniformly contoured root welds. These refinements resolved earlier problems of non-uniform melting of the consumable insert and lack of fusion.

A "continuous" tack weld was made initially to join the insert to the mating forging members to prevent distortion and to seal the back-up purge gas. The schedule was: weld current, 50 to 55 amp; voltage, 9.5 v; surface speed, 6.5 ipm; torch gas flow, 90 cfh; and trailing shield gas flow 90 cfh. (Welding gas mixtures of 75% helium and 25% argon was used in the torch and trailing shield). The tack weld surface was rotary wire brushed and cleaned with Freon prior to welding the root-fusion pass.

The weld schedule used for the root-fusion weld was: weld current, 175 to 185 amp; voltage, 8.9 to 9.3 v; welding speed, 4 ipm; torch and trailing shield gas flows, 85 to 95 cfh. Welding current up and down slope was used to prevent crater cracks.

A photomacrograph showing a cross-section of a weld root pass made using the consumable insert is shown in Figure No. III-1. Additional weld filler material was not required for the root passes.

The root welds of all weld specimens and rotor components were dye-penetrant and radiographically inspected prior to continuing the welding of the joints. Freshly ground tungsten electrodes were used for each weld pass, and the torch gas cup was cleaned periodically when the copper cup became discolored. The weld torch was in the vertical (12 o'clock) position for all tack and root welds. The torch angle was changed as filling of the weld joint progressed.

Four weld cover passes were made using the following schedule: weld current, 170 amp; voltage, 9 v; surface speed, 6.5 ipm; wire feed, 20 to 22 ipm (1/16-in. diameter wire); torch gas flow, 90 cfh; trailing shield gas flow, 60 cfh; torch angle vertical and 10 degrees from 12 o'clock in the direction of rotation of the part. Current slope control was used for all weld passes and the point of arc initiation was overlapped approximately 2-in. prior to initiating the current decay cycle. Each weld pass was inspected by the dye penetrant process and thoroughly cleaned prior to depositing the next cover weld pass. A maximum interpass temperature of 200°F was maintained. The weld torch angle was changed for the remainder of the weld cover passes, alternating from 4-degrees to the right to 4-degrees to the left; all other machine settings

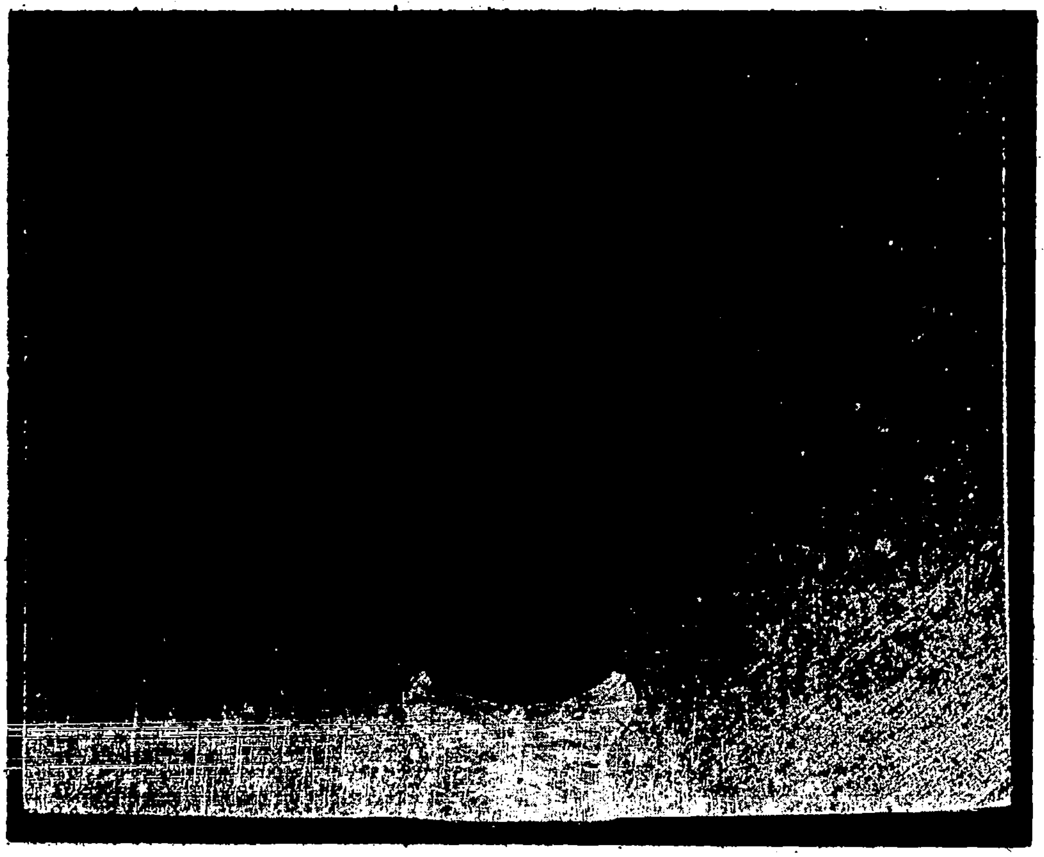

Magnification: 4X

A cross-section of the U-groove joint showing the root pass. A preplaced Alloy 718 consumable insert was fused to both Alloy 718 forgings forming a sound root weld of uniform contour. No additional filler rod was used in this pass.

Figure III-1

Consumable Insert TIG Root Weld in Alloy 718 remained constant for two weld passes. Torch angle was found to be critical in preventing lack of fusion and assuring a sound weld deposit. This is illustrated in Figure No. III-2 which shows a defect resulting from improper positioning of the torch. The Alloy 718 weld puddle is sluggish and does not wash as well as stainless steel.

Dimensional checks were made after the completion of each weld pass to determine the weld shrinkage rate. Progressive welds were initiated at the point where the least shrinkage occurred, thus aiding in maintaining axial alignment of the parts. After the sixth weld cover pass, the weldments were given a stress-relief anneal at 1800°F for one hour. The same weld schedule was used on weld passes 7 through 12 except that the weld wire feed rate was increased to 24-25 ipm. For the thirteenth weld pass, the weld torch was centered in the groove to fill the valley caused by weld passes 11 and 12, which were deposited at each side of the grooved joint. The torch angles were adjusted in this manner throughout the remaining 20 cover passes. The stress-relief anneal was repeated upon completion of the eighteenth and the final weld pass. The 32 weld passes used in this procedure produced the joint illustrated in Figure No. III-3. This procedure eliminated weld cracking and the lack of fusion encountered in the first weld test joints, which were made without interstage anneals.

Three welds of this magnitude were required to joint the four forgings making up the fuel pump rotor assembly. The weld locations are indicated by arrows in Figure No. III-4 (a bladed fuel rotor assembly is seen in the background).

The first weld joint (right arrow) joins the 14-in.-diameter drum forging to the flanged shaft forging. The blade lands were machined after welding. The second weld is at the left arrow and joins two cone forgings. The final or closure weld is indicated by the center arrow. The subassembly weldments (welds 1 and 2) were stress relieved and fully inspected by radiographic and ultrasonic techniques prior to machining the closure weld groove.

The welding setup for making the first joint is illustrated in Figure III-5. The rolls support the heavy forgings and aid in maintaining alignment during welding. A close-up view of the U-groove with the consumable insert root pass completed is seen in Figure No. III-6. The stamped numbers (7 and 8) are two of the twelve stations marked on the periphery of the forgings for checking shrinkage as the weld progressed.

II. <u>TEST RESULTS</u>

A. ALLOY 718 TIG WELDED TO RENE' 41

Type R-3 tensile specimens were machined from the TIG welded outer portion of heat-treated Weldment B. Two typical fractured tensile bars are shown in Figure No. III-7. Results of the tests at room temperature and -320°F are given in Table III-I. Strengths obtained for this dissimilar alloy joint

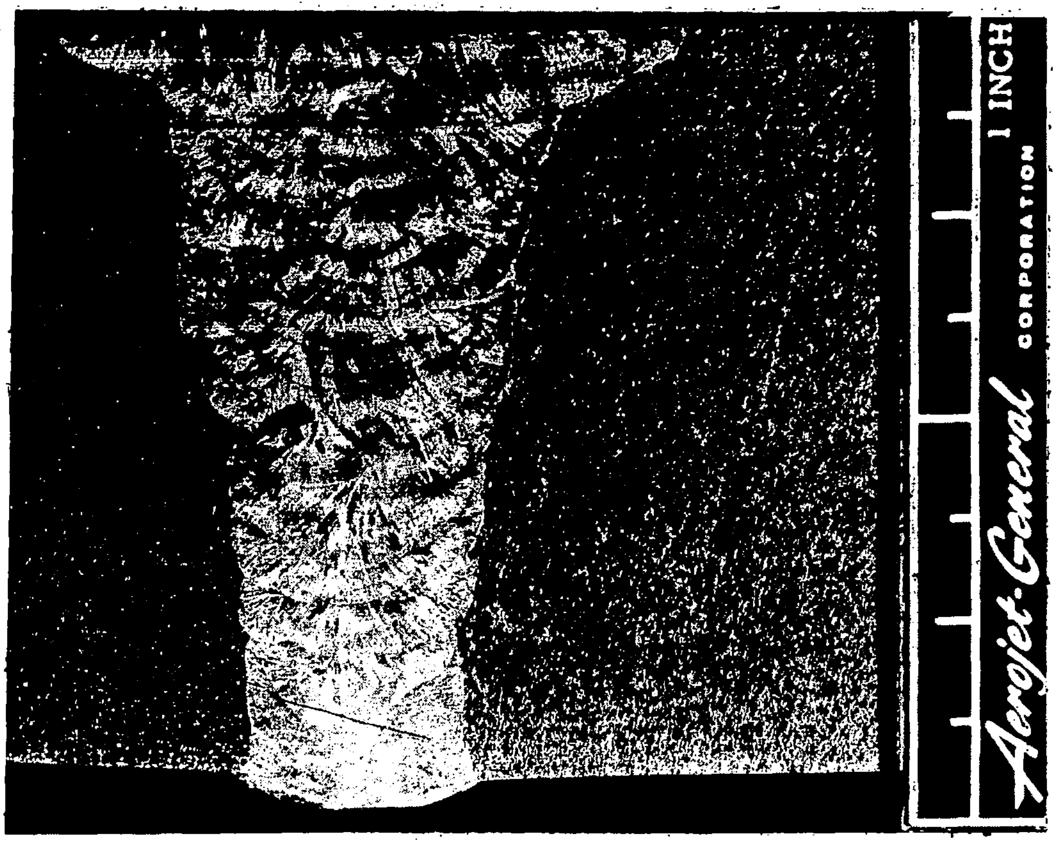

The defect was detected by radiographic inspection. Lack of fusion was corrected by changing the weld torch angle.

Figure III-2

Weld Defect in TIG Butt Weld Joint of Alloy 718

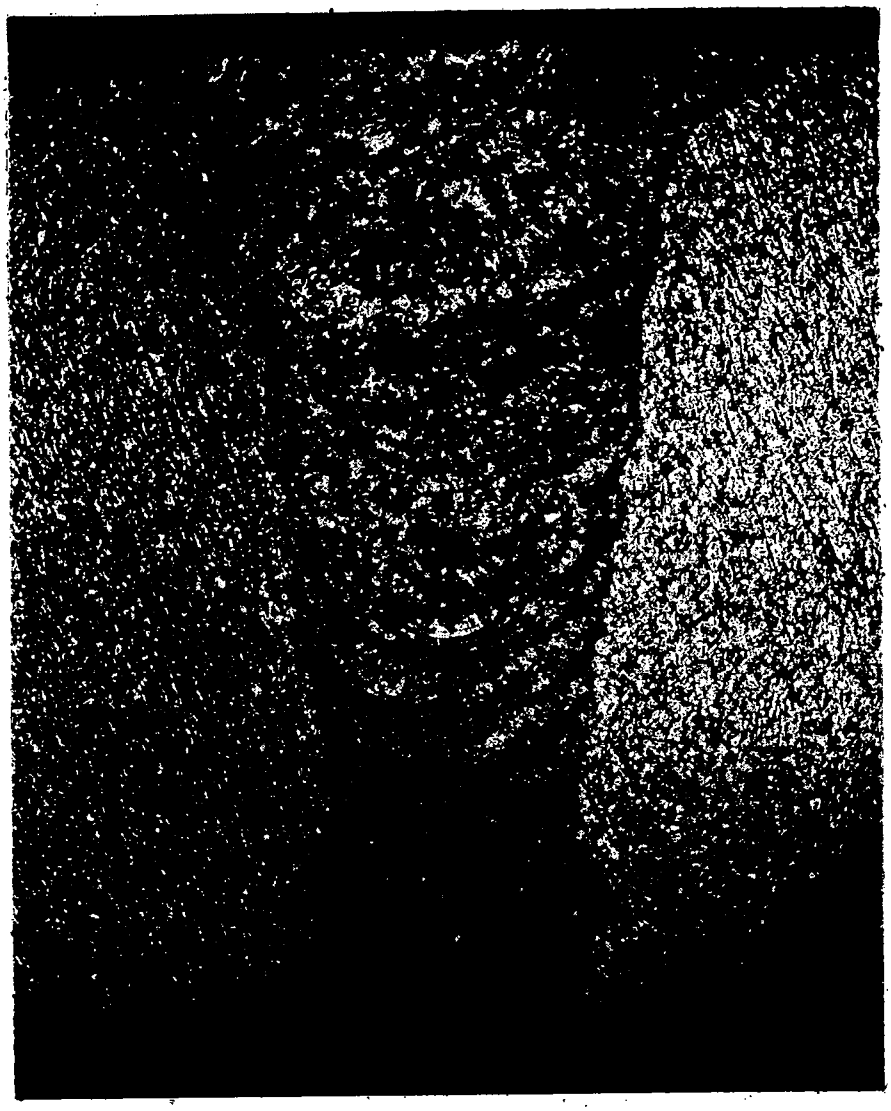

Magnification: 5X

Alloy 718 filler wire was used to make the 32 weld cover passes required to complete the joint.

Figure III-3

Macrostructure of a Sound TIG Butt Weld Joint in Alloy 718

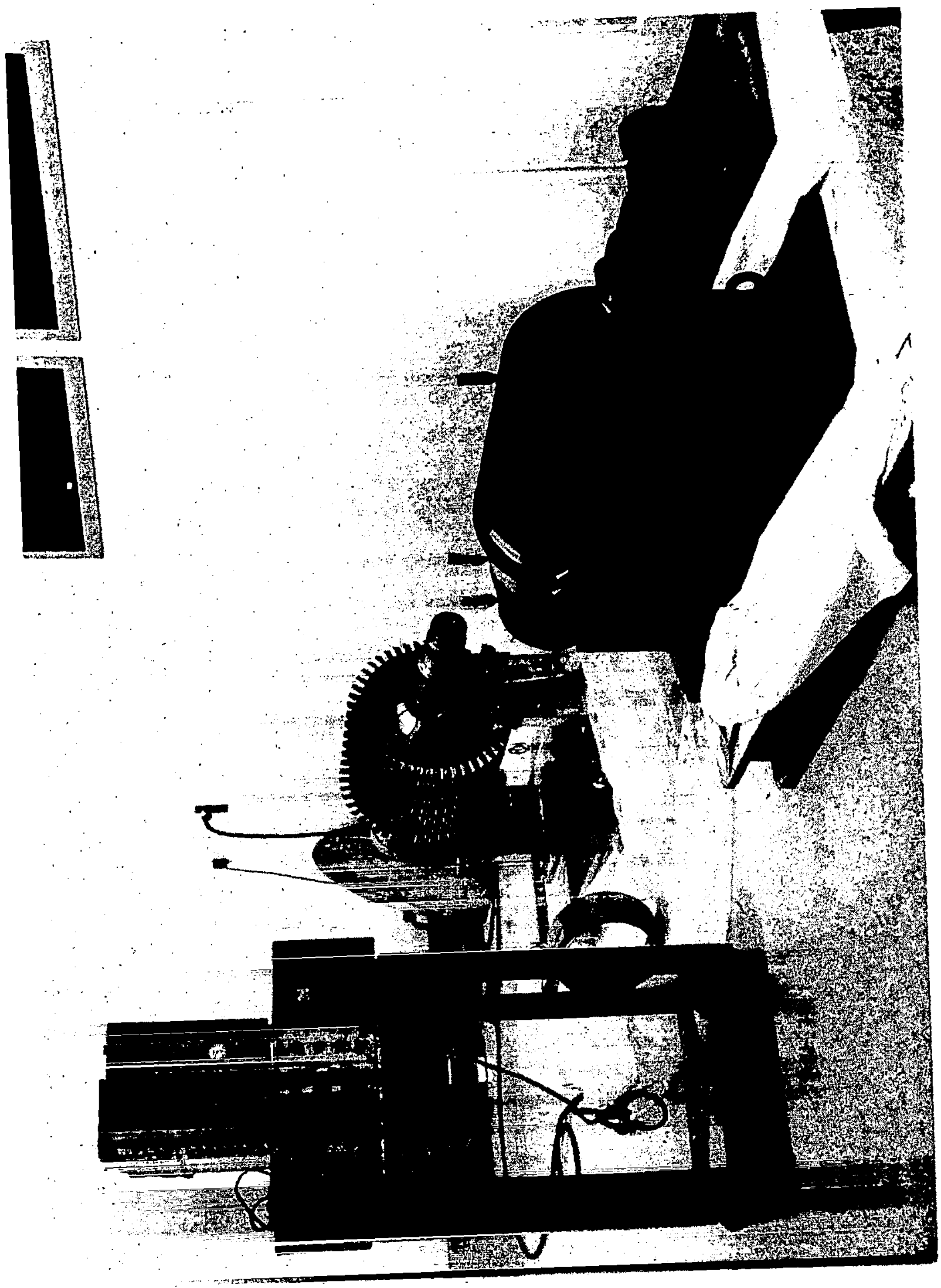

Figure III-4

M-1 Fuel Pump Rotor Assembly

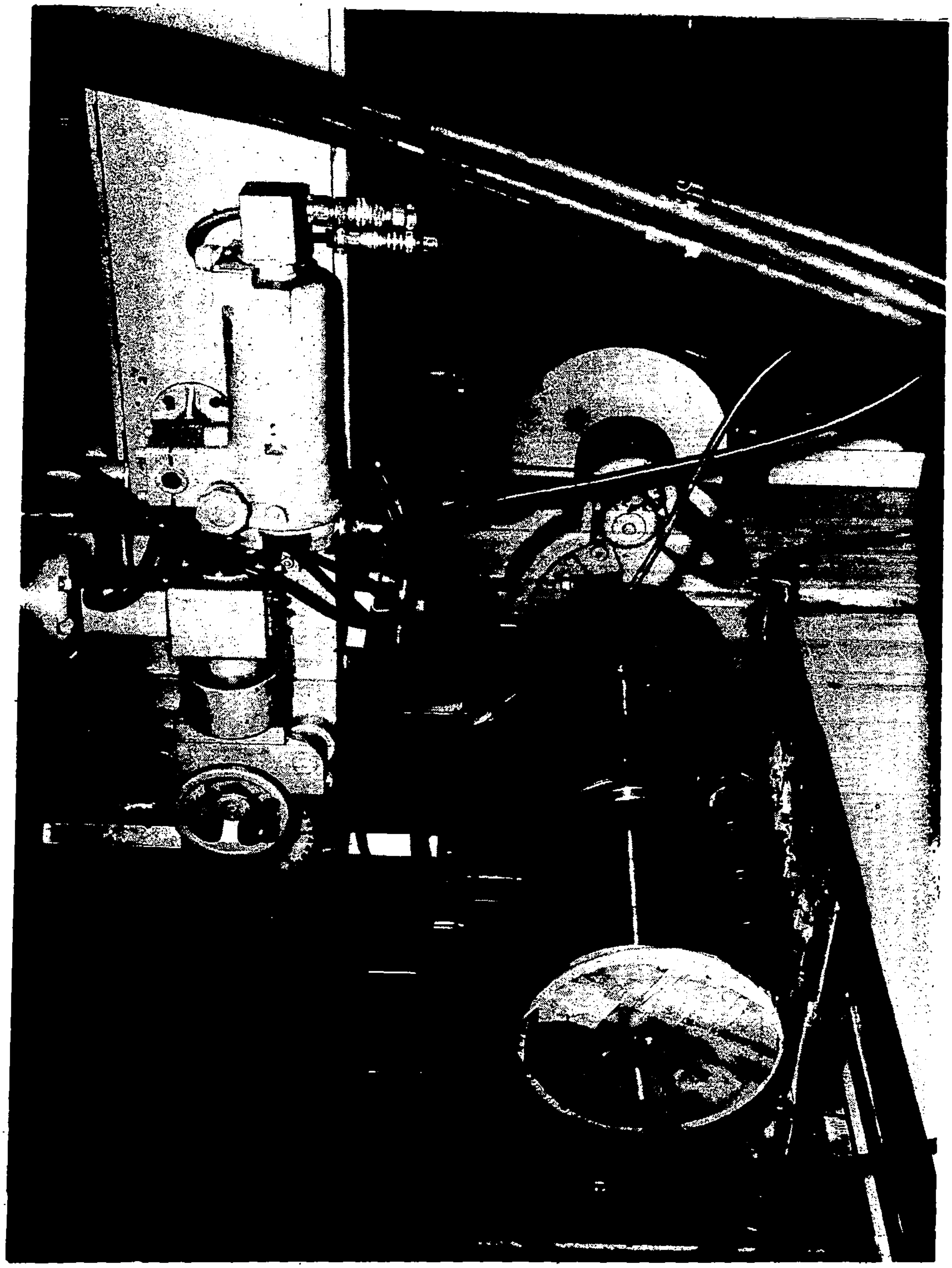

Figure III-5

Welding Setup for TIG Joining Alloy 718 Forgings

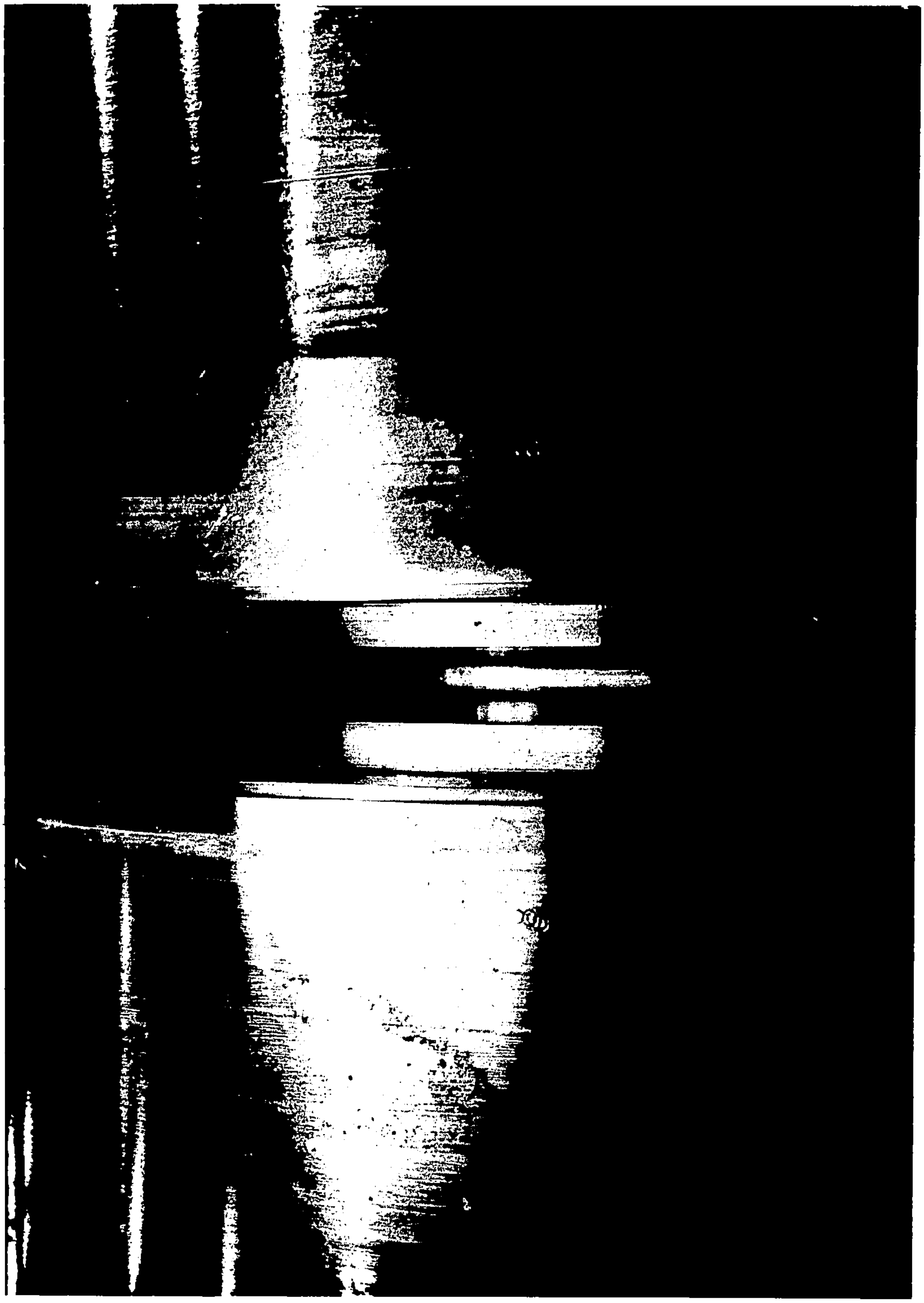

Figure III-6

View of Grooved Joint with Completed Root Fusion Pass

Smooth TIG Weld specimen tested at room temperature showing failure in the heat-affected zone of the Alloy 718 side of the weld.

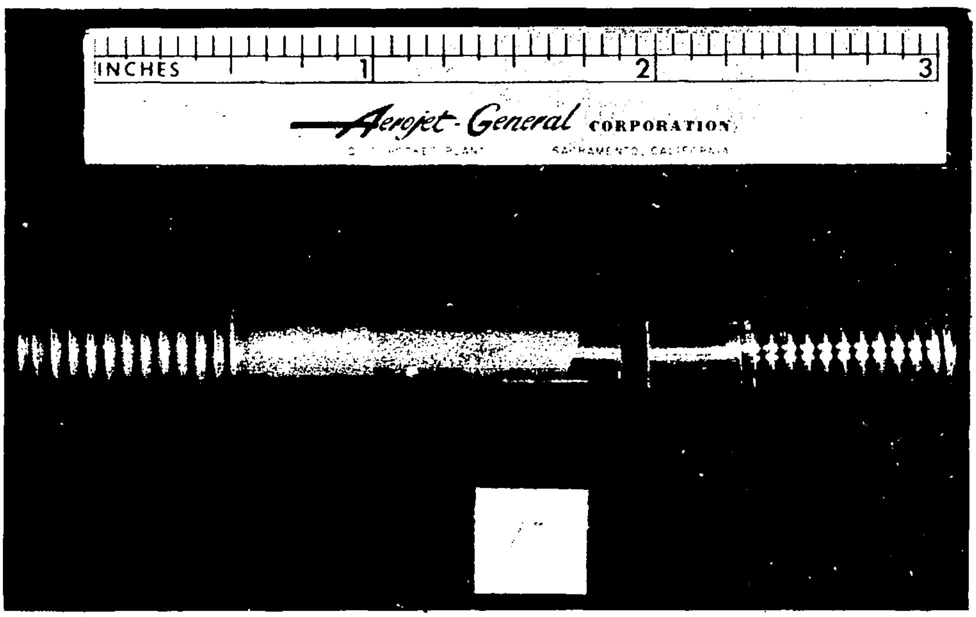

Smooth TIG weld specimen tested at -320°F. Failure occurred in the Rene' 41 parent material.

Figure III-7

TIG Weld Test Specimens

TABLE III-I

MECHANICAL PROPERTIES OF HEAT-TREATED* TIG WELD JOINTS OF ALLOY 718 TO RENE' 41

A. TESTED AT ROOM TEMPERATURE

Smooth Specimen Number	Ftu ksi	Fty (2% Offset) ksi	Elongation (%)	Reduction of Area (%)	Remarks
B-4	187.2	147.4	19.5	40.6	Failure 718 HAZ**
B-18	183.0	146.0	15.5	42.0	Failure 718 HAZ
B-28	174.0	140.0	--	11.4	Failure in R-41
B-45	174.8	146.0	6.5	11.4	Failure in Weld
B-42	183.0	147.6	12.0	13.5	Failure in Weld
Average	180.4	145.4			

Notched Specimen Number	Ftu ksi	
B-1	262.0	$K_t = 6.0$
B-2	263.9	$K_t = 6.4$
B-11	277.9	$K_t = 5.3$
B-44	264.9	$K_t = 5.9$
Average	267.2	Notched tensile ratio = 1.48

B. TESTED AT -320°F

Smooth Specimen Number	Ftu ksi	Fty (2% Offset) ksi	Elongation (%)	Reduction of Area (%)	Remarks
B-10	187.9	166.3	4.0	10.0	Failure in Weld
B-25	199.6	167.5	4.0	7.1	Failure in Weld
B-41	202.3	175.1	4.0	7.8	Failure in Rene'41
B-46	201.6	174.9	3.5	7.0	Failure in Rene'41
Average	197.8	171.0			

Notched Specimen Number	Ftu ksi	
B-3	320.5	$K_t = 5.8$
B-5	309.0	$K_t = 5.2$
B-19	313.7	$K_t = 5.1$
B-24	269.8	$K_t = 5.3$
Average	303.3	Notched tensile ratio = 1.53

* AGC Condition B modified with primary age of 1400°F.
**HAZ - Heat Affected Zone

(Alloy 718/Rene' 41) were very good (145 ksi yield strength) and displayed joint efficiency. Fractures occurred in the welds, in the Rene' 41, and in the Alloy 718 heat-affected zone. The -320°F tests did not show failure in the Alloy 718 heat-affected zones. The notched strengths were excellent and provided a very high notched-smooth bar tensile ratio. A hardness survey was made across the weld and parent metal of the weldment B cross-section. The results are illustrated in Figure No. III-8. The hardness of the heat-treated weldment (Condition B) is quite consistent in the TIG weld, EB weld, and Alloy 718 portions averaging R_C 41. The Rene' 41 parent metal gave somewhat lower hardness readings in response to the Alloy 718 heat treatment cycle.

B. ALLOY 718 PARENT METAL AND TIG WELDED RING FORGING PROPERTIES

Tensile tests of parent metal Alloy 718 and TIG welded Alloy 718 ring forgings were made on notched and smooth bar R-3 (Federal Standard 151a) specimens at ambient, -423°F, and 1200°F. These results are shown in Table III-II. All weldments were heat treated to Condition C. The notch toughness of the parent metal and weld metal are quite consistent and exceed a notched to smooth bar tensile ratio of 1.30 throughout the test temperature range of -423° F to 1200°F. The weld joint efficiency is approximately 93% at -423°F and 95% at ambient and 1200°F.

For ease of comparison, a bar graph is given in Figure No. III-9 illustrating the average strengths of the Alloy 718 joined to itself and to Rene' 41 by both processes discussed in this report: electron-beam welding and gas tungsten arc welding.

III. METALLOGRAPHY

A photomicrograph of the Alloy 718 TIG joint made with Alloy 718 filler wire is shown in Figure No. III-10. The relatively fine dendritic structure of the weld deposit in the 1-1/8-in. thick U-groove butt joint was obtained by using small weld-bead deposits and maintaining a low interpass temperature.

Shrinkage cracks were encountered in the first test joints which were made without interstage stress relief annealing. The cracks illustrated in Figure No. III-11 occurred through the sixth weld pass. This heavily restrained joint required two intermediate anneals in addition to the final anneal to remove the stresses imposed by the weld shrinkage. The in-process stress relief anneals were done at 1800°F for one hour. The final anneal was at 1950°F for one hour.

Proper weld and stress relief control resulted in sound weld fusion.

IV. CONCLUSIONS

Alloy 718 can be successfully TIG welded in heavy sections to itself and to Rene' 41.

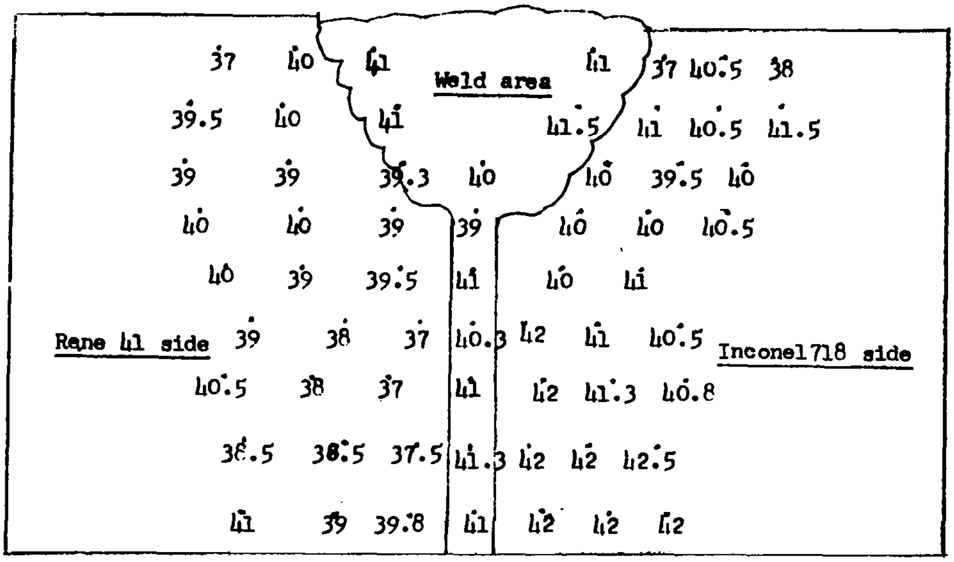

Rockwell C hardness readings taken from Rene' 41 - Alloy 718 welded by EB and TIG processes, heat-treated to Condition B.

Figure III-8

Hardness Survey

TABLE III-II

MECHANICAL PROPERTIES OF HEAT TREATMENT* TIG WELD JOINTS OF ALLOY 718 AND PARENT METAL

A. TESTED AT ROOM TEMPERATURE

Specimen Type	Specimen No.	Ftu (ksi)	Fty (2% Offset) (ksi)	Elongation (%)	Reduction of Area (%)	Notched Tensile Ratio ($K_t = 6.3$)
Smooth-Parent Metal	8-P-11	205.1	162.6	24.5	36.0	
	8-P-12	194.4	165.1	25.0	40.4	
	8-P-13	193.0	(1)	27.0	39.0	
	Average	197.5	163.8	25.5	38.5	
Notched-Parent Metal	8-P-1	290.6				
	8-P-2	266.9				
	8-P-3	261.0				
	Average	272.8				1.38
Smooth-Weld	8-W-11	190.1	(1)	20.0	40.4	
	8-W-12	189.0	162.0	19.0	37.6	
	8-W-13	190.1	169.2	19.0	36.2	
	Average	189.7	165.6	19.3	38.1	
Notched-Weld	8-W-1	266.2				
	8-W-2	262.4				
	8-W-3	260.8				
	Average	263.1				1.39

TABLE III-II (CONT.)

B. TESTED AT -423°F

Specimen Type	Specimen No.	Ftu (ksi)	Fty (2% Offset) (ksi)	Elongation (%)	Reduction of Area (%)	Notched Tensile Ratio (K_t = 6.3)
Smooth-Parent Metal	8-P-5	238.3	198.0	21.0	34.2	
	8-P-6	252.3	208.3	23.0	32.7	
	8-P-7	244.0	198.2	23.0	32.8	
	8-P-8	249.1	210.0	23.0	32.7	
	Average	245.9	203.6	22.5	33.1	
Notched-Parent Metal	8-P-4	325.3				
	8-P-9	323.6				
	8-P-10	322.4				
	Average	323.8				1.32
Smooth-Weld	8-W-5	238.3	205.5	20.0	31.4	
	8-W-6	242.6	202.9	19.0	30.0	
	8-W-8	232.9	194.7	20.0	30.7	
	Average	237.9	201.0	19.7	30.7	
Notched-Weld	8-W-4	312.7				
	8-W-9	308.1				
	8-W-10	305.5				
	Average	308.7				1.30

TABLE III-II (CONT.)

C. TESTED AT 1200°F

Specimen Type*	Specimen No.	Ftu (ksi)	Fty (2% Offset) (ksi)	Elongation (%)	Reduction of Area (%)	Notched Tensile Ratio (K_t = 6.3)
Smooth Parent Metal	9-P-7	143.0	122.1	21.0	44.1	
	9-P-8	144.7	125.6	20.0	43.5	
	9-P-11	144.0	126.3	21.5	35.3	
	9-P-12	144.1	127.3	21.5	39.0	
	9-P-13	143.0	127.0	21.5	41.4	
	Average	143.8	125.7	21.1	40.7	
Notched Parent Metal	9-P-5	206.8				
	9-P-6	211.9				
	9-P-9	206.2				
	9-P-10	204.5				
	Average	207.4				1.44
Smooth-Weld	9-W-7	145.5	127.5	15.5	41.5	
	9-W-8	150.4	130.2	14.0	37.3	
	9-W-11	145.5	126.8	7.5	20.2	
	9-W-12	147.7	124.7	10.5	21.8	
	Average	147.3	127.3	11.9	30.2	
Notched-Weld	9-W-5	209.2				
	9-W-6	214.1				
	9-W-9	196.9				
	9-W-10	196.5				
	Average	204.2				1.39

(1) Extensometer slipped

*Aerojet-General Condition modified with primary age of 1400°F

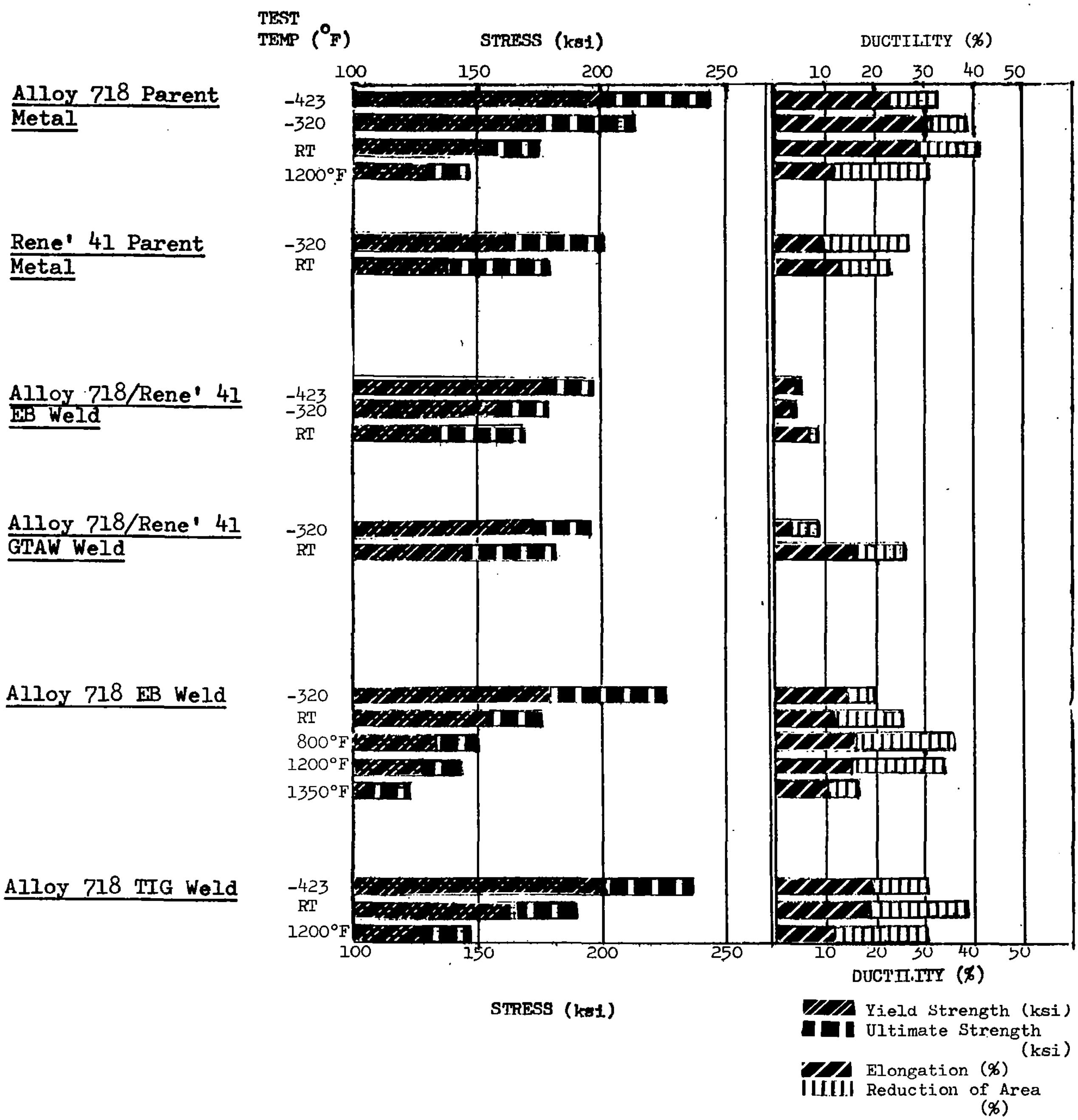

Figure III-9

Mechanical Properties of Alloy 718 and Rene' 41
Parent Material and EB and TIG Weldments

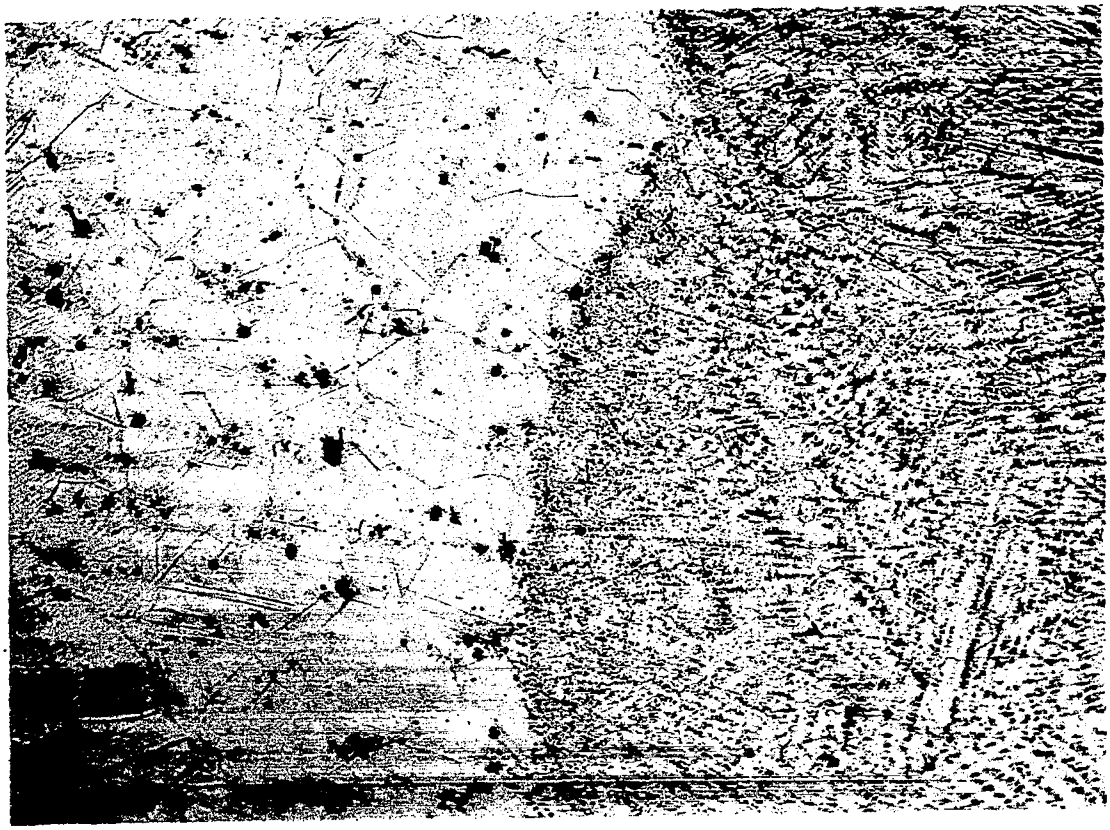

Magnification: 100X

The weld (right side) is Alloy 718 deposited by the TIG process. The weldment was solution-treated and aged prior to sectioning.

Figure III-10

Fusion Zone of TIG Weld in Alloy 718 Forging

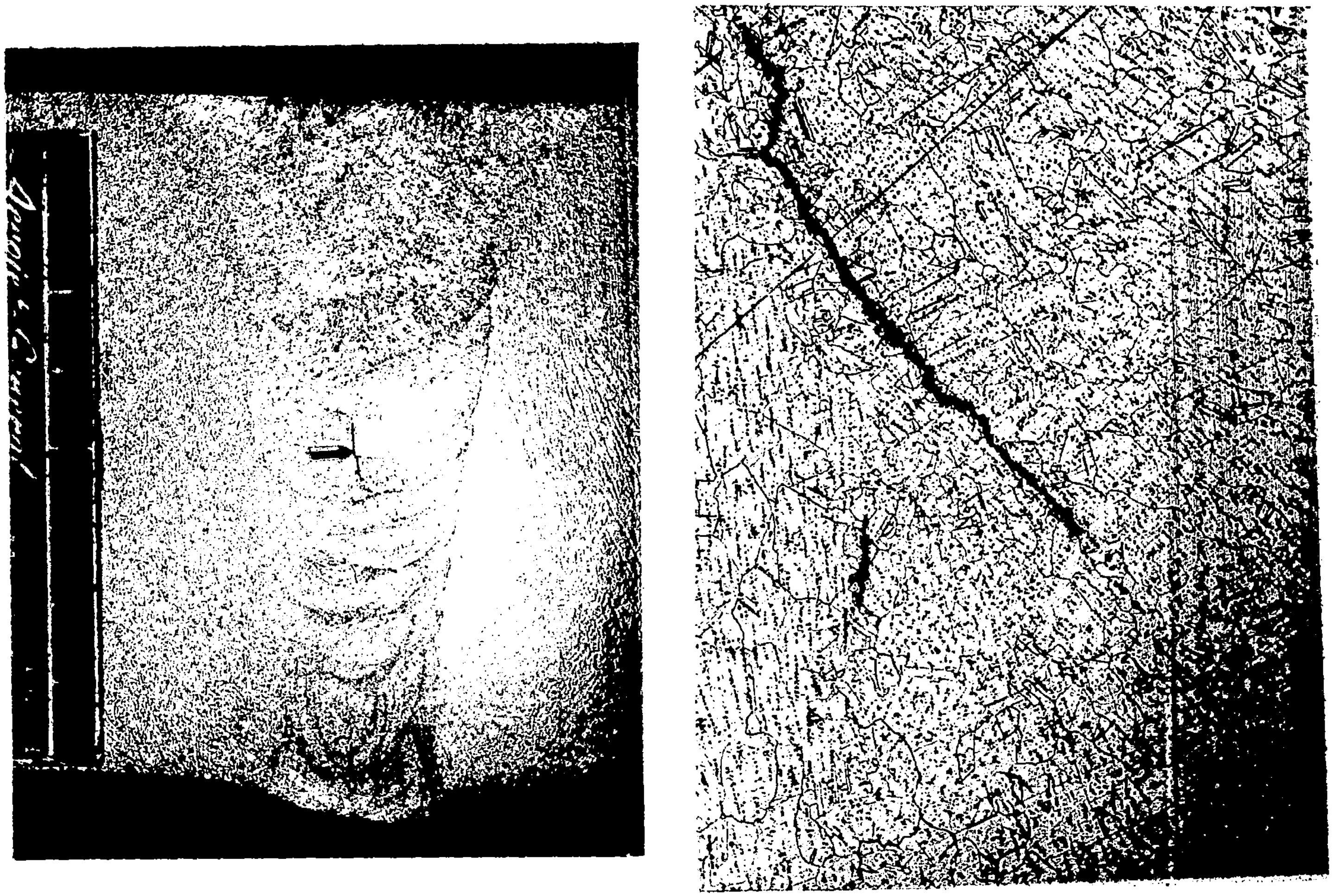

Figure III-11

Shrinkage Crack in TIG Butt Weld in Alloy 718

Magnification: 100X

This is a section of one of the first test joints and required 34 weld passes to fill the "U" groove. The shrinkage crack occurred through the sixth weld pass. To the right is an enlargement of the crack. This cracking problem was resolved by intermediate stress relieving the weldment at 1800°F for 1 hr during the welding operation.

Weld joint efficiencies in excess of 90% can be readily attained in TIG welded Alloy 718 using parent metal filler wire. The weld metal exhibits excellent notch toughness at -423°F.

Close control of welding parameters, part cleanliness, gas purity, and filler wire quality are required to produce sound joints. In welding heavy sections, intermediate (in-process) stress relief is required to prevent cracking caused by shrinkage stresses.

A consumable insert for the root pass assures a uniform weld penetration and a sound weld deposit. The prevention of stress risers caused by uneven weld penetration was essential in the M-1 fuel pump rotor weldment.

V. RECOMMENDATIONS

For quality welding of Alloy 718 in heavy sections, the following considerations must be observed:

The weld schedule should be developed to permit maximum welding speed and weld deposition rate at minimum heat input.

The torch angle is critical in multipass welding of Alloy 718.

The interpass temperature should be controlled so as not to exceed 200°F for multipass welds.

A low angle U-groove design should be used in heavy sections; this will permit accessibility with the least groove volume. The U-groove on the 1-1/8-in. Alloy 718 joints had a 10 degree side-wall angle, a 1/8-in. bottom radius, and a 0.050-in. flat node.

A consumable insert of Alloy 718 should be used to obtain a uniform root pass. A close fit of this insert is required.

Filler wire quality must be closely controlled to assure freedom from laps, seams, surface cracks, and contaminations.

Helium gas should be used for purging, and a 75%-25% helium-argon mixture should be used for the weld torch and trailing shield. A trailing shield is required to assure complete protection of the weld deposit. Gas purity must be controlled.

Good part cleanliness is a standard requirement in all quality welding and is especially critical in welding nickel-base, precipitation-hardened alloys such as Alloy 718 and Rene' 41.

ALLOY 718 DESIGN PROPERTIES

ELASTIC PROPERTIES

Young's Modulus, Torsional Modulus, and Poisson's Ratio vs Temperature

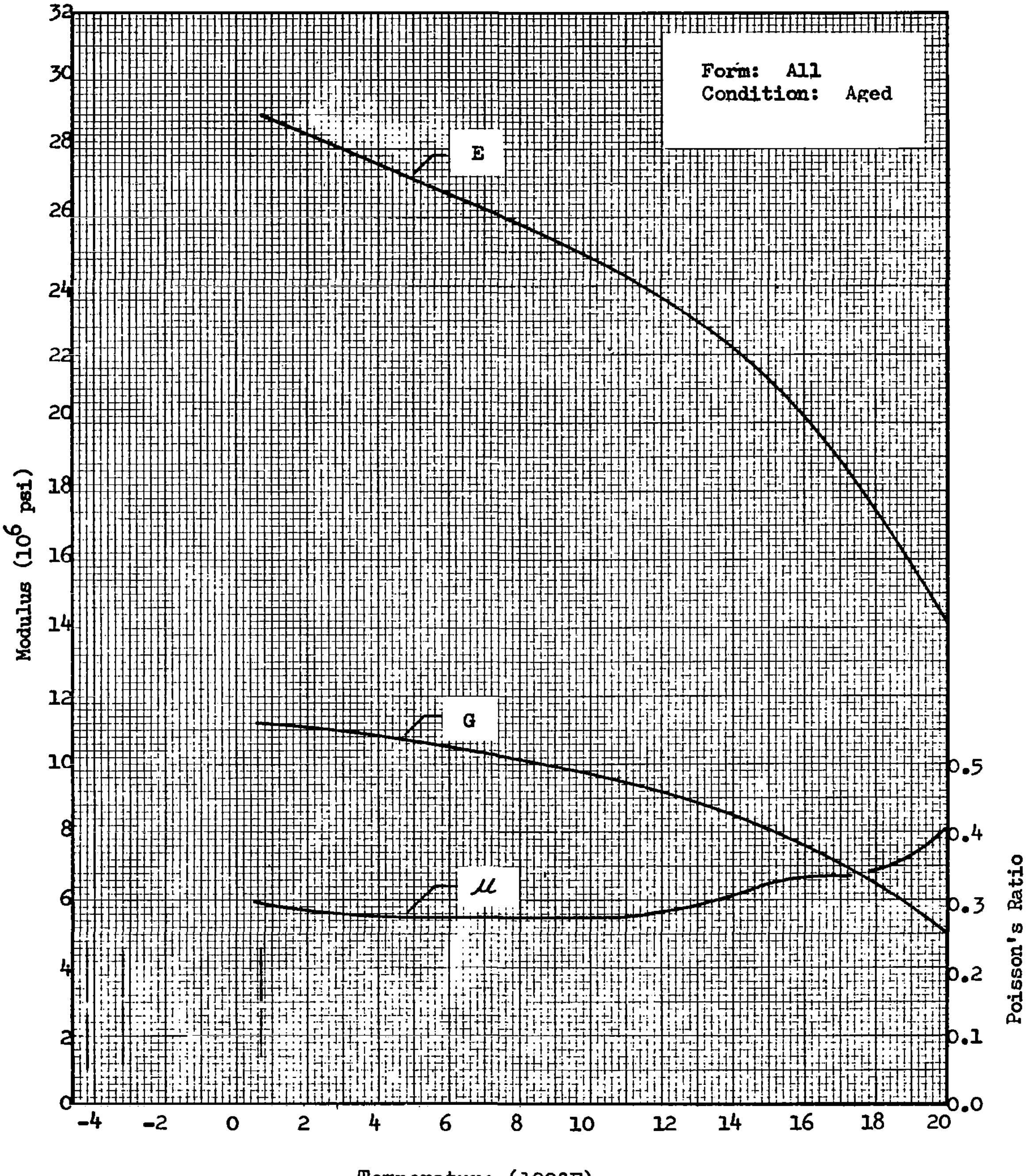

ALLOY 718 DESIGN PROPERTIES

TENSILE PROPERTIES

Ultimate Tensile Stress, 0.2% Yield Stress, and Elongation vs Temperature

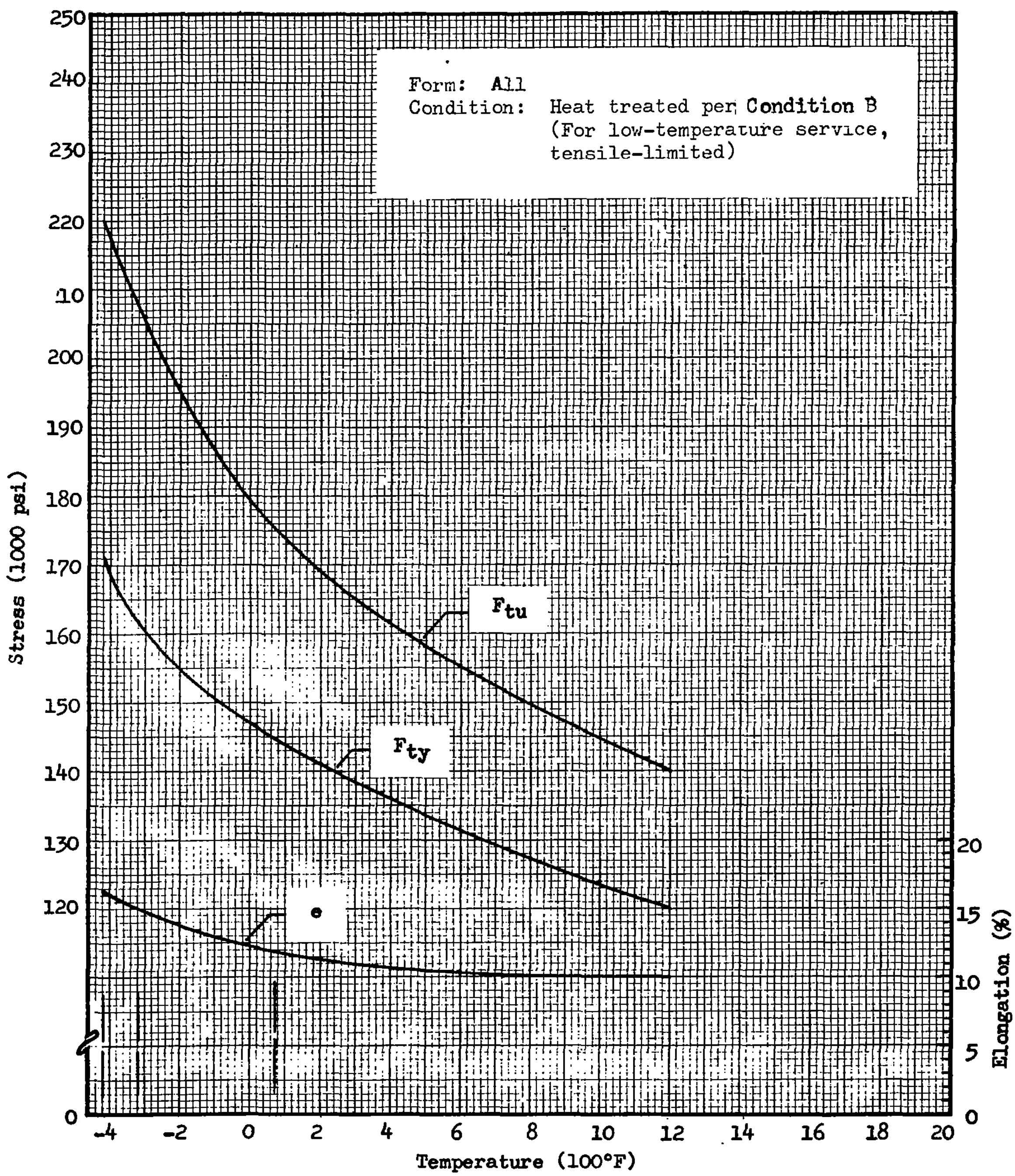

ALLOY 718 DESIGN PROPERTIES

TENSILE PROPERTIES

Ultimate Tensile Stress, 0.2% Yield Stress, and Elongation vs Temperature Also Stress for Rupture in 1 and 10 Hours

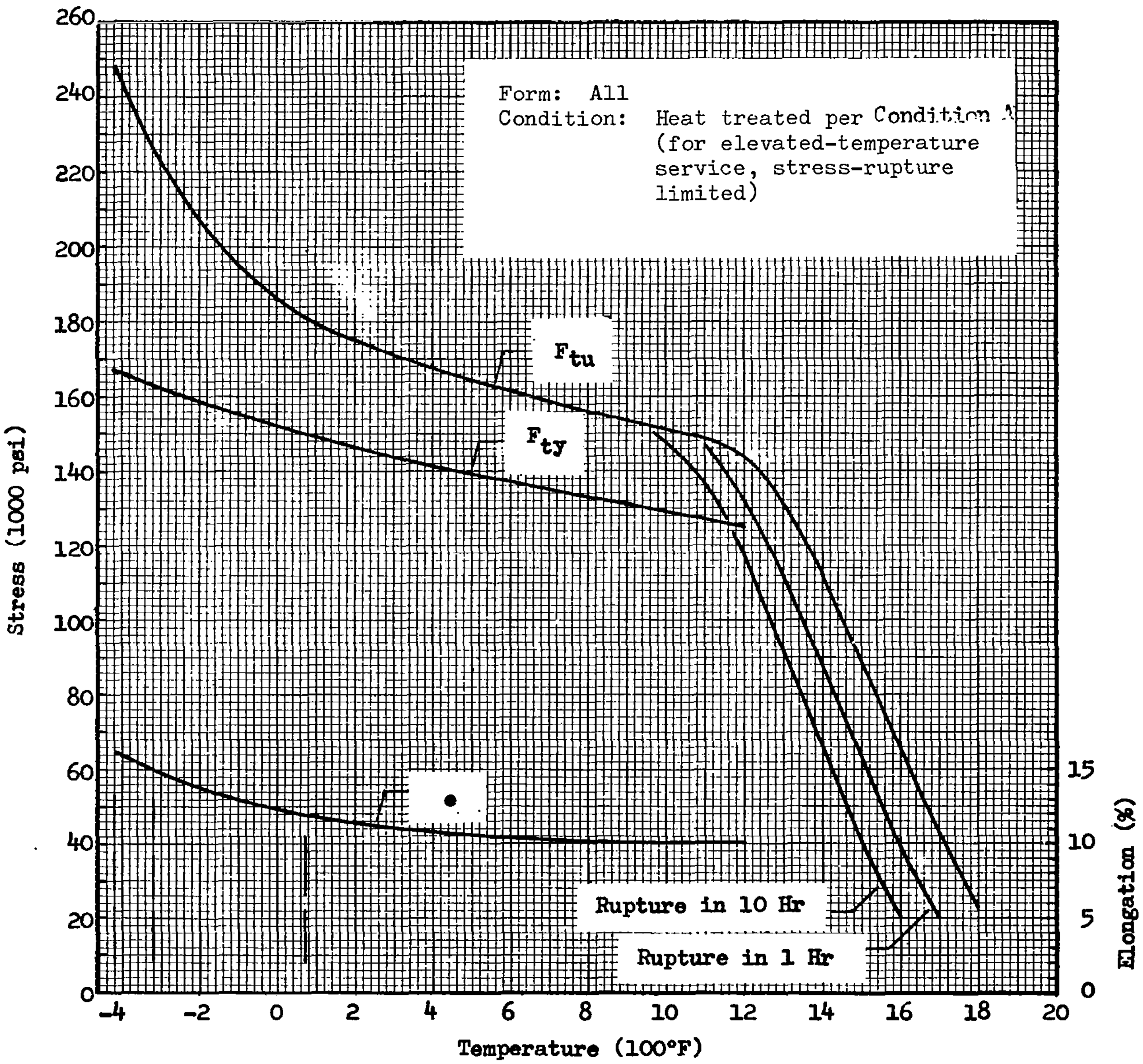

M-1 FUEL TURBOPUMP ASSEMBLY

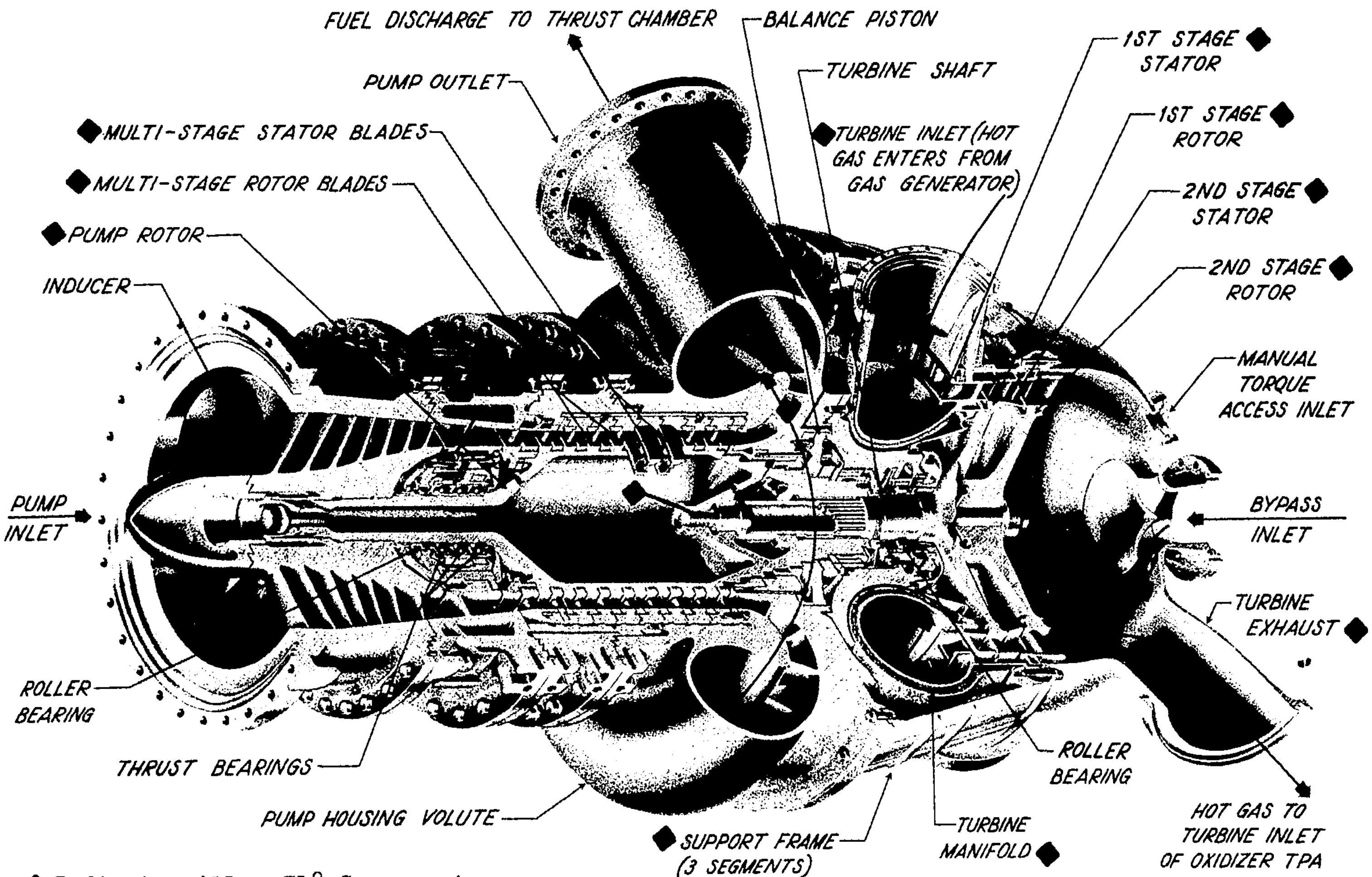

◆ Indicates Alloy 718 Components

M-1 OXIDIZER TURBOPUMP ASSEMBLY

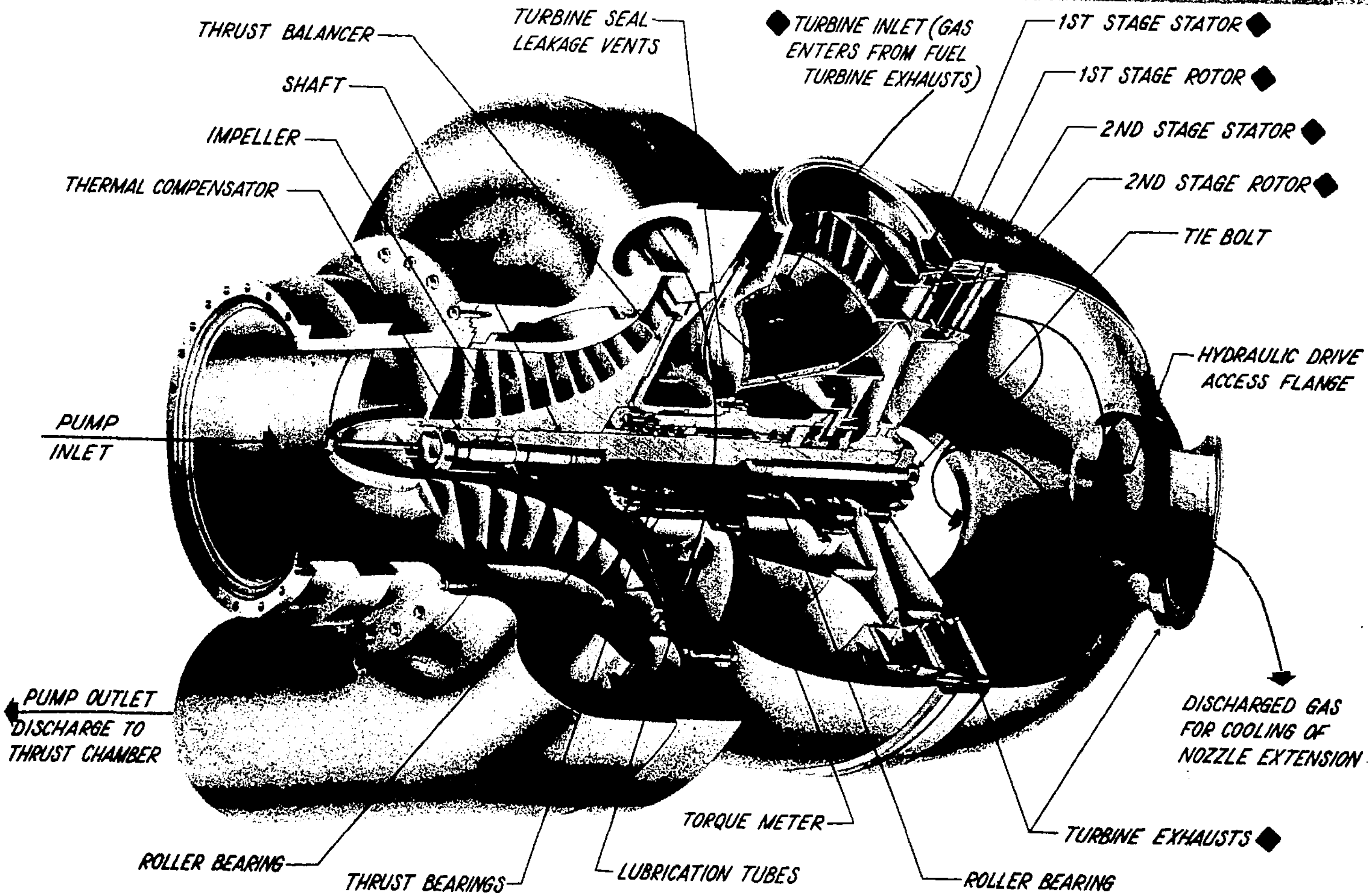

◆ Indicates Alloy 718 Components

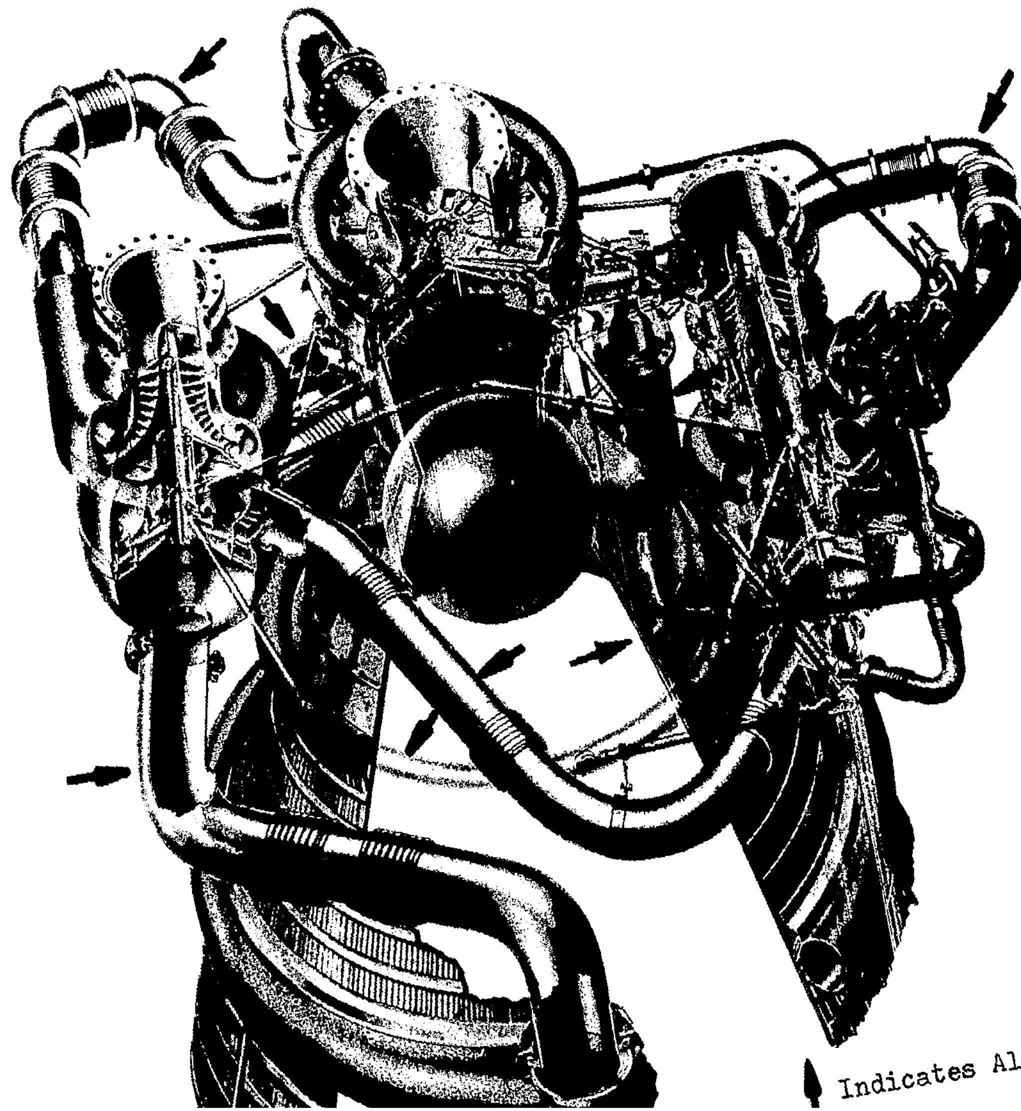

Indicates Alloy 718 Components